UNIVERSITY OF SÃO PAULO
INSTITUTE OF CHEMISTRY
Graduate Program in Chemistry

MARCO ANTONIO DE OLIVEIRA SANTOS MINADEO

Synthesis and characterization of hybrid materials containing gold or platinum nanoparticles and poly(3,4-ethylenedioxythiophenes) for electrochemistry

Versão corrigida da Tese conforme Resolução CoPGr 5890
O original se encontra disponível na Secretaria de Pós-Graduação

São Paulo

Data de depósito na SPG:
05/11/2018

MARCO ANTONIO DE OLIVEIRA SANTOS MINADEO

Synthesis and characterization of hybrid materials containing gold or platinum nanoparticles and poly(3,4-ethylenedioxythiophenes) for electrochemistry

Síntese e caracterização de materiais híbridos contendo nanopartículas de ouro ou platina e poli(3,4-etilenodioxitiofenos) para eletroquímica

Thesis presented to the Institute of Chemistry of the University of São Paulo as part of the requirements for the obtainment of the degree of PhD of Science in Chemistry

Supervisor: Professor Doctor Susana Inés Córdoba de Torresi

São Paulo
2018

I dedicate this Thesis to all those that helped me during my PhD course

AKNOWLEDGEMENTS

To my parents, my friends and all of those that helped me, gave me support and shared good moments during my PhD course.

To the chemists of the past that allowed us extraordinary things with the current science.

To Sci-Hub, for giving back the knowledge to its true owner.

To Professor Paulo Teng An Sumodjo (*in memoriam*), at the Institute of Chemistry of the University of São Paulo (IQ-USP), for the valuable discussions, teachings and advices during my BSc and PhD courses.

To Professor Mauro Bertotti at IQ-USP for the discussions and advices.

To Professor Márcia Temperini and the scientists PhD Tércio, PhD Cláudio and Alessandra at the Laboratory of Molecular Spectroscopy (LEM) of IQ-USP for the infrastructure and the help with the Raman microscopies.

To PhD Aline and other scientists at the Laboratory of Polymeric Biomaterials of IQ-USP for the infrastructure and the help with the gel permeation chromatographies, oven experiments and ultraviolet chamber.

To the scientists at the Laboratory of Electroactive Materials (LME) of IQ-USP (where this work was done): PhD Jadielson (Jadilab), PhD José de Ribamar (Jota) and BSc Rafael Colombo (Dex) for the help with the scanning electron microscopies (SEM); PhD Tatiana Augusto, for the studies of PEDOT; PhD Suélen Harumi, for the help with poly(acrylic acid) hydrogels; BSc Aruã Clayton da Silva, for the collaboration and, syntheses of EDOT-PLA. To BSc Dex for the help with Raman spectra, advices and corrections of this Thesis.

To the Professors at IQ-USP Denise Petri, Flávio Vichi and Mauro Bertotti at my PhD course qualification exam board for the discussion and advices.

To PhD Vinicius Gonçales (Vina) (University of New South Wales), Professor Sergio Humberto Domingues (Mackenzie) and Professor Flavio Vichi (IQ-USP) at the defense board of this Thesis, for the patience, dedication and the valuable discussion, comments, advices and corrections of this Thesis.

To my supervisor, Professor Susana Torresi at LME-IQ-USP, for the supervision, discussions, patience, dedication and help with the academic writing of this Thesis.

To CNPq, process n. 140898/2013-1, for the PhD scholarship granted.

To the Research Support Foundation of the State of São Paulo (Fundação de Amparo à Pesquisa do Estado de São Paulo, FAPESP) for the PhD scholarship granted, process n. 2013/00322-8, vinculated to the processes n. 2009/53199-3 and n. 2015/26308-7 (thematic projects of LME, where this work was done), and for the FAPESP science magazines.

“I think, therefore I am.”

— René Descartes

RESUMO

Minadeo, M. A. O. S. **Síntese e caracterização de materiais híbridos contendo nanopartículas de ouro ou platina e poli(3,4-etilenodioxitiofenos) para eletroquímica**. 2018. 161 p. Tese (Doutorado) – Programa de Pós-Graduação em Química. Instituto de Química, Universidade de São Paulo, São Paulo.

Entre os polímeros orgânicos condutores eletrônicos o PEDOT (poli(3,4-etilenodioxitiofeno)) é largamente utilizado na fabricação de eletrodos em dispositivos miniaturizados, leves e portáteis. As propriedades químicas, mecânicas, eletroquímicas e ópticas dos polímeros condutores são essenciais para planejar a pesquisa futura com eles, e.g., em dispositivos eletrocrômicos transmissivos e reflexivos, sensores cronoamperométricos, sensores voltamétricos e sistemas de liberação controlada de drogas. Degradabilidade também é um fator importante ao considerar o impacto ambiental dos materiais. Nanopartículas (NPs) de Au ou Pt (1–100 nm de tamanho), quando revestidas por um estabilizante, são estáveis, possuem superfícies reativas e funcionalizáveis e catalisam muitas reações de transferência de elétrons. As combinações de nanopartículas de metais nobres com PEDOTs (PEDOT e seus derivados) vêm sendo bastante estudadas nos últimos anos de forma a obter características singulares dos materiais. Os objetivos deste trabalho são estudar a síntese de novos híbridos inorgânicos/orgânicos e o seu comportamento eletroquímico. Foram sintetizados, por reação de oxidorredução em uma etapa em meio aquoso, híbridos de nanopartículas *core-shell* de Au@PEDOT. Por esta mesma estratégia, nanopartículas de Pt dispersas em matrizes de PEDOT foram sintetizadas. As nanopartículas de Au@PEDOT tiveram o seu comportamento eletrocrômico estudado. Com o macromonômero biodegradável EDOT-poli(ácido lático) (EDOT-PLA) foram preparados híbridos de NPsAu/(oligômeros de EDOT-PLA) e também de NPsAu com o novo polímero PEDOT-PLA. Os materiais produzidos foram analisados. As nanopartículas são muito pequenas, com um máximo de distribuição em menos de 10 nm. Observa-se que o PEDOT-PLA é um condutor, de estrutura eletrônica semelhante ao PEDOT e insolúvel em água. Ele também é mais estável em filme do que o PEDOT. NPsAu/PEDOT-PLA demonstra ter atividade eletrocatalítica de redução do peróxido de hidrogênio. Eletrodos de alto desempenho para a redução de peróxido de hidrogênio foram, portanto, obtidos (sensibilidade $8{,}4\times10^{-3}$ A cm^{-2} mol^{-1} L; faixa linear ($5{,}1\times10^{-4}$ – $4{,}5\times10^{-2}$) mol L^{-1}; limite de detecção $1{,}7\times10^{-4}$ mol L^{-1}). Foram feitas também sínteses de hidrogeis acrílicos e a inserção de nanopartículas/PEDOT neles, modificando as suas propriedades.

Palavras-chave: nanopartículas de ouro, polímeros condutores, poli(3,4-etilenodioxitiofeno), eletrocromismo, detecção eletroquímica.

ABSTRACT

Minadeo, M. A. O. S. **Synthesis and characterization of hybrid materials containing gold or platinum nanoparticles and poly(3,4-ethylenedioxythiophenes) for electrochemistry.** 2018. 161 p. PhD Thesis – Graduate Program in Chemistry. Instituto de Química, Universidade de São Paulo, São Paulo.

Among the organic electronic conducting organic polymers PEDOT (poly(3,4-ethylenedioxythiophene)) is largely used in the making of electrodes for miniaturized, light and portable devices. The chemical, mechanical, electrochemical and optical properties of the conducting polymers are essential to plan the future research with them, as in, e.g., electrochromic devices (transmissive and reflective), chronoamperometric sensors, voltammetric sensors and controlled drug release systems. Degradability is also an important factor considering the environmental impact of the materials. Nanoparticles (NPs) of Au or Pt (1–100 nm size), when surrounded by a stabilizer, are stable, have reactive and functionalizable surfaces and catalyze many electron transfer reactions. Combinations of noble metal nanoparticles with PEDOTs (PEDOT and its derivatives) have been studied in the last years to obtain singular characteristics of the materials. The goals of this work are to study the synthesis of new inorganic/organic hybrids and their electrochemical behavior. Through 1-step oxidoreduction reaction in aqueous media, hybrids of core-shell Au@PEDOT nanoparticles were synthesized. Through this same strategy, nanoparticles of Pt dispersed in a matrix of PEDOT were synthesized. The Au@PEDOT nanoparticles had their electrochromic behavior studied. With the biodegradable macromonomer EDOT-poly(lactic acid) (EDOT-PLA) were prepared hybrids of NPsAu/(oligomers of EDOT-PLA) and also of NPsAu with the new polymer PEDOT-PLA. The produced materials were analyzed. The nanoparticles are very small, with a maximum of distribution in less than 10 nm. It's observed that PEDOT-PLA is conducting, electronically similar to PEDOT and insoluble in water. It is also more stable as a film than PEDOT. NPsAu/PEDOT-PLA demonstrates to have electrocatalytic towards the reduction of hydrogen peroxide. Electrodes of high performance towards the reduction of hydrogen peroxide were thus obtained (sensitivity 8.4×10^{-3} A cm^{-2} mol^{-1} L; linear range (5.1×10^{-4} – 4.5×10^{-2}) mol L^{-1}; limit of detection 1.7×10^{-4} mol L^{-1}). Syntheses of acrylic hydrogels and the insertion of nanoparticles/PEDOT in them were also performed, modifying their properties.

Keywords: gold nanoparticles, conducting polymers, poly(3,4-ethylenedioxythiophene), electrochromism, electrochemical detection.

LIST OF EQUATIONS

LIST OF TABLES

Table 3. Potential of detection (E), linear range (LR), sensitivity (Sen), limit of detection (LD) and limit of quantification (LQ) of chronoamperometric sensors of H_2O_2 containing PEDOT hybrids. a: PEDOT and NPsPt hybrid over printed carbon electrode (SPC). b: multiwall carbon nanotubes (MWCNTs) and PEDOT hybrid on GCE. c: hybrid of PEDOT and nanoparticles of Cu and Cu hexacyanoferrate (NPsCu-$Cu_2[Fe(CN)_6]$). d: hybrid of PEDOT nanowiskers (NWs), NPsAu and hemoglobin (Hb). e: PEDOT and Prussian Blue (PB) nanoparticles hybrid. f: PEDOT nanofibers (NFs) and NPsPd (palladium nanoparticles) hybrid. E in this Table refers to Ag/AgCl/$KCl_{(3\ mol\ L-1)}$. The limits of detection are calculated as (3 x standard deviation of blank of analyte / sensitivity). The limits of quantification are calculated as (10 x standard deviation of blank of analyte / sensitivity). Chronoamperometric detection performed in this work: working electrodes: GCEs. Counter electrode: Pt plates. Reference electrode: Ag/AgCl/$KCl_{(3\ mol\ L-1)}$. Electrolyte: dyhydrogenphosphate/hydrogenphosphate buffer 20 mmol L^{-1} pH = 7.4 + NaCl 100 mmol L^{-1}. The electrolyte was deoxygenated by bubbling dry N_2 for at least 15 min prior to the experiment and keeping a N_2 atmosphere over the electrolyte throughout the experiment. NPsAu/PEDOT-PLA deposited on GCE adding a small drop of NPsAu/PEDOT-PLA on GCE and drying it at 40 ºC (313 K) in vacuum. NPsAu/PEDOT-PLA formed from the reaction suspension of NPsAu/o-EDOT-PLA and potassium peroxydisulfate in acetonitrile, under stirring for days.....144

LIST OF SCHEMES

LIST OF FIGURES

the open circuit potentials: ca. +150 mV. Scan rate: 10 mV s^{-1}. Initial potential scans: increasing potential. The current is normalized by the geometrical area of the electrode (7.07 mm^2). 3 cycles were performed. Working electrode: modified ITO. Counter electrode: Pt plate. Reference electrode: $Ag/AgCl/KCl_{(sat)}$. Electrolyte: dyhydrogenphosphate/hydrogenphosphate buffer 20 mmol L^{-1} pH = 7.4 + NaCl 100 mmol L^{-1}. The electrolyte was deoxygenated by bubbling dry N_2 for at least 15 min prior to the experiment and keeping a N_2 atmosphere over the electrolyte throughout the experiment. ITO/silane/f-h-PAAM&NPsAu@PEDOT is the [film hydrogel of polyacrylamide on ITO] with core-shell NPsAu@PEDOT inserted by electroinsertion. The electroinsertion is performed applying a positive potential against an ITO, being the electrolyte reaction suspension of NPsAu@PEDOT. The films of hydrogels of polyacrylamide are formed over ITOs silanized in the surface. ITOs are silanized with tris-(2-methoxyethoxy)(vinyl)silane in toluene, removing and heating the ITOs at 100 ºC (373 K). Hydrogels of polyacrylamide are then formed from acrylamide, polyacrylamide, N,N'-methylenebisacrylamide and 2,2-diethoxyacetophenone in water over ITOs/silane, under ultraviolet radiation. NPsAu@PEDOT formed from $HAuCl_4$, EDOT and NaPSS in water, under stirring for hours.....131

Figure 23. (Continuation). Cyclic voltabsorgrams (i (black curve, solid lines) and T (blue curve, dashed lines) x E) of an ITO/NPsAu@PEDOT (i and T x E). Scan rate: 10 mV s^{-1}. Initial potential: +600 mV. Initial scans: decreasing potential. Wavelength of light: 600 nm. The current was normalized by the geometrical area of electrode (0.5 cm^2). 3 cycles were performed, cycles 2 and 3 showed. Working electrode: modified ITO. Counter electrode: Pt plate. Reference electrode: $Ag/AgCl/KCl_{(sat)}$. Electrolyte:

Figure 25. (Continuation). A: chronoamperogram of a GCE (control) with additions of H_2O_2 to the electrolyte at −300 mV. B: chronoamperogram of a GCE/NPsAu/PEDOT-PLA (deposited by casting, 10 steps) with additions of H_2O_2 to the electrolyte at −300 mV. Working electrodes: GCEs. Counter electrode: Pt plate. Reference electrode: $Ag/AgCl/KCl_{(3\ mol\ L-1)}$. Electrolyte: dyhydrogenphosphate/hydrogenphosphate buffer 20 mmol L^{-1} pH = 7.4 + NaCl 100 mmol L^{-1}. The electrolyte was deoxygenated by bubbling dry N_2 for at least 15 min prior to the experiment and keeping a N_2 atmosphere over the electrolyte throughout the experiment. NPsAu/PEDOT-PLA deposited on GCE adding a small drop of NPsAu/PEDOT-PLA on GCE and drying it at 40 ºC (313 K) in vacuum. NPsAu/PEDOT-PLA formed from the reaction suspension of NPsAu/o-EDOT-PLA and potassium peroxydisulfate in acetonitrile, under stirring for days. 140

LISTS OF SYMBOLS

In the lists the prefixes, superscripts and subscripts are not considered for the order. Symbols of the multiples and submultiples of the elementary units are not listed. Symbols of chemical elements are not listed.

SI units symbols

A.....ampere

C.....coulomb

g.....gram

K.....kelvin

m.....meter

s.....second

V.....volt

Non-SI units symbols

h.....hour = 3600 s

L.....liter = 10^{-3} m^3

min.....minute = 60 s

u.....atomic mass unit = $1.660539040 \times 10^{-27}$ kg

Scale symbols

ºC.....degrees Celsius

LIST OF ACRONYMS, INITIALISMS, PREFIXES, ABBREVIATIONS AND NOTATIONS AND GLOSSARY

Some notations that are not listed here are made combining those listed.

a.....thermodynamic activity

Abs_{600nm}.....absorbance at 600 nm

ACN.....acetonitrile

b-.....bulk form of

c.....mass concentration

ca.....about

CV.....cyclic voltammogram

cyclic voltammetry

CVs.....cyclic voltammograms

cyclic voltammetries

d / d.....derivative relative to

DLS.....dynamic light scattering

E.....electric potential

E^0.....standard reduction potential of reaction

EDOT.....3,4-ethylenedioxythiophene

EDOT-PLA.....3,4-ethylenedioxythiophene-poly(lactic acid)

EDOT-PLAs.....3,4-ethylenedioxythiophene-poly(lactic acid) and its derivatives

EDS.....energy dispersive X ray fluorescence spectrometry

energy dispersive X ray fluorescence spectrometer

f-.....film of

GCE.....glassy carbon electrode

GCEs.....glassy carbon electrodes

h-.....hydrogel of

i.....electric current

ITO.....electrode of glass/(indium tin oxide thin film)

ITOs.....electrodes of glass/(indium tin oxide thin film)

j.....electric current density

j_0.....initial current density

$j_{RED,L}$.....limit current density of reduction

NaPSS.....poly(sodium 4-styrenesulfonate)

NPs.....nanoparticles

NPsAg.....silver nanoparticles

NPsAu.....gold nanoparticles

NPsPt.....platinum nanoparticles

o-.....oligomers of

PAA.....poly(acrylic acid)

PAAs.....samples of poly(acrylic acid)

PAAM.....polyacrylamide

PEDOT.....poly(3,4-ethylenedioxythiophene)

PEDOTs.....poly(3,4-ethylenedioxythiophenes) and its derivatives

PLA.....poly(lactic acid)

PSS.....poly(4-styrenesulfonate)

SEM.....scanning electron microscopy

scanning electron microscope

SHE.....standard hydrogen electrode

T_{600nm}.....transmittance at 600 nm

$T_{600nm(MAX)}$.....maximum transmittance at 600 nm

TEM.....transmission electron microscopy

transmission electron microscope

UV-Vis-NIR.....ultraviolet-visible-near infrared spectrophotometry

@.....core-shell nanoparticles

/.....phase separation

physical separation

substance separation

&.....inserted in

with inserted

[ ].....molar concentration of

Δ.....variation of

v.....wavenumber

→.....react and form

in chemical equilibrium with

-.....covalent bond

hybrid with

SUMMARY

1. INTRODUCTION

Throughout this Thesis the electrochemical convention adopted is the international convention: positive potentials are potentials that favor oxidation, and negative potentials are potentials that favor reduction.

1.1. Nanomaterials

There are several different definitions in literature about nanomaterials, nanoparticles, nanoscience and nanotechnology, from different approaches. There are definitions of nanomaterials as materials with at least 1 dimension 0–100 nm, or materials with at least 1 dimension 0–10 nm. Herein is adopted the one that is suitable for this work: nanomaterials are solid materials with 1 or more external dimensions 1–100 nm (which is called critical size). Among them there are 0-dimension nanomaterials (e.g., nanoparticles (NPs), nanospheres, nanowiskers, nanocubes, nanotetrahedrons, nanooctahedrons, nanopolyhedrons, and nanostars), 1-dimension nanomaterials (e.g., nanorods, nanotubes, nanofibers) and 2-dimension nanomaterials (e.g., nanosheets, nanodiscs). The scale of them is above the atomic scale (several angstroms) and goes up to the colloid particle scale. In 1-dimension nanomaterials the length is much larger than the other sizes, and in 2-dimension nanomaterials width and length are much larger than thickness. Nanoparticles are 0-dimension nanomaterials, i.e., nanomaterials without dominant sizes over the others. All sizes of nanoparticles are in the 1–100 nm

scale, therefore they are the smallest nanomaterials [1]–[3]. In a similar way, herein is adopted that nanoscience is the study of nanomaterials and its properties.

Nanomaterials present chemical and physical properties that differ a lot from the correspondent bulk materials or materials divided in bigger particles, e.g., microparticles. These odd properties are attributed to the great (surface atoms / inner atoms) ratio when compared to bulk materials. As the sizes (length, width, thickness) decrease to the nanometric scale, the (surface area / mass) ratio increases, from bulk materials to micromaterials to nanomaterials to atom clusters. The small sizes and the small numbers of atoms contained in each particle make the electronic structure of the nanomaterials much more discrete, which modifies the way the atoms react. The surface energy is usually higher, and the surface is more reactive but also more easily oxidizable [1]–[3]. This factors contributes to extraordinary rates of reactions in some nanomaterials, to the great surface enhanced Raman scattering effect of gold nanoparticles (due to the plasmonic effect), to high turnover rates of reaction of gases, to high adsorption capacity etc. [1]–[3].

Nanomaterials are usually synthesized by one of the two great approaches: bottom-up or top-down. In bottom-up syntheses the nanomaterials are formed from smaller structures: atoms, molecules or clusters. In top-down syntheses the source material is a large, bulk material that is reduced, milled, excised or etched until the obtainment of the desired nanomaterials. Bottom-up strategies include chemical synthesis, self-assembly of nanomaterials, positional assembly, chemical vapor deposition, physical vapor deposition, electrodeposition, emulsion synthesis, reverse micelle synthesis and sol-gel process. Top-down techniques include nanolithography,

etching, and microengineering and laser ablation. Usually they are more expensive, require more complex equipment and consume more energy and reagents than bottom-up techniques. However, they allow the fast production of highly organized and geometric materials, like, for example, geometric nanostructures on a smooth surface formed by etching the surface with beam techniques, e.g., laser ablation.

Since nanoparticles are the most symmetrical and simplest nanomaterials they are formed as products of many chemical reactions. Nanoparticles can be easily formed from neutral atoms and atom clusters in the presence of stabilizers that adhere to the surface of the nanoparticles, preventing their aggregation. The reduction of metal ions in solutions is a class of reactions widely applied to these syntheses. In these reactions metal-containing cations or anions react with reducing agents; the reduced, neutral metal atoms aggregate and form nanoparticles. The bottom-up syntheses, therefore, are of particular interest for making nanoparticles. In the literature are described chemical syntheses of nanoparticles of gold [4], [5], platinum [6], palladium [7], [8], iron [9], [10], copper [11]–[14], silver [15], [16], rhodium [17], [18], iridium [19], ruthenium [20], [21], lead [22], bismuth [23] etc. In this work were focused on gold and platinum nanoparticles fabricated by bottom-up techniques.

1.2. PEDOT

PEDOT, or poly(3,4-ethylenedioxythiophene), is an organic electronic conducting polymer (these polymers are hereafter called conducting polymers). PEDOT is widely used in electrochemical devices, solar cells and molecular electronic devices, being currently the most used conducting polymer in the world. Its monomer, EDOT (3,4-ethylenedioxythiophene), is a molecule derived from the heterocyclic sulfured aromatic compound thiophene. For neutral undoped PEDOT the band gap e_g = 1.6 eV (which corresponds to 775 nm photon energy (red)), higher than those of polythiophenes and lower than those of many other conducting polymers [24]–[26], which favors PEDOT use in electronics. PEDOT is a cathodic electrochromic polymer, it presents color (intense blue) in the reduced (neutral) state and is colorless (or light blue) in the oxidated (positively charged) state. The blue color comes from the absorption at 775 nm by neutral PEDOT. The insertion of electric charge in PEDOT increases its electronic conductivity. Pure PEDOT is hydrophobic and insoluble in water. The mixture of PEDOT and NaPSS (poly(sodium 4-styrenesulfonate)) has much better solubility and stability in water, since $PSS^-_{(aq)}$ (poly(4-styrenesulfonate)) stabilize PEDOT in solutions. This mixture is the standard commercial PEDOT form. PEDOT has applications in electrochromic layers and electrochemical sensors. In the fully oxidized state PEDOT has 1 positive charge for every 2 monomeric units, and this positive charge is stabilized by 1 negative charge of the sulfonate group of PSS^- anion.

1.3. Inorganic/organic hybrids in electrochemistry

Hybrid materials are solid materials composed by two or more substances with different properties. Hybrid materials of conducting polymers with nanoparticles have been widely used as electrode materials for the assembly of sensors and biosensors in electroanalytics [27]–[37]. Analytes such as glucose [31], [33], [35], [37], ascorbic acid [36], [38], uric acid, dopamine [36], hydrogen peroxide [29], [30], sarin [27], carbamates [27], acetylcholine [34], hydrazine [28], and nitrate [32] were detected by sensors based on these nanohybrids.

Several recent works in the literature have reported the syntheses of hybrids of PEDOT with metal nanoparticles and several electrochemical studies [39]–[44]. They have used strategies like deposition of metallic nanoparticles over previously formed PEDOT films, the polymerization of EDOT around previously formed gold nanoparticles or the synthesis in 1 step of gold nanoparticles surrounded by PEDOT (one-pot synthesis). These nanohybrids have interesting properties as electrode materials because the presence of metallic nanoparticles increase its electric conductivity, and the polymeric network is relatively porous and allows the insertion and removal of molecules and ions in solutions.

Radhakrishnan et al. [43] formed NPsAg (silver nanoparticles) over nanotubes of polypyrrole/PEDOT, chemically synthesizes in two steps. The first was the chemical oxidation of pyrrole, and the second was the formation of the PEDOT coating using $FeCl_3$ as oxidizing agent. NPsAg were chemically synthesized over the walls of the nanotubes from an $AgNO_3$ solution. Semaltianos and coworkers [42] used laser ablation

of bulk Ag piece to form NPsAg in suspension. The same procedure in a PEDOT/PSS-containing aqueous solution leads to the formation of Ag/PEDOT/PSS hybrid. In another strategy, Adibi et al. [45] deposited over a transparent electrode of glass/(indium tin oxide thin film) (ITO) a film of Ag microparticles through spin coating of colloidal Ag, and then spin coated aqueous commercial PEDOT/PSS suspension over it, forming Ag/PEDOT/PSS hybrid. Balamurugan et al. [40], [41] electropolymerized PEDOT by cyclic voltammetry and electrodeposited at constant potential NPsAg with up to 10 nm diameter, for the detection of $H_2O_{2(aq)}$ by chronoamperometry at −450 mV versus $Ag/AgCl/KCl_{(sat)}$. The same group, in other article [41], prepared NPsAg/PEDOT/PSS with 10–15 nm diameter in an one-pot synthesis in aqueous solution containing Ag^+, EDOT and NaPSS. Wang et al. [46] used PEDOT itself in the commercial solution as reducing agent for $AgNO_3$, forming NPsAg with up to 30 nm diameter inside the polymeric network of PEDOT/PSS, which was then deposited as a thin film. Woo et al. [47] performed the chemical syntheses of NPsAu (gold nanoparticles) and NPsAg by reducing $HAuCl_4$ and $AgNO_3$ with $NaBH_4$ in aqueous media containing PEDOT/PSS, obtaining nanoparticles with 20–40 nm diameter. The nanocomposites NPsAu@PEDOT/PSS (core-shell of Au, PEDOT and PSS nanoparticles) and NPsAg/PEDOT/PSS were used as hole conducting layer in organic solar cells, presenting lower electric resistance than the same polymer without metallic nanoparticles. In a similar reaction to that performed by Wang et al. [46], Xu et al. [48] described in a communication the addition of $HAuCl_4$ or $AgNO_3$ to PEDOT/PSS solution containing poly(phenylene vinylene) as stabilizing agent. The reaction was performed to obtain core-shell Au@PEDOT and Ag@PEDOT/PSS/poly(phenylene vinylene)

nanoparticles, with PEDOT oxidation simultaneous to metal reduction. The authors observed the formation of NPsAu with average size of 20 nm, and also other nanostructures as gold nanorods with ca. 2 nm size. Adibi et al. [45] deposited a thin film of silver nanoparticles over ITO by spin coating, and deposited a film of commercial PEDOT/PSS over it by spin coating. The NPsAg in the electrode seem to greatly increase the conductivity.

Among the noble metals used as nanoparticles to form hybrids of interest with conducting polymers the most used is gold. The exceptional electric conductivity and stability towards oxidations and chemical reactions are some of the reasons [49]. As explained behind, metal nanoparticles in general are much less stable and easy to oxidize than the corresponding bulk phases. Atomic scale layers of oxides are formed in the surfaces of NPsAg, copper nanoparticles and palladium nanoparticles, depending on the medium. Nanohybrids of gold nanoparticles with PEDOT have also been studied for electrochromic layer in electrochromic devices, joining the electrochromism of PEDOT with the properties of NPsAu that modify the electronic structure of the polymer [50]–[63].

Gniadek et al. [64] deposited a thin film of polypyrrole containing NPsAu through the oxidation of pyrrole by Au(III). The electrode was sequentially immersed in: a solution of pyrrole, $HAuCl_4$, ethanol, water; for the formation of the film. Ventosa et al. [65] studied the influence of the concentration of oxidant and monomer in the one-pot synthesis of NPsAu@PEDOT. Kumar et al. [66]–[70] used the same strategy synthesis, studied the influence of the stabilizing agents in the properties of nanoparticles and proved the catalytic activity of the nanoparticles for reduction. Zhang et al. [71]

electrodeposited a thin film of PEDOT&NPsAu (PEDOT with inserted NPsAu) voltammetrically cycling GCE (glassy carbon electrode) in $HAuCl_{4(aq)}$ 0,5 mmol L^{-1} with great excess of EDOT, and applied the electrode to the electrooxidation of nitrite. Salsamendi et al. [72] formed a hybrid of PEDOT with Au nanorods. EDOT was polymerized in aqueous media with ammonium peroxydisulfate, using poly(1-ethyl-3-vinylimidazolium bromide) as stabilizer. Following this the suspension of PEDOT was mixed with the Au nanorods suspension, and the film was formed by precipitation with the bis-(trifluoromethanesulfonyl)imide ion.

1.4. Biodegradable conducting materials

New composites and hybrid materials have been studied for the assembly of electrodes for batteries, controlled release drug devices, electrochemical actuators, electrochemical sensors etc. A new class of polymers is the biodegradable conducting polymers, with possible applications in living cells, bacteria and live organisms. Several polymers, polymers combinations and inorganic/organic hybrids have been synthesized and described for this purpose. Boutry et al. [73] prepared the composites PLA-polypyrrole and polycaprolactone-polypyrrole (PLA is poly(lactic acid)) and studied their properties (polycaprolactone is a polymorph material). PLA and polycaprolactone are polyesters, polymers easily degradable by microorganisms, which attack the ester amidic bonds. This strategy allowed the obtaining of a synergic, highly conducting material. Kuang et al. [74] developed a composite of carbon nanotubes and PLA. Yet Xu et al. [75] synthesized polyurethanes with 10-camphorsulfonic acid. The polyurethanes presented great elasticity and feasible electric conductivity when hydrated. Moradpour et al. [76] prepared a material of cellulose/carbon-based paste functionalized with palladium nanoparticles/ethylenediamine, which showed catalytic activity for the production of hydrogen and was characterized by cyclic voltammetry. In an article published in *RSC Advances*, Mondal et al. [77] described the preparation of a nanoblend of poly(butylene-adipate-*co*-terephtalate) with polypyrrole, by electrospun. The blend is hydrophilic, biocompatible and conducting. These works used more than 1 polymer or component, being at least 1 of them a π-conjugated polymer.

1.5. Hydrogels with inserted nanoparticles in electrochemistry

Hydrogels are soft materials made of networks of organic polymer chains that are hydrophilic and have the capacity of absorb and release water. Hydrogels can retain large amounts of water, and its properties can vary with the hydration state of the gel, from the fully-dehydrated state to the fully-hydrated state (maximum absorption possible). The hydration process is called swelling, and it depends greatly on the size, structure and chemical composition of the gel. Hydrogels possess polymer chains with cross-linked bonds that form the 3-dimension, highly porous networks and make them insoluble in water [78], [79]. It's clear thus that they have the potential to be hosts for materials of interest.

Several noble metal nanoparticles have been inserted or synthesized inside insulating hydrogels. The developed strategies allow the modification of with different nanomaterials, resulting in hybrids with different properties. Norton et al. [80] polymerized a layer of PEDOT over silica (amorphous silicon dioxide) nanoparticles through chemical oxidation in solutions, obtaining core-shell inorganic/organic nanoparticles with silica core. The nanoparticles were added to a solution of ethyleneglycol, which was photopolymerized under ultraviolet radiation to form a poly(ethylene glycol) hydrogel with Si@PEDOT nanoparticles inside. In another work [81] the authors used dimethylviologen dichloride, KBr and tris(2,2'-bipyridil)ruthenium(II) as redox mediators of PEDOT inside the hydrogel, characterizing the electrochemistry of the hybrid material.

Odaci et al. [82] prepared a poly(ethylene glycol) hydrogel containing NPsAu and glucose oxidase in one step through the simultaneous reaction: gel formation assisted by DL-camphoroquinone and $HAuCl_{4(aq)}$ reduction, in the presence of glucose oxidase. The reactions were induced by blue light. The hybrid was used as biosensor for glucose, and the results showed that NPsAu improved the contact with the catalytic active site of the enzyme.

Dai et al. [83] synthesized a triple network conducting hydrogel composed by PAA (poly(acrylic acid)) and PEDOT. For this the chemical synthesis of PAA was made at 80 ºC (353 K), from acrylic acid and cross-linker precursor solution. Then the resulting hydrogel was immersed in: acrylic acid solution for the second polymerization; solution of EDOT; solution of NaPSS; $FeCl_{3(aq)}$. $Fe^{3+}{}_{(aq)}$ acts as oxidant of EDOT, forming polymeric chain of PEDOT/PSS inside PAA. [84] used this same method [83] and synthesized NPsAu inside the PAA&PEDOT/PSS hydrogel, immersing the gel in an Au(III) solution; Au(III) oxides PEDOT. The 2 works demonstrate *in situ* synthesis of NPsAu. In a communication Sekine et al. [85] obtained a flexible electrode material through PEDOT electropolymerization in an agarose gel. Core-shell nanoparticles with Au nuclei and PEDOT shell were synthesized by one-pot oxidative chemical syntheses in suspension, as described in the works by Augusto et al. in the Laboratory of Electroactive Materials [86], [87]. In this work this approach was used to synthesize Au@PEDOT, Pt/PEDOT and other inorganic/organic hybrid materials.

2. GOALS

Based on the need for new advanced electroactive materials today, like biodegradable electronic conducting materials and high volume 3-dimensional conducting matrixes, the general goal of this work is to study the syntheses of hybrids of PEDOTs (PEDOT and its derivatives) with Au or Pt nanoparticles and to study their electrochemical behaviors. The specific goals are to investigate the detailed syntheses and the techniques of deposition of these hybrids and how they affect the electroactivity of their films.

3. EXPERIMENTAL

3.1. Chemicals

3,4-ethylenedioxythiophene was acquired from Sigma-Aldrich. It was distilled under reduced pressure in the dark and stored at 4 ºC (277 K) in the dark when not in use. Poly(sodium 4-styrenesulfonate) (massed average molecular mass is ca. 70000 u), acrylic acid, acrylamide, tetrachloroauric acid, hexachloroplatinic acid, N,N,N',N'-tetramethylethane-1,2-diamine and tris(2-methoxyethoxy)(vinyl)silane were acquired from Sigma-Aldrich and used as received. Poly(acrylic acid) and polyacrylamide were acquired from Acros Organics. N,N'-methylenebisacrylamide was acquired from Invitrogen. All others reagents and solvents are analytical grade and were used as received. All water was deionized by using an Elga UHQ deionizer.

3.2. Materials

Copper/(carbon films) TEM (transmission electron microscopy) grids (circular, diameter = 3 mm, 400 mesh) were acquired from Ted Pella. Glass electrodes covered with indium tin oxide thin films (ITOs, resistivity 15–25 Ω cm^{-1}) were acquired from Ossila. They were cut, washed with water, sonicated in propanone for 5 min, sonicated in ethanol for 5 min, sonicated in water for 5 min, washed with water and dried with N_2 flow. Glassy carbon electrodes (GCEs) with diameter = 3 mm (area = 7.07 mm^2) with polytetrafluoroethene bodies were acquired from BASi and CHI. Prior to use the GCEs were polished with a politrix, with suspensions of 1000 nm size, 500 nm size and 300 nm size of alumina nanoparticles. The electrodes were immersed in $HCl_{(conc)}$:H_2O 1:1 (v/v), washed with water, immersed in HNO_3:H_2O 1:1 (v/v), washed with water and, when necessary, electrochemically cycled in $H_2SO_{4(aq)}$ 1 mol L^{-1} between −1.2 V and +400 mV (versus Ag/AgCl/$KCl_{(sat)}$) at 50 mV s^{-1} for 20 cycles. The Pt plates used as counter electrodes were acquired from Impalla Metals and weld to Pt wires. As reference electrodes were used homemade Ag/AgCl/$KCl_{(sat)}$ and commercial Ag/AgCl/$KCl_{(3\ mol\ L-1)}$ electrodes, acquired from BASi. The electric potentials hereafter refer to Ag/AgCl/$KCl_{(sat)}$ reference electrode, except when mentioned that they refer to Ag/AgCl/$KCl_{(3\ mol\ L-1)}$ or to other electrodes, and except for the zeta potentials, that always refer to the vacuum.

3.3. Instrumentation

The electrochemical experiments were performed with the bipotentiostat PGSTAT 302N and with the multipotentiostat M101 from Metrohm Autolab, controlled by the softwares NOVA 1.8, NOVA 1.10, NOVA 1.11 and NOVA 2.1 from Metrohm Autolab. The Raman microscopies were performed with a Renishaw inVia Raman microscope with a Renishaw red laser of 636 nm wavelength at the Laboratory of Molecular Spectroscopy of the Institute of Chemistry of University of São Paulo. The UV-Vis-NIRs (ultraviolet-visible-near infrared spectrophotometries) were performed in a HP HP8453 spectrophotometer with optical cuvettes of quartz and plastic. The scanning electron microscopy images were acquired with a JEOL FESEM JSM-7401F microscope and with a JEOL NeoScope JCM-5000 microscope. The TEM were performed with a JEOL JEM-2100 microscope (potential difference of acceleration = 200 kV, LaB_6 filament) coupled with a silicon drift-type X-MaxN 80T EDS (energy dispersive X ray fluorescence spectrometer) from Oxford Instruments, controlled by software AZtec INCA, and with a JEOL JEM-3010 (potential difference of acceleration = 300 kV). A Karl-Fisher 831 coulometer from Metrohm Autolab was used to measure water fractions in the samples. Gel permeation chromatographies were performed in a Viscotek VE2001 gel permeation chromatographer at the Laboratory of Polymeric Biomaterials. The photochemical syntheses were performed in an ICH2 ultraviolet chamber from Luzchem, with 360 nm wavelength emission ultraviolet lamps, at the Laboratory of Polymeric Biomaterials. The sonochemical syntheses were performed in a Vibracells Sonics ultrasound chamber with 20 kHz vibration frequency. The ultrasound cleanings were performed in an Unique

USC1400 ultrasound bath. The spectroelectrochemical experiments were performed with a monochromatic system from LEDLite, with an electric source optical fiber and photomultiplier from WPI. The system was coupled to a potentiostat to acquire and synchronize data with electrochemical data. The particles analyses were performed in a Malvern Zetasizer Nano ZS90 equipment.

3.4. Experimental methods

Unless stated otherwise:

i: all experiments were performed at ambient pressure (ca. 100 kPa) and ambient temperature (ca. 25 ºC (298 K)) in open atmosphere.

ii: all samples were stored at ambient pressure and temperature in closed vessel, in the dark, when not in use.

iii: all electrochemical experiments were performed in 3-electrode conventional cells with Pt as counter electrode, $Ag/AgCl/KCl_{(sat)}$ as reference electrode and dyhydrogenphosphate/hydrogenphosphate buffer 20 mmol L^{-1} pH = 7.4 + NaCl 100 mmol L^{-1} as electrolyte.

iv: all electrochemical experiments dependent on dissolved oxygen, like measurements of current in common electrodes, were made after deoxygenating the electrolyte by bubbling dry N_2 in the solution for at least 15 min and keeping a N_2 atmosphere over the electrolyte throughout the experiments. In the experiments described in this Thesis this procedure was enough to prevent O_2 from interfering in the results.

3.4.1. Syntheses of hybrids of metal nanoparticles and PEDOTs

3.4.1.1. Syntheses of EDOT-derived hybrids

The hybrid NPsAu@PEDOT/PSS shall hereafter be called simply NPsAu@PEDOT. The reaction of synthesis of NPsAu@PEDOT was performed as follows: in a reaction vessel, under vigorous magnetic stirring (1800 rpm) and in closed vessel, were added slowly, in this order: H_2O, NaPSS; EDOT; $HAuCl_{4(aq)}$ 10 mmol L^{-1}. The amounts of reagents were varied. The optimized analytical molar concentrations of the reagents are (in 10,26 mL of H_2O): [NaPSS] = $1.39x10^{-6}$ mol L^{-1}, [EDOT] = $8.9x10^{-3}$ mol L^{-1} and [$HAuCl_4$] = $2.4x10^{-4}$ mol L^{-1}. The optimized theoretical molar concentration of 4-styrenesulfonate monomeric units is thus $4.8x10^{-4}$ mol L^{-1}. The limiting reagent is $HAuCl_4$. PEDOT in the flask can be further oxidized to the positively-charged state, which consumes more H_2PtCl_6.

The syntheses were also performed in cuvettes to follow the reactions with UV-Vis-NIR (ultraviolet-visible-near infrared spectrophotometry). For this, 20% of all reagents were taken (ca. 2 mL total volume). The spectra of water and of the mixture (H_2O + NaPSS + EDOT) were acquired and the syntheses were timed. Spectra were acquired throughout the reaction.

The hybrid NPsPt/PEDOT/PSS shall hereafter be called simply NPsPt/PEDOT (NPsPt are platinum nanoparticles). Hybrids of Pt nanoparticles and PEDOT polymer were also synthesized by one-pot radical oxidative chemical syntheses in aqueous

suspension. The reaction is equivalent to $HAuCl_4$ + EDOT + NaPSS reaction, substituting $HAuCl_4$ by H_2PtCl_6.

In detail: in a reaction vessel, under vigorous magnetic stirring (1800 rpm) and in closed vessel, were added slowly, in this order: H_2O; NaPSS; EDOT; $H_2PtCl_{6(aq)}$ 10 mmol L^{-1}. The amounts of reagents were varied. The optimized analytical concentrations of the reagents are (in 10,26 mL of H_2O): [NaPSS] = $1.39x10^{-6}$ mol L^{-1}, [EDOT] = $8.9x10^{-3}$ mol L^{-1} and [H_2PtCl_6] = $2.4x10^{-4}$ mol L^{-1}. The optimized theoretical molar concentration of 4-styrenesulfonate monomeric units is thus $4.8x10^{-4}$ mol L^{-1}. The limiting reagent is H_2PtCl_6. PEDOT in the flask can be further oxidized to the positively-charged state, which consumes more H_2PtCl_6.

The syntheses were also performed in cuvettes to follow the reactions with UV-Vis-NIR. For this, 20% of all reagents were taken (ca. 2 mL total volume), the syntheses were timed, and spectra of water and of the mixture (H_2O + NaPSS + EDOT) were acquired. Spectra were acquired throughout the reaction.

3.4.1.2. Syntheses of lactic acid-derived hybrids

The hybrid NPsAu/o-EDOT-PLA/PSS shall hereafter be called simply NPsAu/o-EDOT-PLA (o- are oligomers of). The hybrid NPsAu/PEDOT-PLA/PSS shall hereafter be called simply NPsAu/PEDOT-PLA.

EDOT-PLA (3,4-ethylenedioxythiophene-poly(lactic acid) is a new molecule derived from EDOT. It is EDOT with a lateral chain of poly(lactic acid) attached to the carbon of oxyethylene ring [87], [88]. PLA is formed from a racemic mixture of lactic acid, a chiral compound. Its synthesis was described in an article from the literature [88]. EDOT-PLA is a macromonomer and was synthesized through a reaction between δ-hydroxymethyl-EDOT (EDOT-CH_2-OH) and 3,6-dimethyl-1,4-dioxane-2,5-dione (a lactide). 3,6-dimethyl-1,4-dioxane-2,5-dione (2.76 g = 20 mmol), δ-hydroxymethyl EDOT (100 mg = 0.6 mmol) and Sn(II)-2-ethylhexanoate (0.016 mL = 0.05 mmol) were stirred at 110°C (383 K) with 7 mL of toluene for 24 hours. The solvent was removed by distillation under reduced pressure (2000 Pa, 60 °C (333 K)). The obtained solid product was purified by recrystallization with a (1:4) hexane/methanol mixture, separated by decantation and vacuum dried until constant mass. The yield obtained from this procedure was 98% [88]. The organic syntheses, the studies of biodegradation and chain lengths of the lactic acid-derived polymers were performed by Aruã Clayton da Silva in our Laboratory. ^{1}H-nuclear magnetic resonance spectrometry and ^{13}C- nuclear magnetic resonance spectrometry experiments demonstrated that the purified product has the expected chemical structure (which is shown in **Chapter 4, Results and Discussion**). Gel Permeation Chromatograph indicated average molecular mass =

3779 u and a polydispersity index of 1.46 (24.82 average units of -$C_6H_8O_4$- per molecule of EDOT-PLA). These experiments were performed by Aruã Silva at the Laboratory of Electroactive Materials.

PEDOT-PLA is the polymer of EDOT-PLA produced by radical oxidative polymerization of the thiophene ring. In PEDOT-PLA, as in PEDOT, the carbons vicinal to the sulfur are linked to the other monomeric units. One step of the strategy to synthesize PEDOT-PLA is the oxidation of EDOT-PLA by $HAuCl_4$, and was performed through the following procedure: in a reaction vessel under vigorous magnetic stirring (1800 rpm) and in closed vessel, were added slowly, in this order: ACN (acetonitrile); NaPSS; EDOT-PLA 169 g L^{-1}; $HAuCl_4$ 10 mmol L^{-1}. The optimized analytical concentrations (in 10,45 mL ACN) are: $c_{NaPSS} = 9.6x10^{-2}$ g L^{-1}, $c_{EDOT\text{-}PLA} = 3.2$ g L^{-1} and $[HAuCl_4] = 2.4x10^{-4}$ mol L^{-1} (c is the mass concentration). This step, at the same time, produces oligomers of EDOT-PLA and gold nanoparticles.

The following step is the oxidation of the oligomers of EDOT-PLA to longer chains of the PEDOT-PLA polymer. It was performed through the following procedure: 2 mL of the product of the previous step were added to an UV-Vis-NIR cuvette, under magnetic stirring (300 rpm) and in closed vessel. 20 µmol potassium peroxydisulfate were added (analytical molar concentration: [potassium peroxydisulfate] = $1.0x10^{-2}$ mol L^{-1}). The reagents and products were analyzed by UV-Vis-NIR spectrophotometry, which shows the absorption band in NIR due to longer polymer chains of PEDOT-PLA that are formed.

Scheme 1 summarizes the inorganic/organic hybrids synthesized in this work.

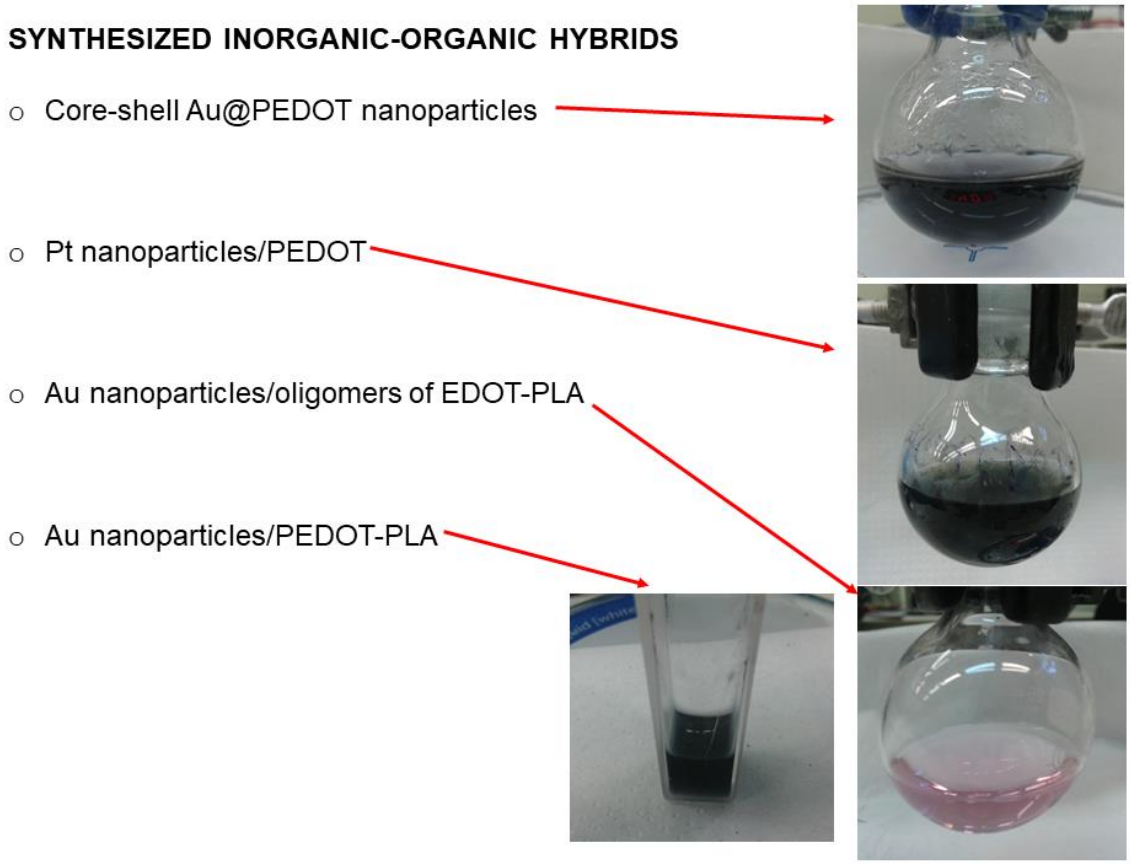

Scheme 1. Summary of the hybrids of noble metals nanoparticles and PEDOTs which were synthesized in this work, and the photographs of their reaction suspensions. NPsAu@PEDOT: core-shell Au@PEDOT nanoparticles synthesized from $HAuCl_4$, EDOT and NaPSS in water under stirring for hours. NPsPt/PEDOT: Pt nanoparticles and PEDOT synthesized from H_2PtCl_6, EDOT and NaPSS in water under stirring for days. NPsAu/o-EDOT-PLA: Au nanoparticles and oligomers of EDOT-PLA synthesized from $HAuCl_4$, EDOT-PLA and NaPSS in acetonitrile under stirring for days. NPsAu/PEDOT-PLA: Au nanoparticles and PEDOT-PLA synthesized through the oxidation of NPsAu/o-EDOT-PLA with potassium peroxydisulfate in acetonitrile under stirring for days.

3.4.2. Characterizations of hybrids

The hybrids of nanoparticles and conducting polymers described were characterized by:

Transmission electron microscopy: the nanoparticles suspensions were casted (ca. 2 µL) on TEM grids and let dry. The grids were analyzed in TEM coupled with EDS modules. EDS was performed in selected areas of the samples.

Scanning electron microscopy: the nanoparticles suspensions were casted (ca. 2 µL) on TEM grids and let dry. The grids were analyzed in SEM (scanning electron microscope) coupled with EDS modules. EDS was performed in selected areas of the samples.

Raman microscopy: samples of the nanoparticles suspensions were analyzed in a Raman microscope with a He/Ne laser of wavelength 636 nm, integration time of 10–100 s and 10% laser power. Commercial PEDOT/PSS suspensions were also analyzed. PEDOT/PSS shall hereafter be called PEDOT. The suspensions were diluted 100 x with their own solvents previous to the experiments. The suspensions were casted on glass slides and let dry at ambient temperature, or added to small flasks, and then analyzed.

UV-Vis-NIR spectrophotometry: UV-Vis-NIR spectra of the nanoparticles suspensions were acquired.

Dynamic light scattering: the nanoparticles suspensions were analyzed through dynamic light scattering to investigate the size and zeta potentials of the nanoparticles.

3.4.3. Syntheses of hydrogels

3.4.3.1. Hydrogels of PAA

PAA hydrogels were synthesized by 2 techniques i: uncatalyzed oxidative chemical synthesis and ii: catalyzed oxidative chemical synthesis. In technique i, N,N'-methylenebisacrylamide was used as cross-linker and potassium peroxydisulfate as initiator. Hydrogel precursor solutions with 2.5 mol L^{-1} acrylic acid (monomer), 12–250 µmol L^{-1} N,N'-methylenebisacrylamide (cross-linker) and 50 mmol L^{-1} potassium peroxydisulfate (initiator) were prepared. The reaction was performed at ambient temperature and at 80 ºC (353 K) until complete drying, since the reaction at ambient temperature is very slow. Potassium peroxydisulfate was added at last, just after neutralizing the pH of the mixture and deoxygenating it by bubbling dry N_2 for at least 15 min. The optimized analytical molar concentrations are: [AA] = 2.5 mol L^{-1}, [N,N'-methylenebisacrylamide] = 24 µmol L^{-1} and [potassium peroxydisulfate] = 50 mmol L^{-1}.

In technique ii precursor solutions contained 2.5 mol L^{-1} acrylic acid, 0.18–1.80 g L^{-1} PAA (polymer), 12–250 µmol L^{-1} N,N'-methylenebisacrylamide, 25 mmol L^{-1} N,N,N',N'-tetramethylethane-1,2-diamine (catalyzer) and 50 mmol L^{-1} potassium peroxydisulfate. In this technique the precursor solutions is let polymerize and dry at ambient temperature. Potassium peroxydisulfate is added at last, just after neutralizing the pH of the solution and deoxygenating it by bubbling dry N_2 for at least 15 min. The optimized analytical concentrations are [acrylic acid] = 2.5 mol L^{-1}, c_{PAA} = 1.80 g L^{-1},

[N,N’-methylenebisacrylamide] = 250 μmol L^{-1}, [N,N,N',N'-tetramethylethane-1,2-diamine] = 25 mmol L^{-1} and [potassium peroxydisulfate] = 50 mmol L^{-1}.

Cylindrical templates were used to shape the bulk hydrogels. The PAA hydrogels were also synthesized as films on ITOs through technique ii. For this purpose specific controlled areas were delimited on ITOs surface using inert, insulant coatings, and the precursor solutions were casted on ITOs (ca. 20 μL) and let dry at ambient temperature.

3.4.3.2. Hydrogels of PAAM

Hydrogels of PAAM (polyacrylamide) were synthesized as films over ITOs through technique iii: photochemical syntheses of ITOs/silane/f-h-PAAM (f- is a film of; h- is hydrogel of). In detail: ITOs were first submitted to a silanization process in the surface. For this N_2 was bubbled in toluene for at least 15 min. Then N_2 atmosphere was kept over toluene, and was added 5% (v/v) tris-(2-methoxyethoxy)(vinyl)silane. ITOs were immersed in the solution for 10 min, removed and dried at 100 ºC (373 K) for 2 h to drive the silanization reaction. The surface of ITOs was delimited with insulant coatings. Precursor solutions containing 0.679–2.5 mol L^{-1} acrylamide (monomer), 0.18–1.8 g L^{-1} PAAM (polymer), 12–250 mmol L^{-1} N,N'-methylenebisacrylamide, 12–32 mmol L^{-1} N,N,N',N'-tetramethylethane-1,2-diamine, 17 mmol L^{-1} 2,2-diethoxyacetophenone, the photoinitiator) and 50 mmol L^{-1} potassium peroxydisulfate were casted over ITOs/silane (ca. 20 µL). They were irradiated with ultraviolet radiation for 2 h. The optimized analytical concentrations are [acrylamide] = 0.679 mol L^{-1}, c_{PAAM} = 0.18 g L^{-1}, [N,N'-methylenebisacrylamide] = 21 mmol L^{-1}, [N,N,N',N'-tetramethylethane-1,2-diamine] = 32 mmol L^{-1}, [2,2-diethoxyacetophenone] = 17 mmol L^{-1} and [potassium peroxydisulfate] = 50 mmol L^{-1}. The silane molecule covalently bond to the surface of ITO and to the hydrogel network. **Equation 1** shows the reaction of modification of ITOs surface with tris-(2-methoxyethoxy)(vinyl)silane. ITO/$SiC_9H_{21}O_6$ and ITO/silane are interchangeable forms.

$$ITO + SiC_{11}H_{24}O_{6(toluene)} \rightarrow ITO/SiC_9H_{21}O_6$$

Equation 1. Non-stoichiometric reaction of silanization of ITOs surface with tris(2-methoxyethoxy)(vinyl)silane ($SiH_{24}C_{11}O_6$) in toluene. Only the species shown are considered. This reaction is the first step of the photopolymerization of films of hydrogels of polyacrylamide on ITOs surface. The reaction is performed bubbling N_2 in toluene for at least 15 min, keeping N_2 atmosphere over the toluene, adding 5% (v/v) tris-(2-methoxyethoxy)(vinyl)silane, immersing ITOs in the solution for 10 min, removing and drying them at 100 ºC (373 K) for 2 h.

After the syntheses the bulk hydrogels were stuck by Pt wires to make electric connection with the electrochemical systems (potentiostats) and, then, stored in air, in the dark, at 4 ºC (277 K) when not in use. The ITOs/hydrogels were stored in air, in the dark, at 4 ºC (277 K) when not in use.

3.4.4. Deposition of hybrids

3.4.4.1. Deposition of hybrids on ITOs

Electrodeposition: working electrode ITOs were immersed in the reaction suspensions (electrolytes). A potential of +1.15 V versus counter electrode ITOs was applied to the working electrode (the nanoparticles are negatively charged). The deposition times were varied. The modified ITOs were then washed with water to remove the excess material and stored in the dark when not in use. **Scheme 2** illustrates the electrodeposition.

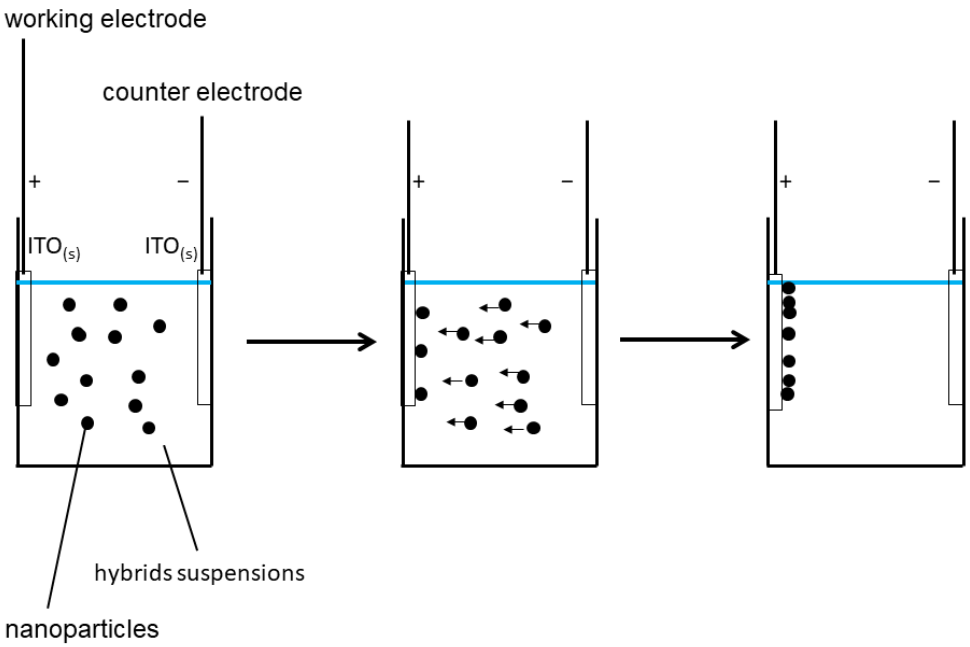

Scheme 2. Electrodeposition of the hybrids NPsAu@PEDOT and NPsPt/PEDOT on ITOs. Two ITOs are connected to the potentiostat through copper tapes and glimpses. The electrolyte is the reaction suspension of NPsAu@PEDOT or NPsPt/PEDOT. A constant electric potential difference is applied between the two ITOs for different times for the electrodeposition, being the working electrode positive relative to the counter electrode to promote the migration of the nanoparticles to the working electrode. NPsAu@PEDOT formed from $HAuCl_4$, EDOT and NaPSS in water, under stirring for hours. NPsPt/PEDOT formed from H_2PtCl_6, EDOT and NaPSS in water, under stirring for days.

3.4.4.2. Deposition of hybrids on GCEs

The deposition of NPsAu@PEDOT and NPsAu/PEDOT-PLA on GCEs was performed by casting. For it at first 1 mL of the reaction suspensions were centrifuged in *Eppendorfs* in an appropriate centrifuge at 13400 rpm for 30 min, in order to precipitate the nanoparticles. The supernatants were discharged, 1 mL dymethylsulfoxide was added to the *Eppendorfs* and the suspensions were sonicated in an ultrasound bath for the time necessary to resuspend the hybrids in dymethylsulfoxide. For the casting deposition 7 μL of the suspension in dymethylsulfoxide were added to the GCEs, which were taken to an oven at 40 ºC (313 K) in vacuum to dry the suspensions for at least 10 min. This procedure was repeated up to 10 x. The modified GCEs were then washed with water to remove the excess material and stored in air, in the dark, at 4 ºC when not in use. The procedure is illustrated in **Scheme 3**.

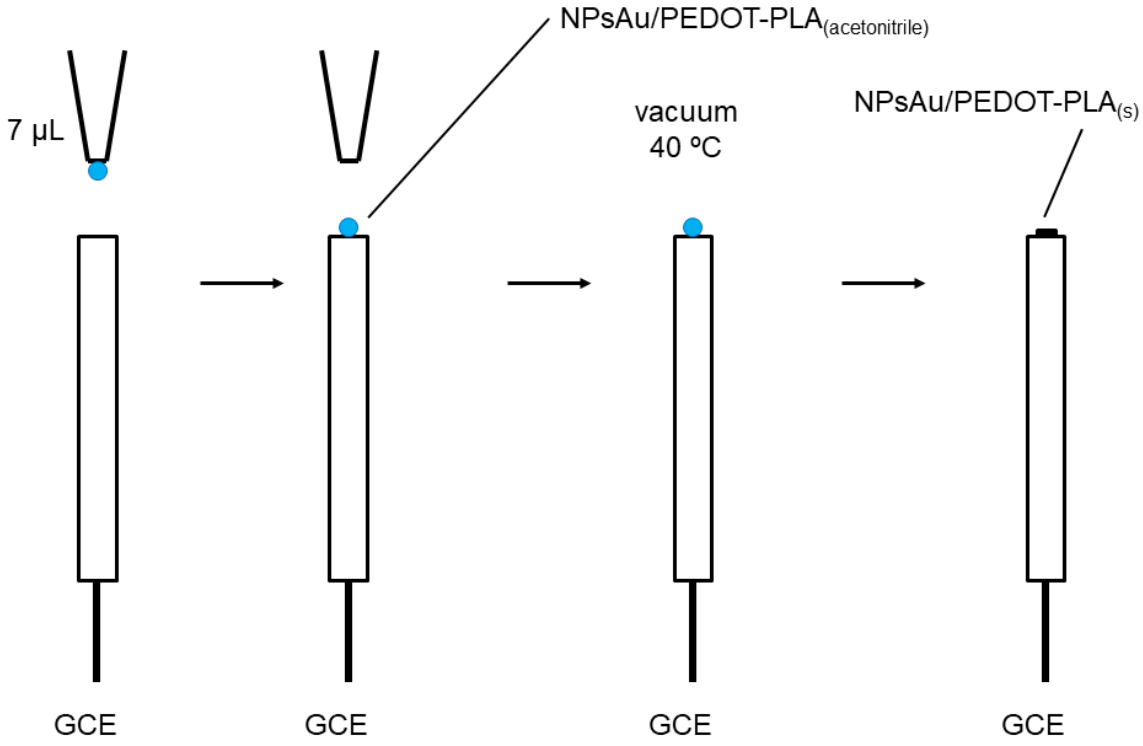

Scheme 3. Deposition of NPsAu/PEDOT-PLA on GCEs by casting. In each step of casting 7 µL of NPsAu/PEDOT-PLA are added to the electrodes, which are taken to an oven and let dry in vacuum at 40 ºC (313 K) for at least 10 min. Up to 10 steps of casting are done. The electrodes are then immersed in water to remove the excess material. NPsAu/PEDOT-PLA formed from the reaction suspension of NPsAu/o-EDOT-PLA and potassium peroxydisulfate in acetonitrile, under stirring for days. The reaction suspension of nanoparticles was centrifuged at 13400 rpm at 30 min. The supernatant was discarded, 1 mL of dymethylsulfoxide was added to the precipitate and NPsAu/PEDOT-PLA were resuspended in dymethylsulfoxide by ultrasonicating the mixture for the time necessary.

3.4.4.3. Insertion of hybrids in hydrogels

NPsAu@PEDOT were synthesized *in situ* in PAA hydrogels, through the following procedure: bulk PAA hydrogels were immersed in $HAuCl_{4(aq)}$ 1 mmol L^{-1} overnight, in the dark, at 4 ºC (277 K). They were removed and immersed in $8.9x10^{-3}$ mol L^{-1} EDOT 100 mg L^{-1} NaPSS in water for different times, in the dark, at 4 ºC (277 K). The hydrogels were washed with water and stored in water at the same temperature, in the dark, when not in use. The same procedure was applied to synthesize NPs *in situ* in ITOs/f-h-PAA and ITOs/f-h-PAAM hydrogels. The final step of the syntheses in ITOs/f-h-PAA and ITOs/f-h-PAAM, alternatively, was performed in cuvettes and followed through UV-Vis-NIR, at ambient temperature. **Scheme 4** illustrates this *in situ* formation.

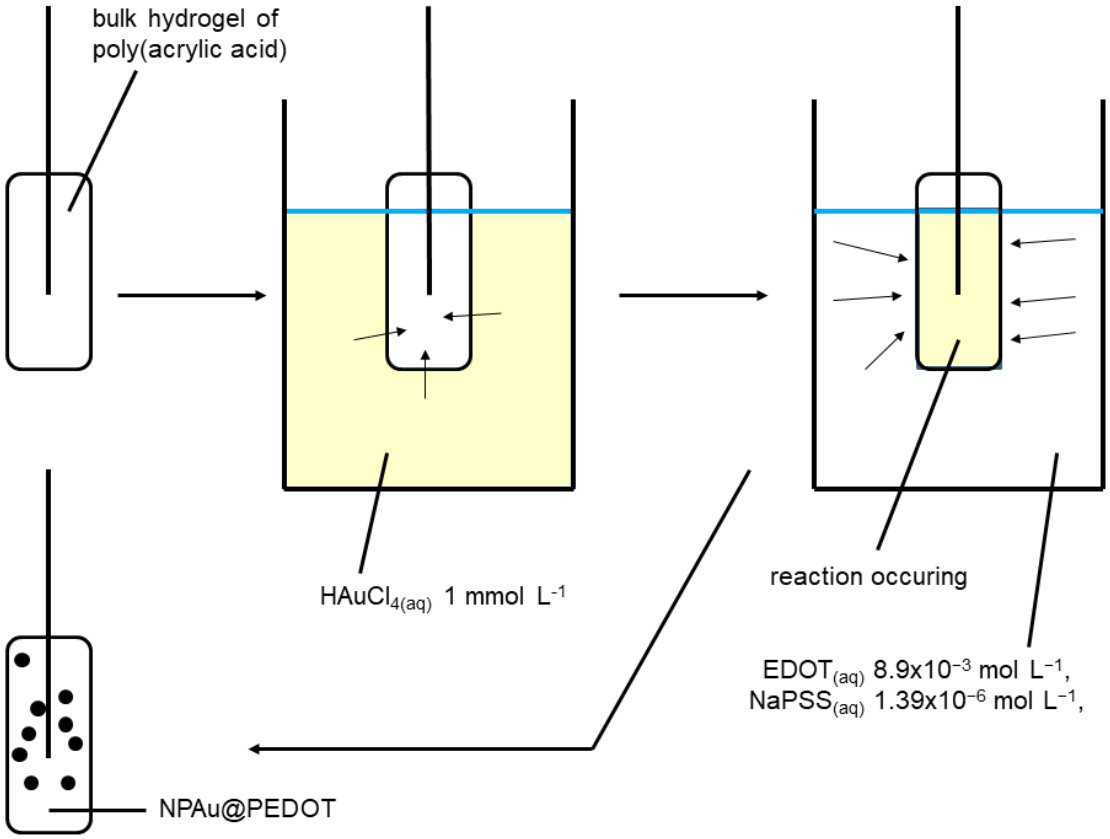

Scheme 4. *In situ* one-pot synthesis of NPsAu/PEDOT inside bulk hydrogels of poly(acrylic acid) stuck by Pt wires. The hydrogels are inserted in $HAuCl_4$, overnight, in the dark, at 4 ºC (277 K). Then, they are removed and inserted in EDOT and NaPSS. The bulk hydrogels of poly(acrylic acid) were synthesized through uncatalyzed or catalyzed chemical synthesis. Uncatalyzed synthesis: acrylic acid, N,N'-methylenebisacrylamide and potassium peroxydisulfate in water at 80 ºC (353 K). Catalyzed synthesis: acrylic acid, poly(acrylic acid), N,N'-methylenebisacrylamide, N,N,N',N'-tetramethylethane-1,2-diamine and potassium peroxydisulfate in water.

NPsAu@PEDOT were electroinserted in b-PAA (b- is bulk form of) and f-PAAM hydrogels through electroinsertion. For this the hydrogels were immersed in the reaction suspensions of NPsAu@PEDOT (in the case of bulk hydrogels they were electrically connected to the potentiostat system through the Pt wires (as described previously). Then constant positive potentials versus ITOs counter electrodes were applied to the hydrogels to promote migration and insertion of the negatively charged nanoparticles. The potentials applied were +1.15 V and +2.3 V, and the times of electroinsertion were varied (nanoparticles are negatively charged). After this the hydrogels were immersed in water for 20 min, washed and stored in water at 4 ºC (277 K) when not in use. **Scheme 5** and **Scheme 6** illustrate the process of electroinsertion.

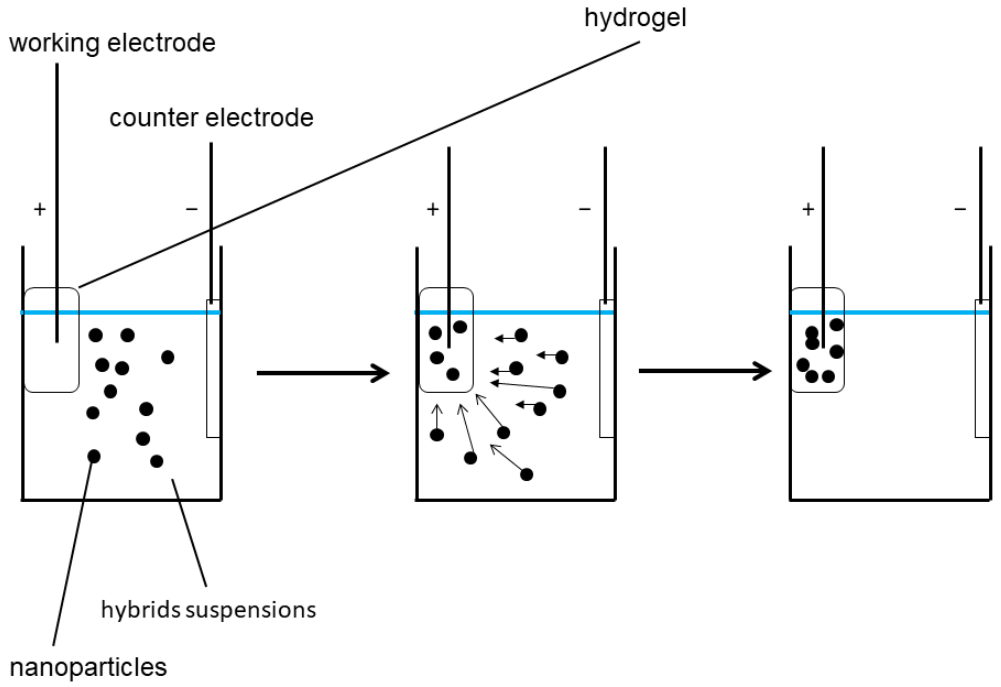

Scheme 5. Electroinsertion of NPsAu@PEDOT in bulk hydrogels of poly(acrylic acid). The hydrogel is the working electrode and an ITO is the counter electrode. The electrolyte is the reaction suspension of NPsAu@PEDOT or NPsPt/PEDOT. Constant electric potential differences are applied between the electrodes for different times, being the hydrogel positive relative to the ITO to promote the migration of nanoparticles to the hydrogel. The bulk hydrogels of poly(acrylic acid) were synthesized through uncatalyzed or catalyzed chemical synthesis. Uncatalyzed synthesis: acrylic acid N,N'-methylenebisacrylamide and potassium peroxydisulfate in water at 80 ºC (353 K). Catalyzed synthesis: acrylic acid, poly(acrylic acid), N,N'-methylenebisacrylamide, N,N,N',N'-tetramethylethane-1,2-diamine and potassium peroxydisulfate in water. NPsAu@PEDOT formed from $HAuCl_4$, EDOT and NaPSS in water, under stirring for hours. NPsPt/PEDOT formed from H_2PtCl_6, EDOT and NaPSS in water, under stirring for days.

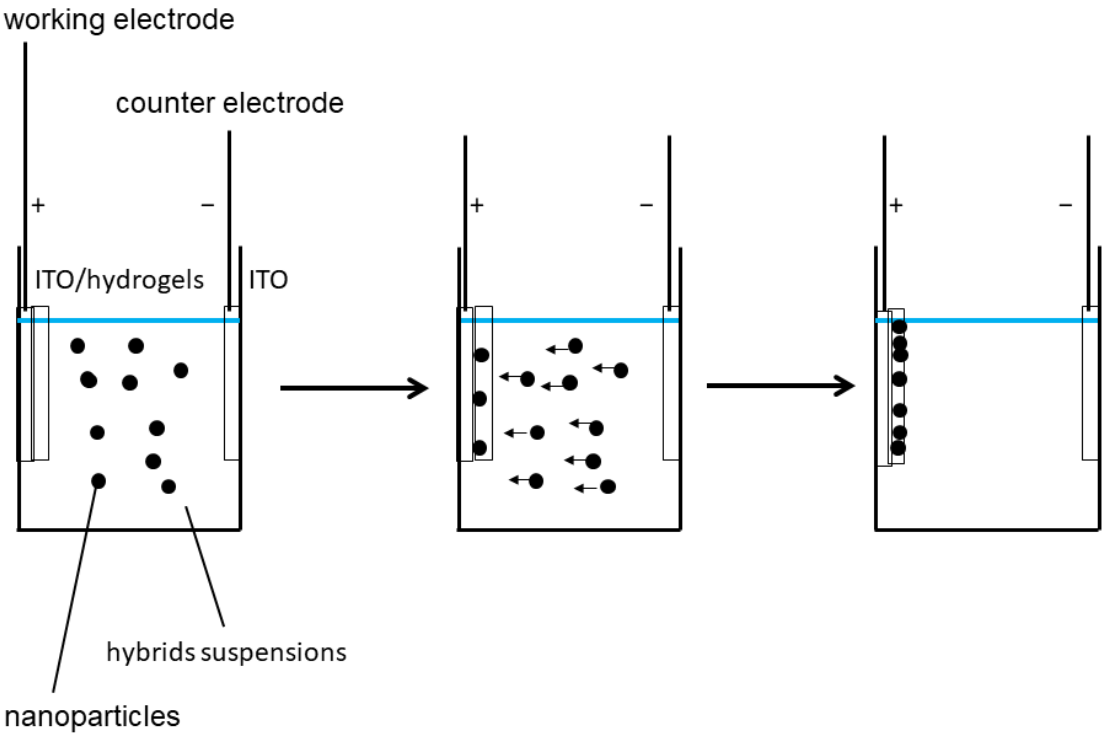

Scheme 6. Electroinsertion of NPsAu@PEDOT in films of hydrogels of polyacrylamide on ITOs. The hydrogel on ITO is the working electrode. The counter electrode is an ITO. The electrolyte is the reaction suspension of NPsAu@PEDOT. A constant electric potential difference is applied between the electrodes, being the working electrode positive relative to the counter electrode to promote the migration of nanoparticles to the hydrogel. The films of hydrogels of polyacrylamide were formed over ITOs silanized in the surface. ITOs were silanized with tris-(2-methoxyethoxy)(vinyl)silane in toluene at 100 ºC (373 K). Hydrogels of polyacrylamide were then formed from acrylamide, polyacrylamide, N,N'-methylenebisacrylamide and 2,2-diethoxyacetophenone in water over ITOs/silane, under ultraviolet radiation. NPsAu@PEDOT formed from $HAuCl_4$, EDOT and NaPSS in water, under stirring for hours. NPsPt/PEDOT formed from H_2PtCl_6, EDOT and NaPSS in water, under stirring for days.

Scheme 7 summarizes the experimental strategies adopted for the substrates and the immobilization techniques of inorganic/organic hybrids used in this work. These deposition techniques were subsequently tried in order to obtain stable films on the electrodes, then optimized.

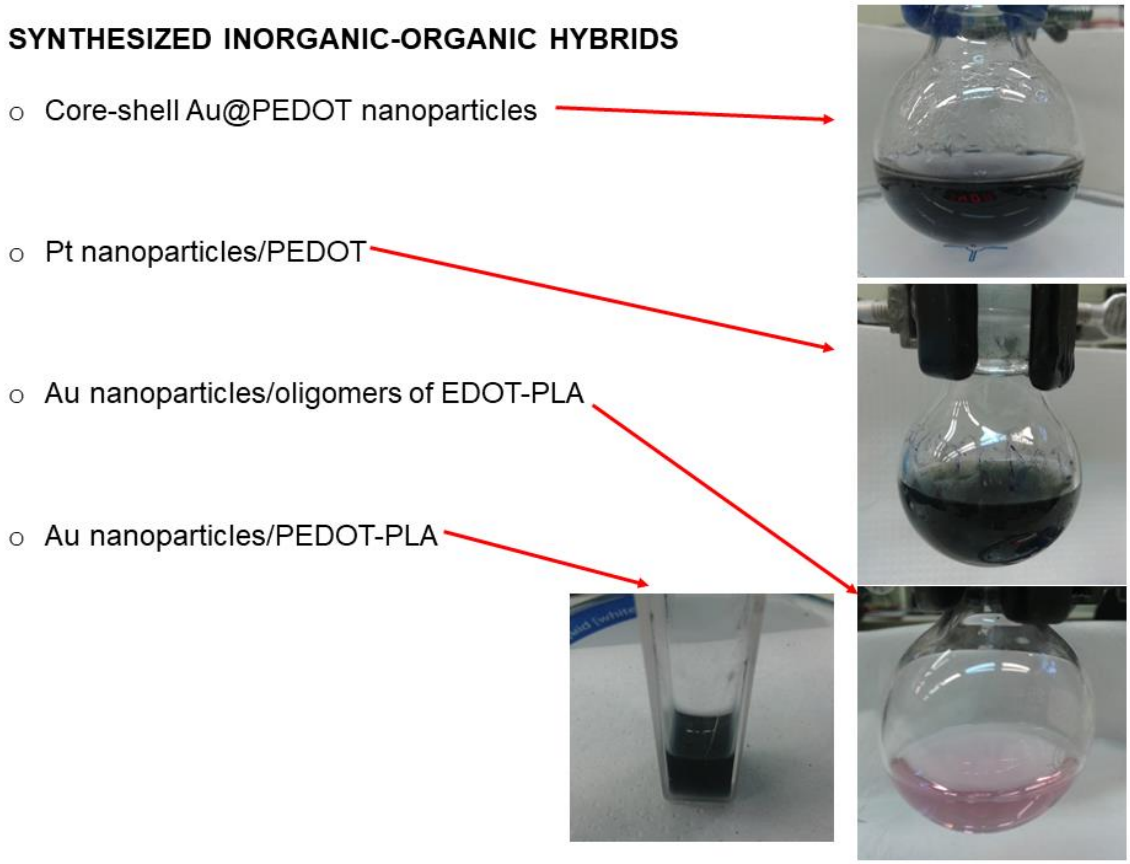

Scheme 7. Summary of strategies used to deposit hybrids of nanoparticles and PEDOTs on electrodes and photographs of these electrodes. Deposition methods: GCEs: casting. ITOs: electrodeposition at constant electric potential difference. Bulk hydrogels: *in situ* synthesis of nanoparticles; electroinsertion. Films of hydrogels on ITOs: electroinsertion.

3.4.5. Characterization of modified electrodes

The electrodes modified with inorganic/organic hybrids were characterized by the following techniques (electrochemical techniques are not cited here):

Scanning electron microscopy: modified ITOs were analyzed through SEM, as well as some modified GCEs electrodes. However, most GCEs do not fit the sample support of SEM. In the case of the modified hydrogels they were dried under vacuum to the dehydrated state previous to the microscopies.

Raman microscopy: modified GCEs were analyzed in the Raman microscope with a red, 636 nm laser, 10–100 s integration time and 10% laser power.

UV-Vis-NIR spectrophotometry: modified ITOs were analyzed through UV-Vis-NIR, positioning the ITOs parallel to the optical walls of the cuvettes and perpendicular to the optical path, which passed through ITOs surface. They were analyzed in air and also immersed in electrolyte, under severed applied potentials. For this, electrochemical cells were assembled in UV-Vis-NIR cuvettes.

3.4.6. Electrochemical experiments

The electrochemical experiments with ITOs were performed in UV-Vis-NIR cuvettes, assembled in a LEDLite light measurement system in the case of spectroelectrochemical experiments. Chronoamperometries with additions of $H_2O_{2(aq)}$, cyclic voltammetries and cyclic voltabsormetries were performed to study the systems. ITOs working electrodes were positioned parallel to the optical walls and perpendicular to the optical path, which passes through the electrode. The systems are illustrated in **Scheme 8**.

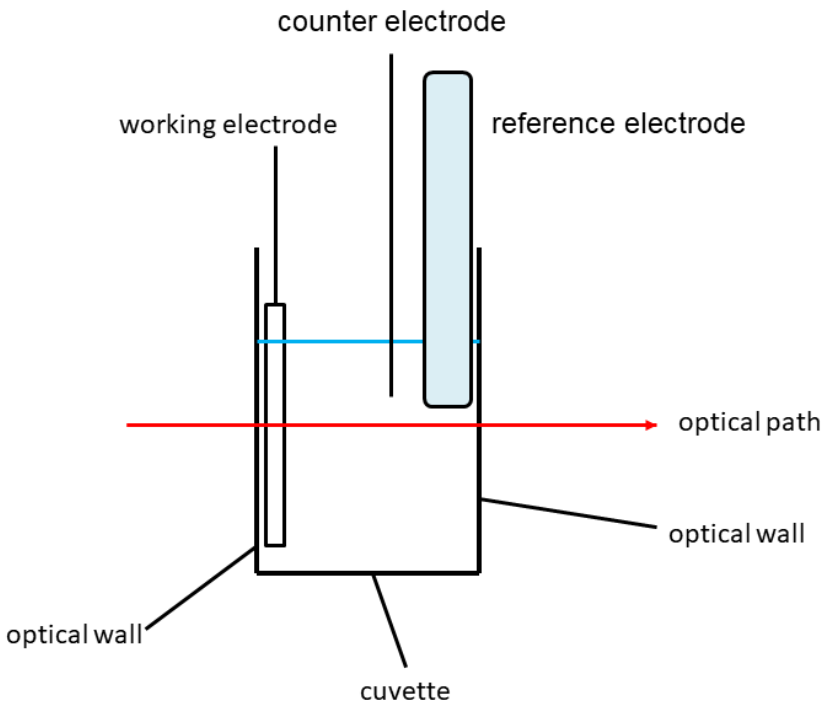

Scheme 8. Experimental design of spectroelectrochemical experiments with the modified ITOs. The experiments are performed in an UV-Vis-NIR cuvette with 1 cm optical path. The ITOs (working electrodes) are positioned at one optical wall, parallel to it, in the way of the optical path. The counter electrode and the reference electrode are positioned out of the optical path.

4. RESULTS AND DISCUSSION

4.1. Syntheses of hybrids of metal nanoparticles and PEDOTs

4.1.1. Au@PEDOT core-shell nanoparticles

In this work, as described in **Subsection 3.4.1**, bottom-up synthesis of noble metal nanoparticles were performed. In the synthesis of NPsAu@PEDOT, precursor $HAuCl_4$ is reduced through the half-reaction in **Equation 2**. E is electric potential. E^0 is standard reduction potential of reaction.

$$HAu^{III}Cl_{4(aq)} + 3e^- + H_2O_{(l)} \rightarrow Au^0_{(s)} + 4Cl^-_{(aq)} + H_3O^+_{(aq)} \qquad E^0 = +930 \text{ mV versus SHE}$$

Equation 2. Half-reaction of reduction of $HAu^{III}Cl_4$ to Au^0 in acidic medium. E^0 is the potential at the conditions: (*a* is thermodynamic activity) $a_{HAuCl4} = 1$, $a_{Cl-} = 1$ and $a_{H3O+} = 1$ (pH = 0). E is pH dependent: when pH increases, E increases. In this work this reaction is performed at non-buffered solution with pH ca. 4. SHE: standard hydrogen electrode.

Instead of a specie that acts only as reducer for $HAuCl_4$ for the Au nanoparticles, EDOT was used. EDOT polymerizes usually through an oxidative radical mechanism, in which the Cα-H bonds are broken and new intermonomer Cα-Cα bond are formed. EDOT is easily oxidized by Au(III) precursor, which presents a high E^0 to form Au^0. The new intermonomer bonds between EDOT molecules are head-to-head bonds. Each inner EDOT molecule in the chain donates 2 electrons and produces 2 H_3O^+ in the whole process. The polymer PEDOT is formed. The reaction $HAuCl_4$ + EDOT + NaPSS produces NPsAu and PEDOT in one step, and therefore is an one-pot reaction,

performed in aqueous solution. There is also the possibility of forming Au(I) species in solution. $HAuCl_4$ also partially oxidizes PEDOT, introducing positive charges in its polymer chain. PSS^- negative charge stabilizes PEDOT positive charges. Au@PEDOT core-shell nanoparticles are formed because of the high affinity of gold for sulfur. The synthesis is showed in **Equation 3**. **Scheme 9** shows the non-stoichiometric synthesis and **Scheme 10** shows the stoichiometric synthesis. For each mole of $HAuCl_4$ 1.5 moles of EDOT are necessary for the theoretical complete reaction. As described in **Subsection 3.4.1.1**, the optimized analytical molar concentrations found are: [NaPSS] = $1.39x10^{-6}$ mol L^{-1}, [EDOT] = $8.9x10^{-3}$ mol L^{-1} and [$HAuCl_4$] = $2.4x10^{-4}$ mol L^{-1}. The optimized theoretical molar concentration of 4-styrenesulfonate monomeric units is $5.3x10^{-4}$ mol L^{-1}. $HAuCl_4$ is the limiting reagent for the reaction, and thus it determines the amount of PEDOT that can be formed. This also implies that the polymer cannot be in excess to the gold nanoparticles in the product, and the layer cannot be too thick to block the surface of gold, which could decrease the conductivity of the material. However, as explained ahead, PEDOT formed in the flask bonds to gold and also limits the growth of gold nanoparticles. PEDOT can be and is in part further oxidized to positively-charged states, which consumes more $HAuCl_4$, since 1 $HAuC_4$ molecule is necessary to receive every 3 e^- from PEDOT.

$$EDOT_{(aq)} + HAuCl_{4(aq)} + NaPSS_{(aq)} \rightarrow NPsAu@PEDOT_{(aq)}$$

Equation 3. Non-stoichiometric EDOT + $HAuCl_4$ + NaPSS reaction in aqueous medium, forming core-shell NPsAu@PEDOT. NaPSS is omitted in the products, as adopted in this Thesis. The reaction is done adding, in this order, NaPSS, EDOT and $HAuCl_4$ in water and stirring for hours.

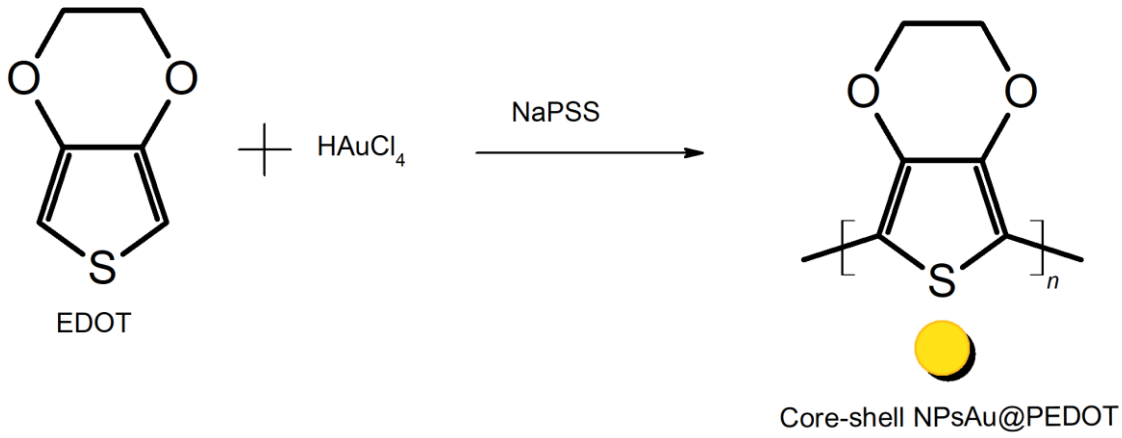

Scheme 9. Non-stoichiometric reaction EDOT + $HAuCl_4$ + NaPSS in aqueous medium, forming core-shell NPsAu@PEDOT. Only the species shown are considered. The Scheme does not imply a 1:1 proportion between gold nanoparticles and EDOT monomeric units in PEDOT. The reaction is done adding, in this order, NaPSS, EDOT and $HAuCl_4$ in water, and stirring for hours.

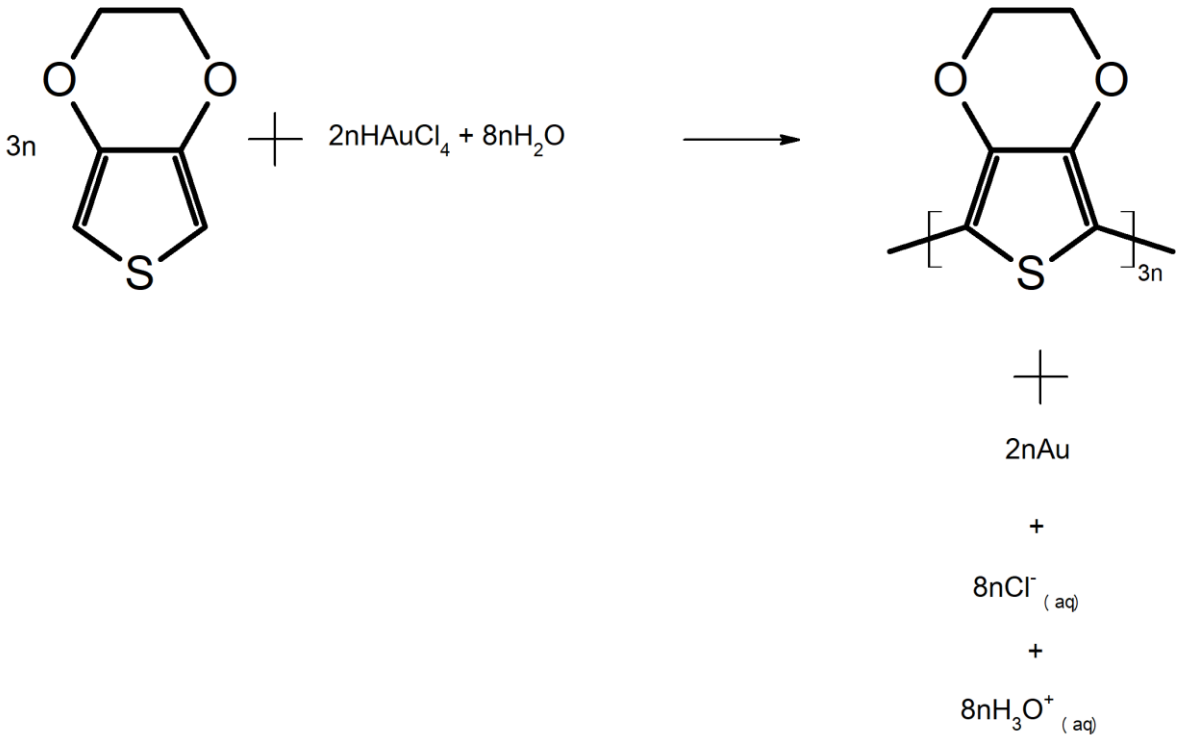

Scheme 10. Stoichiometric reaction EDOT + $HAuCl_4$ in acidic medium, forming core-shell NPsAu@PEDOT. Only the species shown are considered. $2nAu_{(NPs)}$ means 2n mols of atoms of Au in the form of nanoparticles, and not 2n nanoparticles of Au. The reaction is done adding, in this order, NaPSS, EDOT and $HAuCl_4$ in water, and stirring for hours.

After the addition of $HAuCl_4$ in the flask the reaction mixture changes from light yellow (color due to $HAuCl_4$) to light green, to light blue, to dark blue, in a few minutes. **Figure 1** presents a photograph of the product. The blue color is due to the oxidized PEDOT present, and it is so intense that it masks the characteristic pink color of Au nanoparticles, also present in the sample.

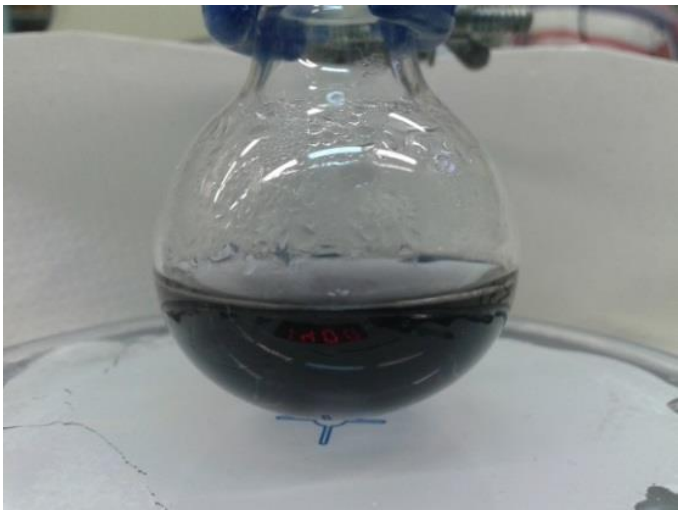

Figure 1. Photograph of NPsAu@PEDOT after 4 h of synthesis. The reaction is done adding, in this order, NaPSS, EDOT and $HAuCl_4$ in water, and stirring for hours.

UV-Vis-NIR was performed as the reaction proceeded. The spectra are shown in **Figure 2**. The bottom spectrum (black curve, solid line) belongs to the mixture previous to the addition of $HAuCl_4$, and the absorbance is practically null throughout the spectrum. The second bottom spectrum (red curve, dashed line) was taken 30 s after the addition and shows a peak in UV at ca. 307 nm due to $HAuCl_4$. As time flows the backgrounds grows a lot and the plasmonic band rises in green, changing its maximum from 532 nm to 548 nm. This redshift implies the growing of Au nanoparticles. The peak in 307 nm disappears and 2 large bands in NIR at 802 nm and 918 nm rise. These bands are due to PEDOT polymer, which greatly contributes to the dark aspect of the solution. In articles about PEDOT Garreau et al. [89]–[93] state that the occurrence of bands in the near infrared is due to PEDOT in the oxidized bipolaron state, but oxidized PEDOT has little absorption in the visible region. The 2 bands in NIR may be due to PEDOT of controlled chain sizes in the shells of core-shell nanoparticle. The spectra demonstrate the formation of the nanoparticles and of the polymer.

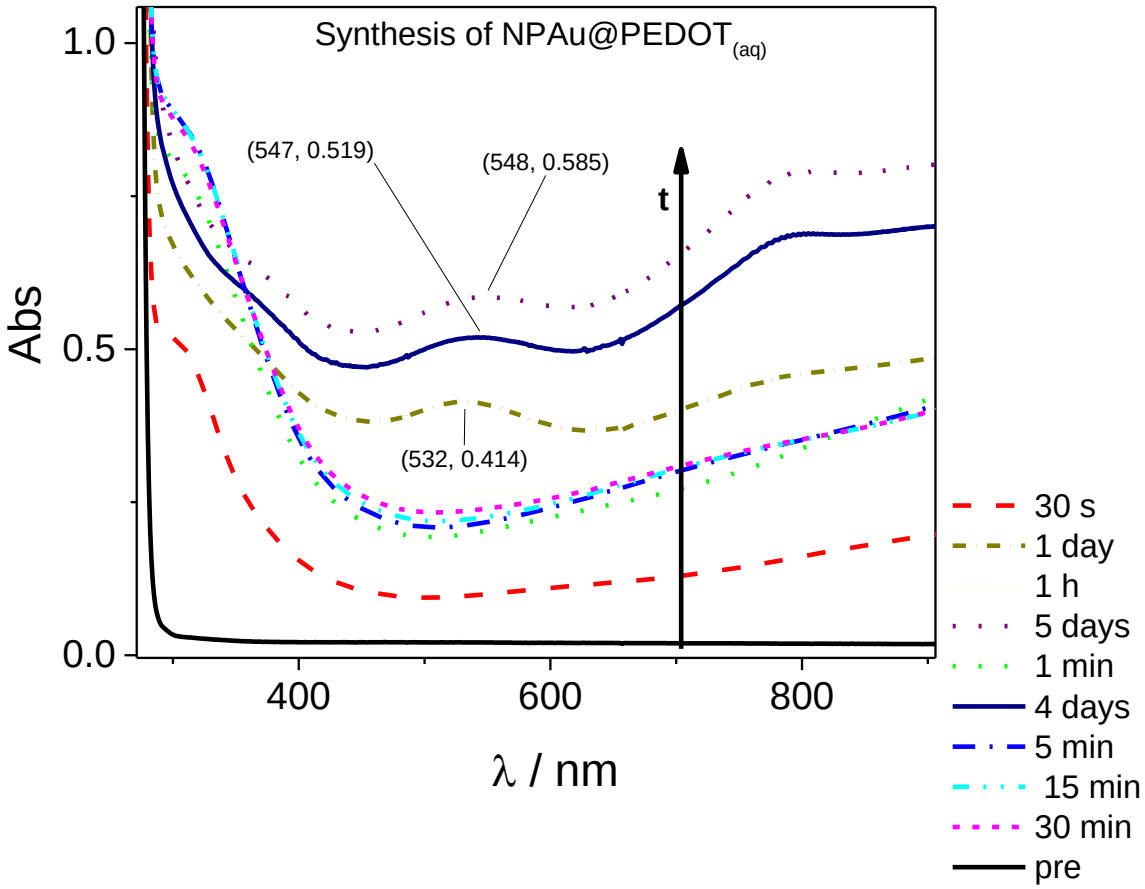

Figure 2. UV-Vis-NIR spectra acquired during the synthesis of NPsAu@PEDOT. Blank of UV-Vis-NIR: water. Bottom spectrum (black curve, solid line) acquired of the mixture of H_2O, NaPSS and EDOT, previous to the $HAuCl_4$ addition. The reaction is done adding, in this order, NaPSS, EDOT and H_2PtCl_6 in water, and stirring for days.

4.1.2. Pt/PEDOT hybrids

The reaction H_2PtCl_6 + EDOT + NaPSS was studied for the synthesis of NPsPt/PEDOT hybrids. Platinum is a noble metal of high interest in electrochemistry, and catalyzes many redox reactions. H_2PtCl_6 was used as platinum precursor, and another one-pot reaction with EDOT was planned. **Equation 4** is the half-reaction of reduction of H_2PtCl_6 and in **Equation 5** is the reaction of synthesis of NPsPt/PEDOT.

$$H_2Pt^{IV}Cl_{6(aq)} + 4e^- + 2H_2O_{(l)} \rightarrow Pt^0_{(s)} + 6Cl^-_{(aq)} + 2H_3O^+_{(aq)} \qquad E^0 = +1484 \text{ mV versus SHE}$$

Equation 4. Half-reaction of reduction of $H_2Pt^{IV}Cl_6$ to Pt^0 in acidic medium. E^0 is the potential at the conditions: $a_{H2PtCl6} = 1$, $a_{Cl-} = 1$, $a_{H3O+} = 1$ (pH = 0). E is pH-dependent: when pH increases, E increases. In this work this reaction was performed at non-buffered solution with pH ca. 4.

$$EDOT_{(aq)} + H_2PtCl_{6(aq)} + NaPSS_{(aq)} \rightarrow NPsPt/PEDOT_{(aq)}$$

Equation 5. Non-stoichiometric EDOT + H_2PtCl_6 + NaPSS reaction in aqueous medium. Only the species shown are considered. The reaction is done adding, in this order, NaPSS, EDOT and H_2PtCl_6 in water and stirring for days.

H_2PtCl_6 is reduced to Pt^0 and forms nanoparticles, while EDOT polymerizes, forming PEDOT. The non-stoichiometric reaction is shown in **Scheme 11** and the stoichiometric reaction is shown in **Scheme 12**. For each mole of H_2PtCl_6 2 moles of EDOT are necessary for the theoretical complete reaction. The optimized analytical molar concentrations of NaPSS and EDOT in the synthesis are [NaPSS] = 1.39×10^{-6} mol L^{-1}, [EDOT] = 8.9×10^{-3} mol L^{-1}, [H_2PtCl_6] = 2.4×10^{-4} mol L^{-1}. H_2PtCl_6 is the limiting reagent. PEDOT is in part further oxidized to positively-charged states, which consumes

more H_2PtCl_6. **Figure 3** shows a photograph of the product. The dark color of the solution is due to PEDOT.

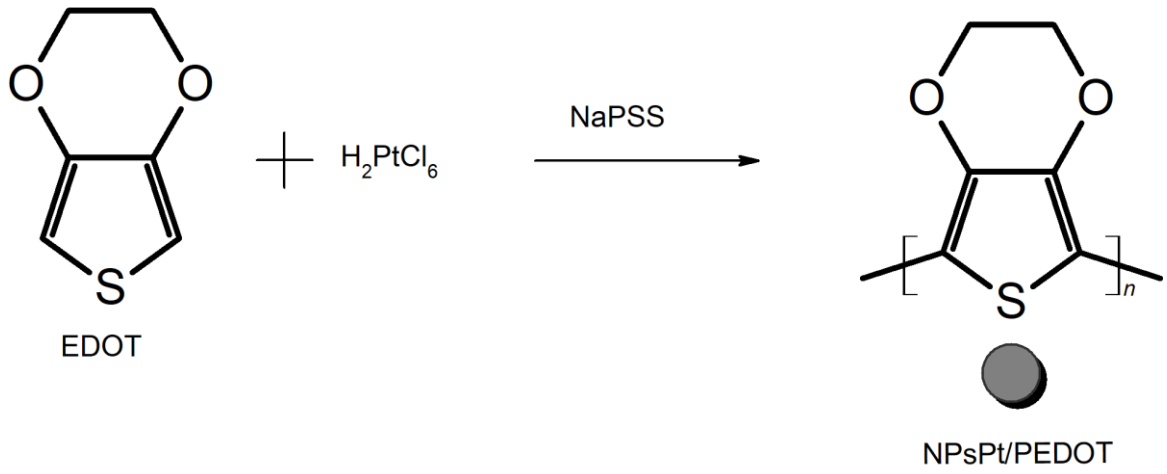

Scheme 11. Non-stoichiometric H_2PtCl_6 + EDOT + NaPSS reaction in aqueous medium forming NPsPt/PEDOT hybrid. Only the species shown are considered. The Scheme does not imply a 1:1 proportion between platinum nanoparticles and EDOT monomeric units in PEDOT. The reaction is done adding, in this order, NaPSS, EDOT and H_2PtCl_6 in water, and stirring for days.

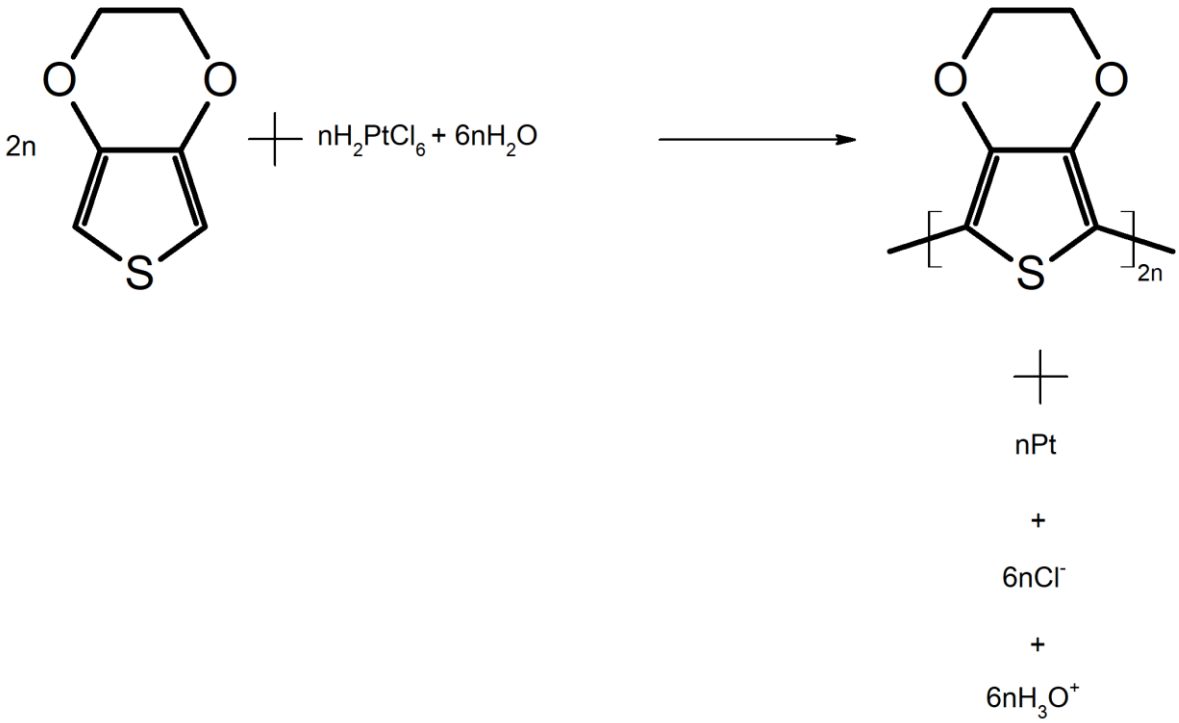

Scheme 12. Stoichiometric H_2PtCl_6 + EDOT reaction in acidic medium forming NPsPt/PEDOT hybrid. Only the species shown are considered. The reaction is done adding, in this order, NaPSS, EDOT and H_2PtCl_6 in water, and stirring for days.

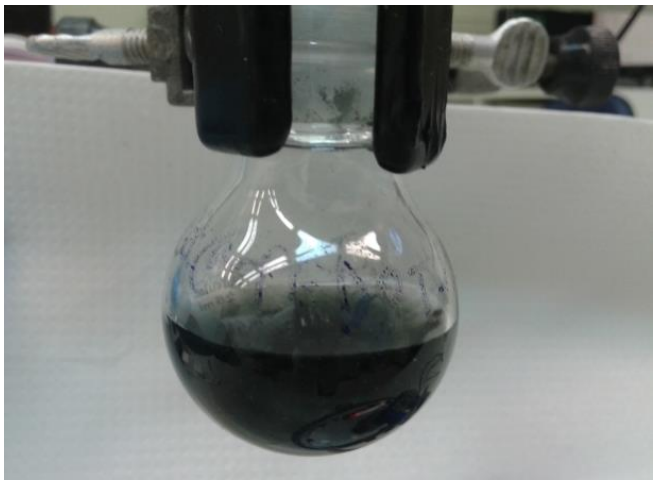

Figure 3. Photograph of NPsPt/PEDOT after 4 h of synthesis. The reaction is done adding, in this order, NaPSS, EDOT and H_2PtCl_6 in water, and stirring for days.

Figure 4 presents the UV-Vis-NIR spectra of the reaction suspension (up to 6 days of reaction). The bottom spectrum of **Figure 4** (black curve, solid line) is the spectrum previous to the addition of H_2PtCl_6, in which absorbance is practically null. The second bottom spectrum (red curve, dashed line) was taken ca. 30 s after the addition of H_2PtCl_6, and depicts a shoulder in UV at ca. 370 nm of H_2PtCl_6. After some hours the plasmonic band of NPsPt rises in green and changes its maximum from 516 nm to 526 nm. This redshift is due to the growing of Pt nanoparticles. The background increases and a broad band in NIR (maximum at ca. 850 nm) rises. This band is due to PEDOT. The inexistence of well-defined bands in NIR may indicate that these bands are due to confined and size-controlled PEDOT in core-shell nanoparticles, which is not the case for the hybrid NPsPt/PEDOT.

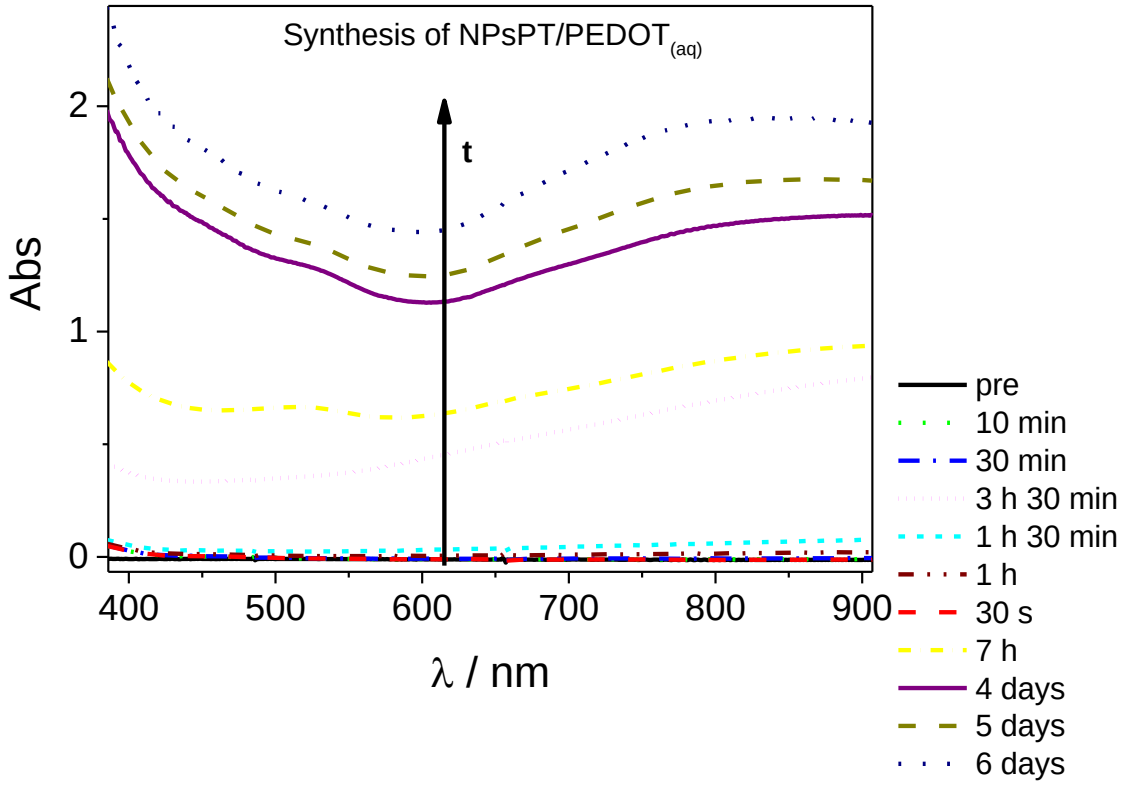

Figure 4. UV-Vis-NIR spectra acquired during the synthesis of NPsPt/PEDOT. Blank of UV-Vis-NIR: water. Bottom spectrum (black curve, solid line) of mixture of H_2O, EDOT and NaPSS, previous to the H_2PtCl_6 addition. The reaction is done adding, in this order, NaPSS, EDOT and H_2PtCl_6 in water, and stirring for days.

4.1.3. Lactic acid-derived hybrids

Novel hybrids of gold nanoparticles with polymers derived from EDOT-PLA were also studied. EDOT-PLA is a macromonomer and new biodegradable molecule, which in this work is desirable to be polymerized in order to obtain an easy to process, conducting, and biodegradable electrode material. This is very important to electrodes of wearable electrochemical sensors or sensors that are inserted in live organisms (*in vivo* sensors), a rising scientific field.

Although it is predicted to be oxidized in the same way EDOT does it is much more difficult to be oxidized than EDOT due to its huge molecular volume and steric hindrance caused by the PLA side chain. PLA itself is a biodegradable polymer extensively used in implants due to its compatibility with living organisms [94], [95], but has found little use in electrochemistry so far. **Scheme 13** shows the synthesis of EDOT-PLA. Sn(II) 2-ethylhexanoate is an organometallic compound that catalyzes the opening of the oxygenated ring of 3,6-dimethyl-1,4-dioxane-2,5-dione, which originates the carbonic chain of EDOT-PLA.

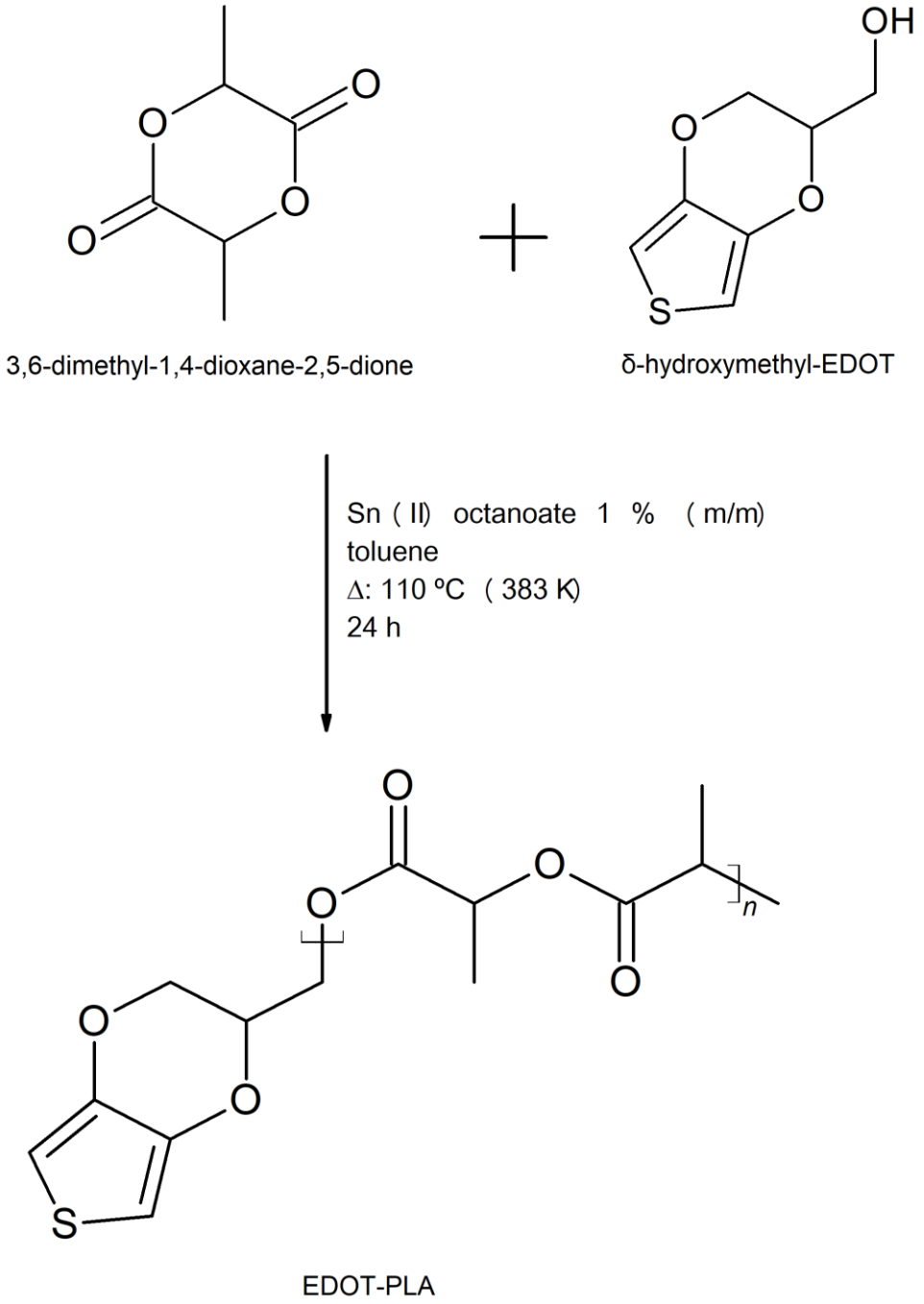

Scheme 13. Non-stoichiometric 3,6-dimethyl-1,4-dioxane-2,5-dione + EDOT-CH_2-OH reaction in toluene forming EDOT-PLA. Only the species shown are considered. Sn(II) 2-ethylhexanoate is the catalyzer of the reaction, and toluene is toluene is the solvent. EDOT-CH_2-OH, 3,6-dimethyl-1,4-dioxane-2,5-dione and Sn(II) 2-ethylhexanoate are heated to 110 ºC (383 K), under reflux, for 24 h.

EDOT-PLA is insoluble in water, and therefore the reactions were performed in organic solvent, and acetonitrile was chosen. The one-pot reaction HAuCl4 + EDOT-PLA + NaPSS forms at the same time: gold nanoparticles; oligomers of EDOT-PLA with intermonomer Cα-Cα bonds, in head-to-head, head-to-tail or tail-to-tail configurations. There is also the possibility of forming Au(I) species in solution. The gold nanoparticles interact with the polymer through the sulfur atoms. The synthesis is described in **Equation 6** and illustrated in **Scheme 14**. Each mole of $HAuCl_4$ requires 1.5 moles of EDOT-PLA to the theoretical complete reaction to neutral o-EDOT-PLA. The optimized analytical concentrations are [NaPSS] = $1.4x10^{-6}$ mol L^{-1}, [$HAuCl_4$] = $2.4x10^{-4}$ mol L^{-1}, $c_{EDOT\text{-}PLA}$ = 3.2 g L^{-1}. Based on the average molecular mass of EDOT-PLA it is calculated that, for the optimized analytical concentrations, $HAuCl_4$ is the limiting reagent. o-EDOT-PLA formed can be further oxidized to positively-charged states, which consumes more $HAuCl_4$. The product, NPsAu/o-EDOT-PLA, is presented in **Figure 5**. The light pink color is due to the Au nanoparticles.

$$\text{3,6-dimethyl-1,4-dioxane-2,5-dione}_{(\text{toluene})} + \text{EDOT-CH}_2\text{-OH}_{(\text{toluene})} \rightarrow \text{EDOT-PLA}_{(\text{toluene})}$$

Equation 6. Non-stoichiometric 3,6-dimethyl-1,4-dioxane-2,5-dione + EDOT-CH_2-OH reaction in toluene forming EDOT-PLA. Only the species shown are considered. The reaction is done with toluene, EDOT-CH_2-OH, 3,6-dimethyl-1,4-dioxane-2,5-dione and Sn(II) 2-ethylhexanoate at 110 ºC (383 K), under reflux, for 24 h.

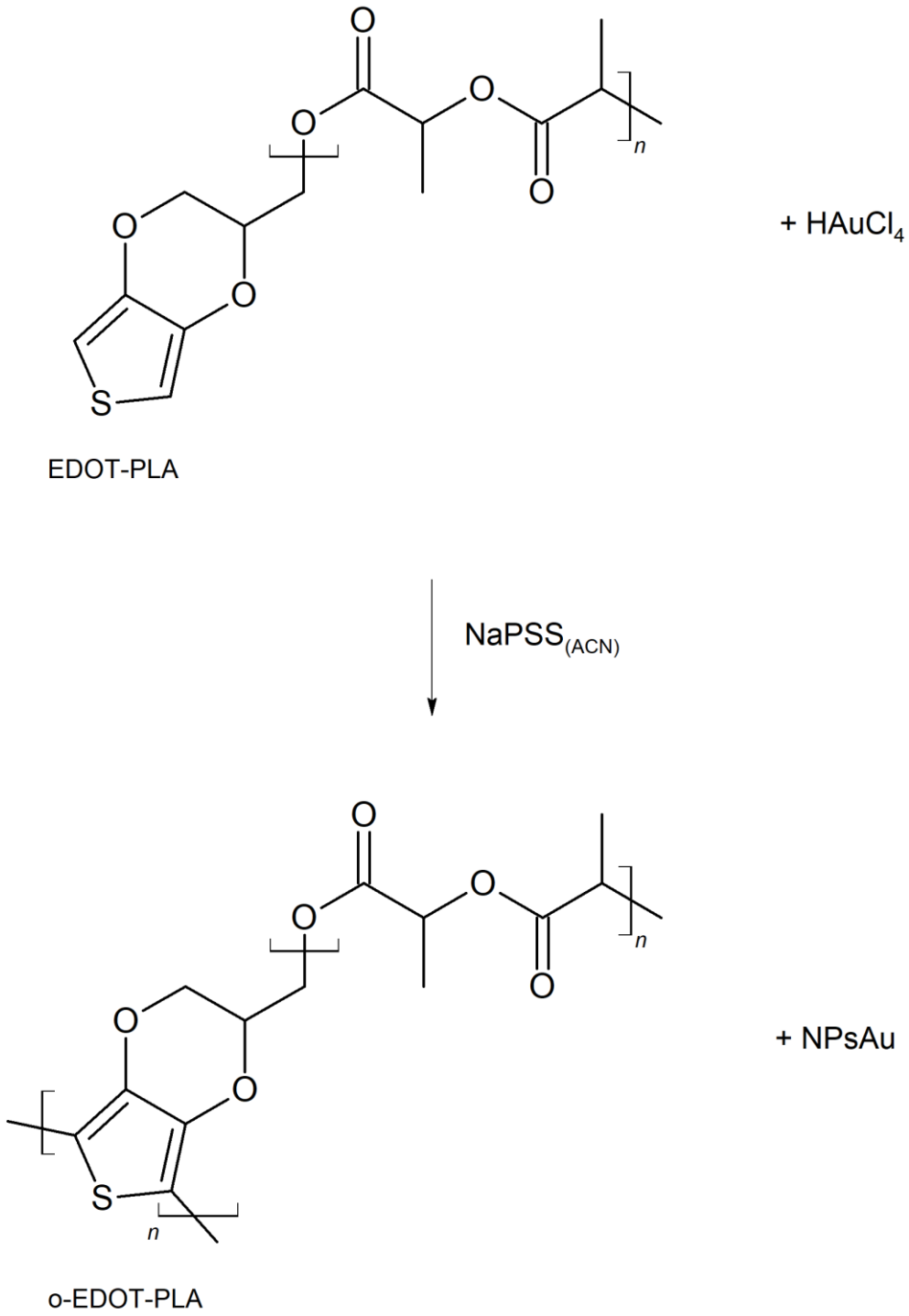

Scheme 14. Non-stoichiometric reaction EDOT-PLA + $HAuCl_4$ in acetonitrile forming NPsAu and oligomers of EDOT-PLA hybrid. NaPSS is omitted in the products, as adopted in this Thesis. Only the species shown are considered. Only the neutral states of EDOT-PLAs are considered (3,4-ethylenedioxythiophene-poly(lactic acid) and its derivatives). The reaction is done adding to acetonitrile, in this order, NaPSS, EDOT-PLA and $HAuCl_4$, and stirring for days.

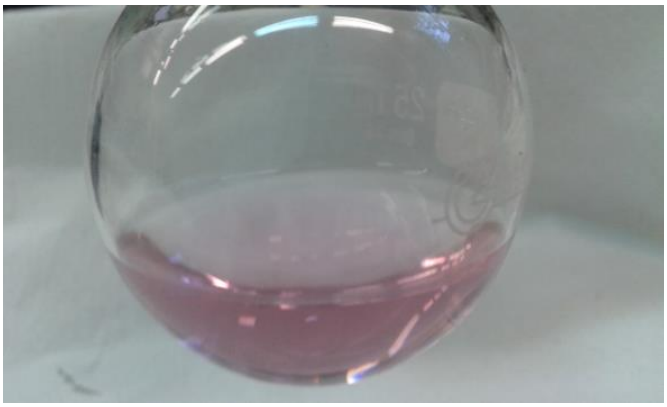

Figure 5. Photograph of NPsAu/o-EDOT-PLA after 4 h of synthesis. The reaction is done adding to acetonitrile, in this order, NaPSS, EDOT-PLA and $HAuCl_4$, and stirring for days.

Figure 6 presents the spectra taken during the reaction. The absorbance of (EDOT-PLA + NaPSS + ACN) mixture (black curve, solid line) is very low. It is observed that the plasmonic band of Au (green, 538 nm) rises as the reaction proceeds. There are only minor peaks in the near infrared, therefore, no PEDOTs polymers are present in the sample. Outside the selected range of this spectrum there is an ultraviolet peak of $HAuCl_4$ at 322 nm, which decreases with time. Oligomers of EDOT-PLA (o-EDOT-PLA) are formed in the oxidation of EDOT-PLA consuming $HAuCl_4$.

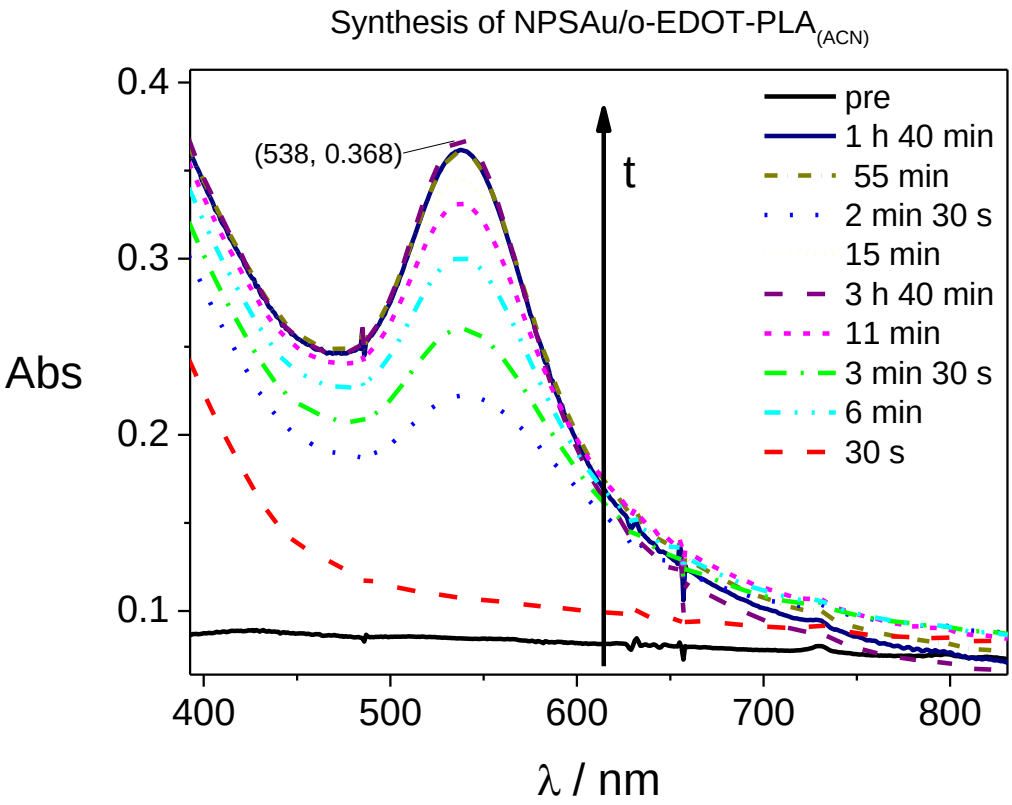

Figure 6. UV-Vis-NIR spectra acquired during the synthesis of NPsAu/o-EDOT-PLA in acetonitrile. Blank of UV-Vis-NIR: water. Bottom spectrum (black curve, solid line) of mixture of acetonitrile, NaPSS and EDOT-PLA, previous to the $HAuCl_4$ addition. The reaction is done adding to acetonitrile, in this order, NaPSS, EDOT-PLA and $HAuCl_4$, and stirring for days.

The oligomers of EDOT-PLA can theoretically be further polymerized to form the corresponding polymer through the reaction with an oxidizer. In this work potassium peroxydisulfate, a very strong oxidizer, was used for this purpose. The reaction NPsAu/o-EDOT-PLA + potassium peroxydisulfate was performed adding $1.0x10^{-2}$ mol L^{-1} potassium peroxydisulfate to the reaction suspension of NPsAu/o-EDOT-PLA, which darkens due to the formation of the polymer. **Figure 7** shows the suspension before and after the oxidation with potassium peroxydisulfate. PEDOT-PLA is formed in this step. **Equation 7** brings the half-reaction of reduction of potassium peroxydisulfate. **Equation 8** is the half-reaction of oxidation of Au^0 back to $HAu^{III}Cl_4$, which also occurs when potassium peroxydisulfate is added, as explained ahead. **Equation 9** is the complete reaction. Au^0 can also be oxidized to Au^{3+}, shown in **Equation 10** (oxidation half-reaction) and **Equation 11** (reduction half-reaction). **Equation 12** is the complete reaction with potassium peroxydisulfate.

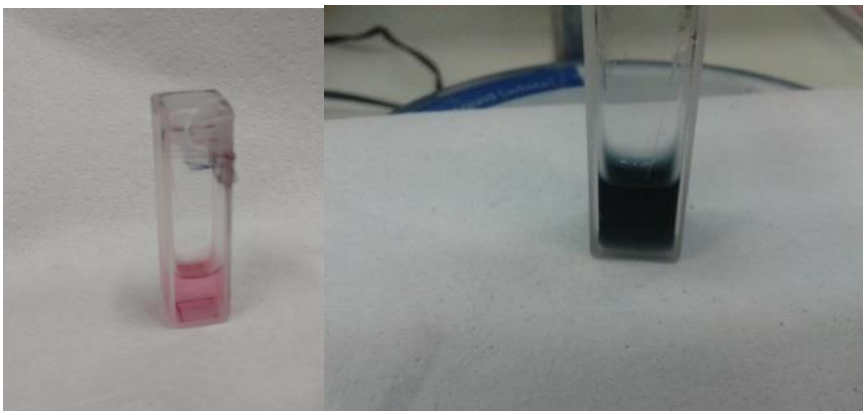

A **B**

Figure 7. **A**: photograph of NPsAu/o-EDOT-PLA after 4 h of synthesis. The reaction is done adding to acetonitrile, in this order, NaPSS, EDOT-PLA and $HAuCl_4$, and stirring for days. **B**: photograph of NPsAu/PEDOT-PLA after 4 days of synthesis. The reaction is done by adding potassium peroxydisulfate to the reaction suspension of NPsAu/o-EDOT-PLA, and stirring it for days.

$S_2O_8^{2-}{}_{(aq)} + 2e^- \rightarrow 2SO_4^{2-}{}_{(aq)}$ $E^0 = +2120$ mV versus SHE

Equation 7. Half-reaction of reduction of potassium peroxydisulfate to sulfate. E^0 is the potential at the conditions: $a_{S2O82-} = 1$, $a_{SO42-} = 1$.

$$Au^0{}_{(s)} + H_3O^+{}_{(aq)} + 4Cl^-{}_{(aq)} \rightarrow HAu^{III}Cl_{4(aq)} + H_2O_{(l)} + 3e^-$$

Equation 8. Half-reaction of oxidation of Au^0 to $HAu^{III}Cl_4$, the inverse half-reaction of **Equation 2**.

$$2Au^0{}_{(s)} + 2H_3O^+{}_{(aq)} + 8Cl^-{}_{(aq)} + 2S_2O_8^{2-}{}_{(aq)} \rightarrow 2HAu^{III}Cl_{4(aq)} + 2H_2O_{(l)} + 6SO_4^{2-}{}_{(aq)}$$
$$E^0 = +1190 \text{ mV versus SHE}$$

Equation 9. Reaction of oxidation of Au^0 to $HAu^{III}Cl_4$ by peroxydisulfate. E^0 is the potential at the conditions: $a_{H3O+} = 1$ (pH = 0), $a_{Cl-} = 1$, $a_{S2O82-} = 1$, $a_{HAuCl4} = 1$, $a_{SO42-} = 1$. E is pH-dependent: when pH is increased, E decreases. In this work this reaction was performed at non-buffered pH ca. 4.

$Au^{3+}{}_{(aq)} + 3\ e^- \rightarrow Au^0{}_{(s)}$ $E^0 = +1520$ mV versus SHE

Equation 10. Half-reaction of reduction of Au^{3+} to Au^0 in aqueous medium. E^0 is the potential at the conditions: $a_{Au3+} = 1$.

$$Au^0{}_{(s)} \rightarrow Au^{3+}{}_{(aq)} + 3\ e^-$$

Equation 11. Half-reaction of oxidation of Au^0 to Au^{3+} in aqueous medium. Inverse half-reaction of **Equation 10**.

$2Au^0{}_{(s)} + 3S_2O_8^{2-}{}_{(aq)} \rightarrow 2Au^{3+}{}_{(aq)} + 6SO_4^{2-}{}_{(aq)}$ $E^0 = +600$ mV versus SHE

Equation 12. Reaction of oxidation of Au^0 to Au^{3+} by potassium peroxydisulfate. E^0 is the potential at the conditions: $a_{S2O82-} = 1$, $a_{Au3+} = 1$, $a_{SO42-} = 1$.

4.2. Characterization of hybrids

4.2.1. DLS and TEM results

The synthesized hybrids or Au and Pt nanoparticles were analyzed by transmission electron microscopy (TEM) on Cu/C grids.

Figure 8 shows the size histogram of NPsAu@PEDOT measured by DLS (dynamic light scattering); **Figure 9** shows the zeta potential measurement of NPsAu@PEDOT; **Figure 10** shows 4 TEM micrographs. In the micrographs the Au nanoparticles appear in black, while the surrounding polymer around is lighter, grey. The images show high polydispersity of nanoparticles from less than 1 nm up to ca. 5 nm. In the size histogram of **Figure 8** there are 3 peaks: 1 between 1 nm and 10 nm, 1 between 10 nm and 100 nm and 1 between 100 nm and 1000 nm (microparticles). The peak between 1 nm and 10 nm correspond to the nanoparticles of the micrographs and to the core-shell Au@PEDOT nanoparticles, inside the matrix of PEDOT in **Figure 10**. It can be observed in **Figure 10** that the nanoparticles outside the matrix are bigger than the nanoparticles inside, which may indicate that, during the synthesis, PEDOT blocked the surface of gold nanoparticles and prevent them from growing. The peaks of larger sizes can correspond to aggregates of Au nanoparticles or to PEDOT. In an article about the same nanoparticles [86] TEM micrographs were also performed and it was demonstrated that the smaller nanoparticles are hybrid and have a core-shell structure. **Figure 9** shows a peak in ca. −25 mV, the nanoparticles are negatively charged due to PSS^- in the shell or to adsorbed Cl^- (Cl^- tends to adsorb on gold). Nanoparticles require

a high zeta potential (in module) to be stable in solution and do not underwent coalescence.

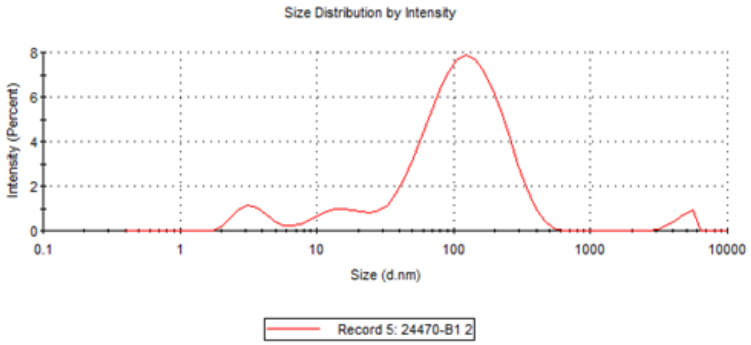

Figure 8. Dynamic light scattering histogram of size distribution of core-shell NPsAu@PEDOT. x axis is in logarithmic scale. NPsAu@PEDOT formed from $HAuCl_4$, EDOT and NaPSS in water, under stirring for hours.

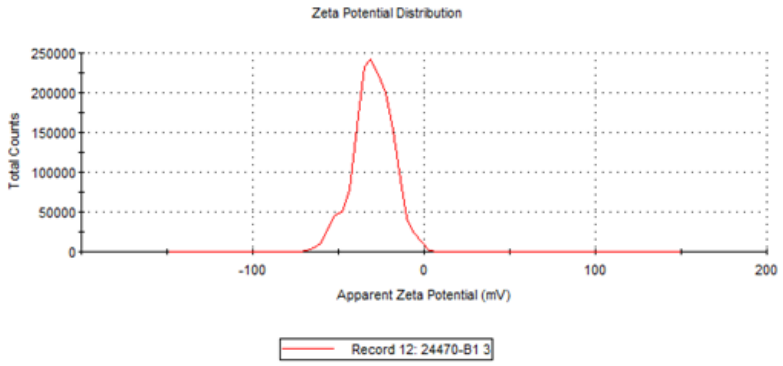

Figure 9. Zeta potential measurements of core-shell NPsAu@PEDOT by dynamic light scattering. NPsAu@PEDOT formed from $HAuCl_4$, EDOT and NaPSS in water, under stirring for hours.

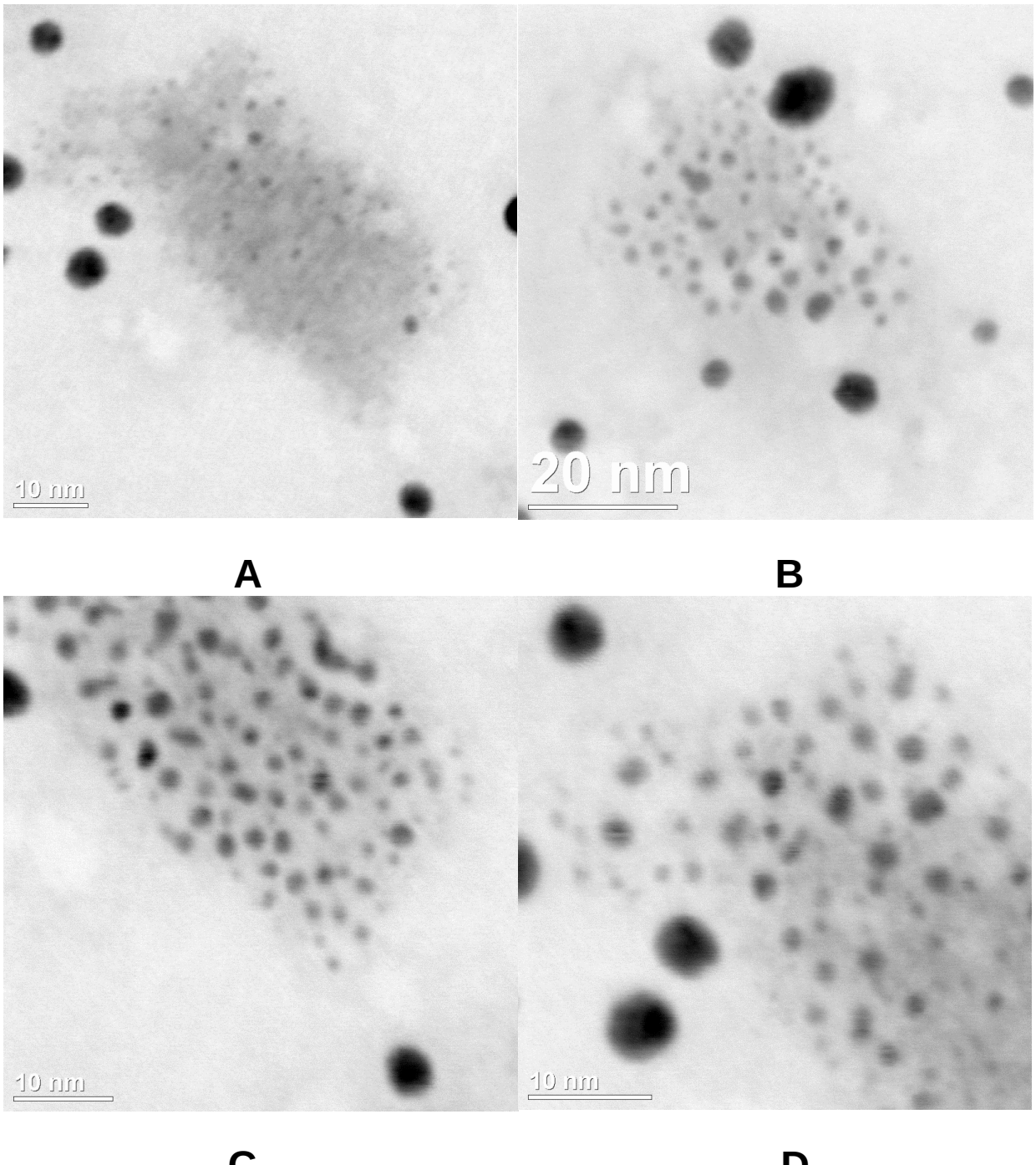

Figure 10. Transmission electron micrographs of different nominal magnifications of NPsAu@PEDOT. These images show NPsAu in the matrix of PEDOT. The reaction suspension of NPsAu@PEDOT is casted (ca. 2 μL) on transmission electron microscopy grids and let dry. NPsAu@PEDOT formed from $HAuCl_4$, EDOT and NaPSS in water, under stirring for hours.

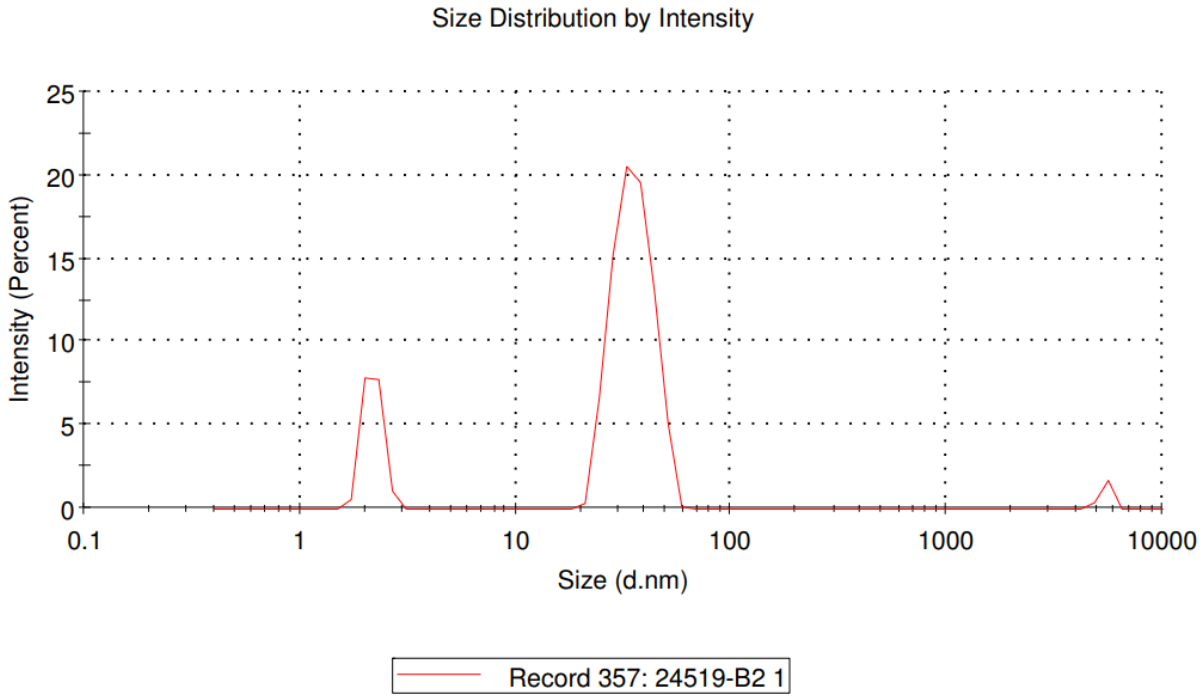

Figure 11 shows the size histogram; **Figure 12** shows the zeta measurements; **Figure 13** shows TEM micrographs of NPsPt/PEDOT. The histogram presents 2 sharp peaks: ca. 2 nm and between 10 nm and 100 nm. The micrographs show highly homogenous platinum nanoparticles with low polydispersity and well distributed in the PEDOT matrix. These NPs correspond to the 2 nm peak in the histogram. **Figure 12** shows that the particles in NPsPt/PEDOT are mostly negatively charged, as in the sample NPsAu@PEDOT. EDS measurements were performed in the depicted regions 1 and 2 of **Figure 13E**. **Figure 14** and **Figure 15** present the EDS spectra of these 2 regions, respectively. In **Figure 14** (EDS performed in a small dark nanoparticle) there are peaks of Pt and Cu. Cu due to the TEM grid and Pt from the nanoparticle. In **Figure 15** (EDS performed in a larger region englobing dark nanoparticles and the grey matrix) there are peaks of Pt, Cu, Cr, Co, Si and S. Si signal is from the X rays detector; Co and

Cr are from the microscope; Cu is from the TEM grid and Pt and S are from the sample. Therefore EDS demonstrates that sulfur-containing polymers PEDOT and PSS^- are present in the matrix, surrounding the Pt nanoparticles.

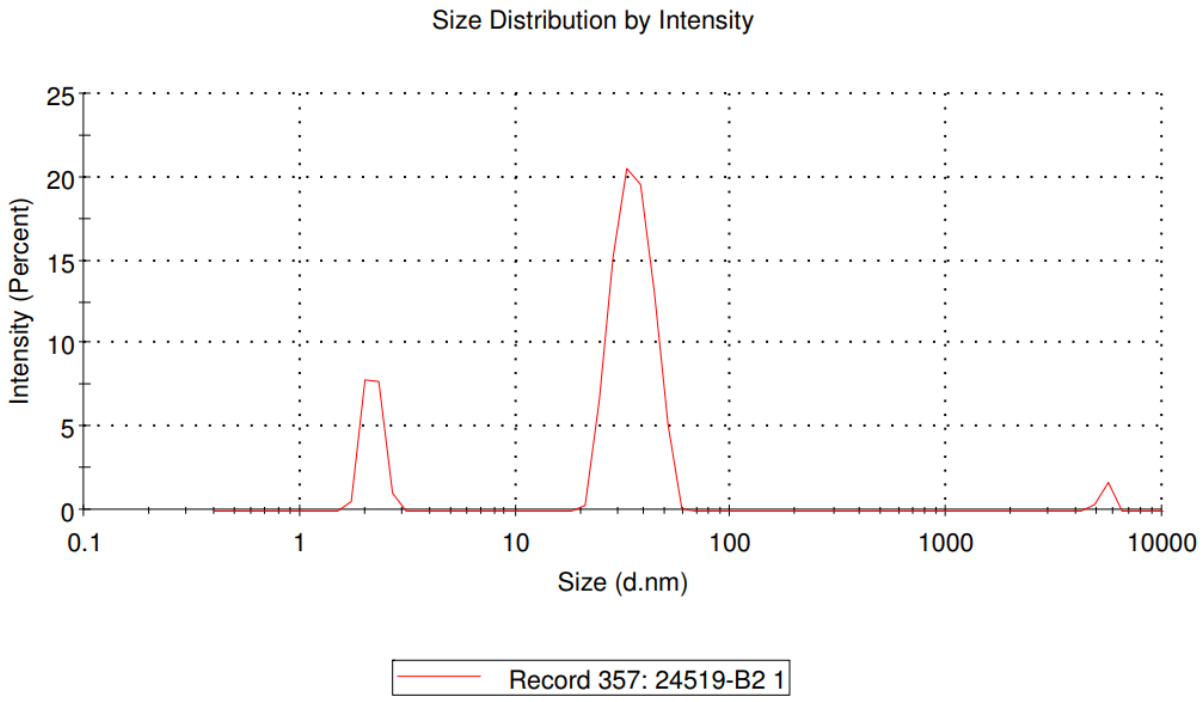

Figure 11. Dynamic light scattering histogram of size of Pt nanoparticles on NPsPt/PEDOT hybrid. x axis is in logarithmic scale. NPsPt/PEDOT formed from H_2PtCl_6, EDOT and NaPSS in water, under stirring for days.

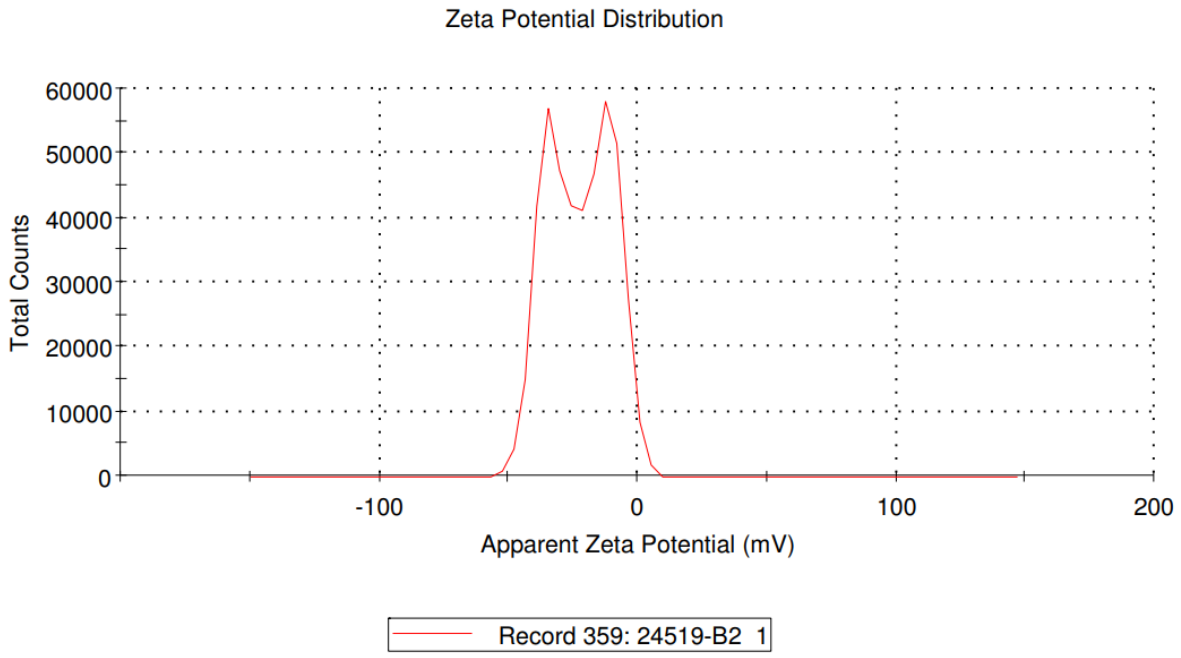

Figure 12. Zeta potential measurement of Pt nanoparticles on NPsPt/PEDOT hybrid. NPsPt/PEDOT formed from H_2PtCl_6, EDOT and NaPSS in water, under stirring for days.

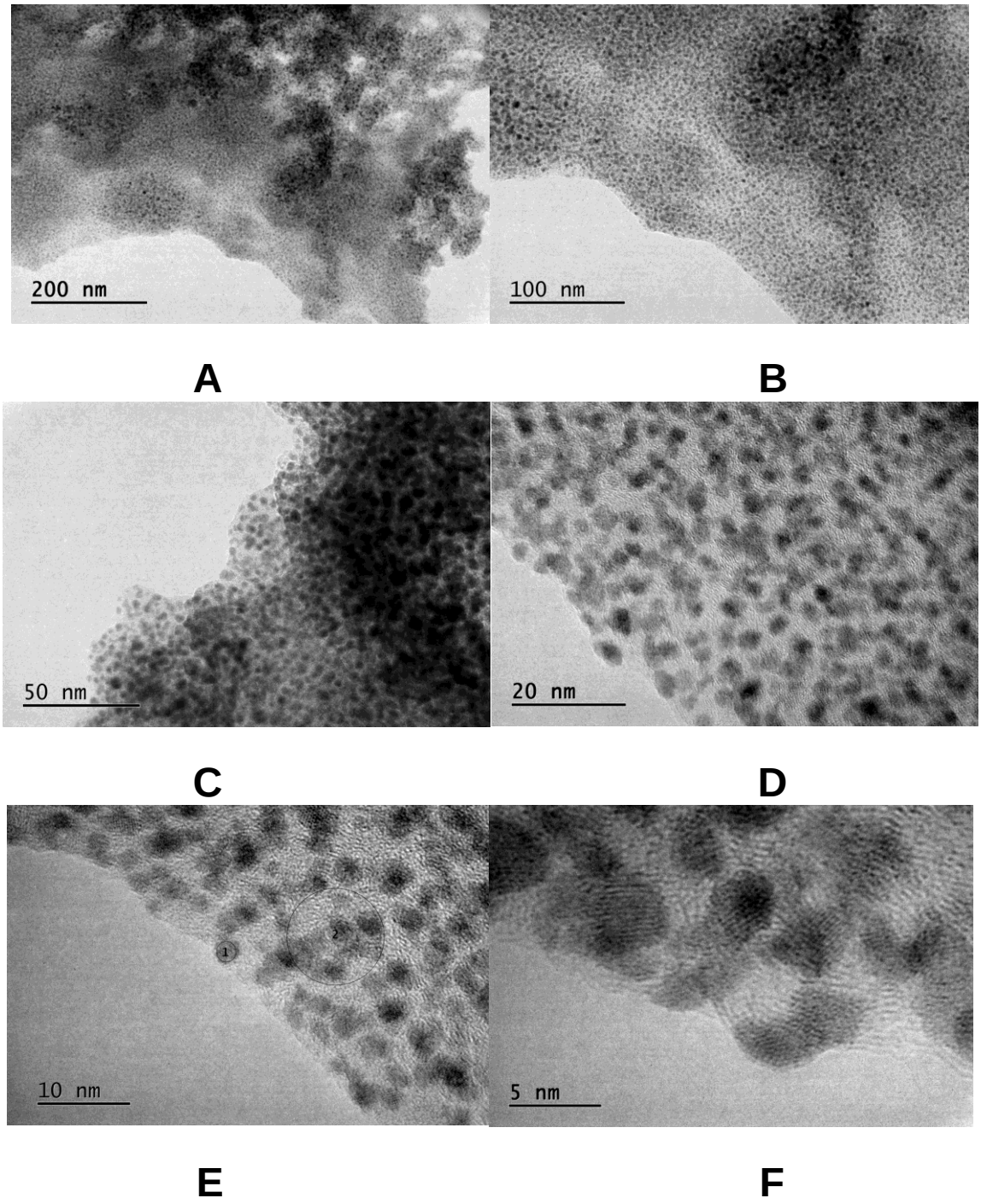

Figure 13. Transmission electron micrographs of different nominal magnification of NPsPt/PEDOT hybrid. EDS was performed in the depicted regions of E. The reaction suspension of NPsPt/PEDOT is casted (ca. 2 µL) on transmission electron microscopy grids and let dry. NPsPt/PEDOT formed from H_2PtCl_6, EDOT and NaPSS in water, under stirring for days.

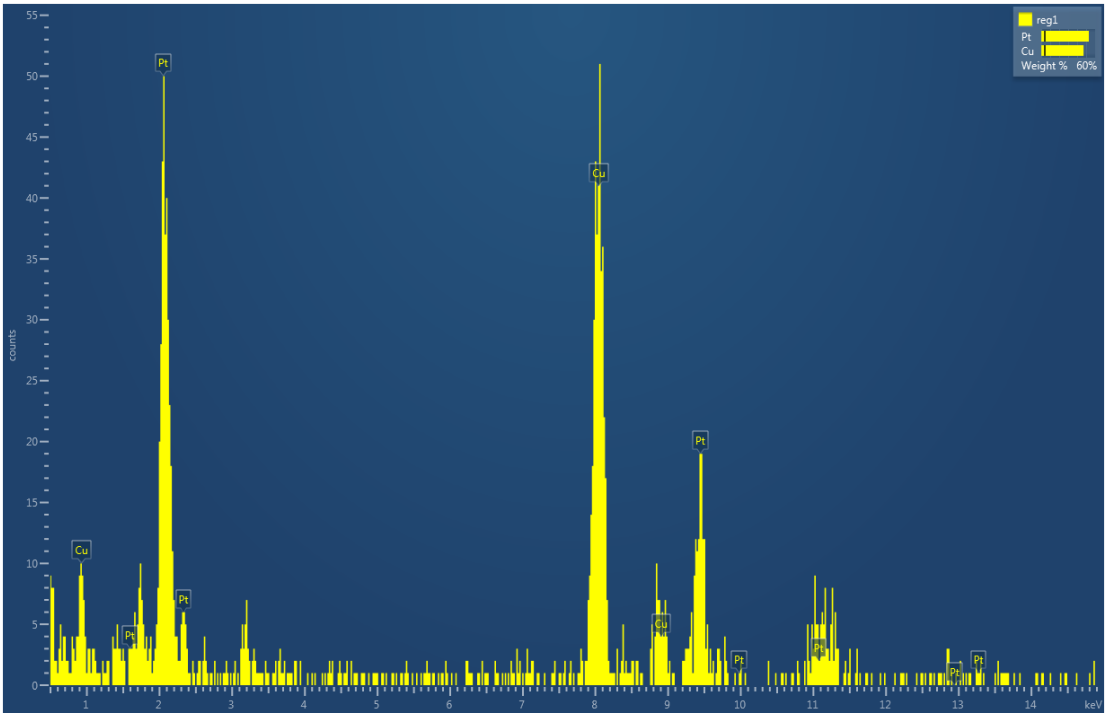

Figure 14. EDS spectrum of region 1 of the transmission electron micrograph of **Figure 13E**, a region containing 1 nanoparticle. The sample is NPsPt/PEDOT. The reaction suspension of NPsPt/PEDOT was casted (ca. 2 μL) on transmission electron microscopy grids and let dry. NPsPt/PEDOT formed from H_2PtCl_6, EDOT and NaPSS in water, under stirring for days.

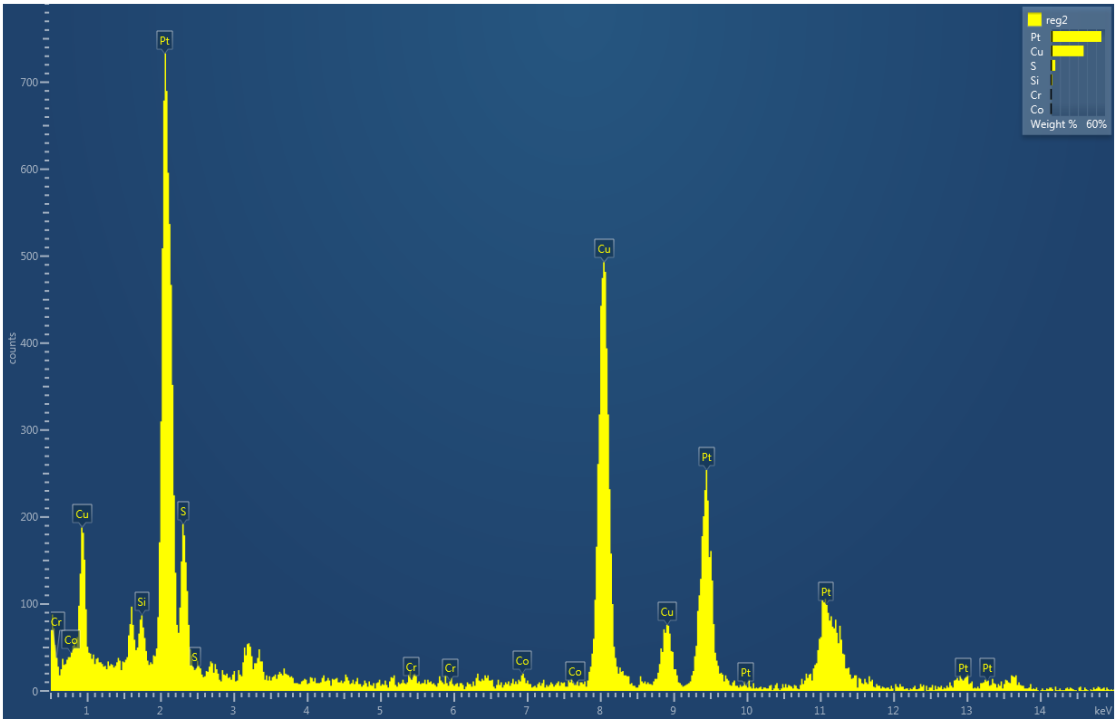

Figure 15. EDS spectrum of region 2 of transmission electron micrograph of **Figure 13E**, a region containing both the matrix and nanoparticles. The sample is NPsPt/PEDOT. The reaction suspension of NPsPt/PEDOT was casted (ca. 2 µL) on transmission electron microscopy grids and let dry. NPsPt/PEDOT formed from H_2PtCl_6, EDOT and NaPSS in water, under stirring for days.

Figure 16 presents the size histogram of nanoparticles and **Figure 17** presents the zeta measurements of NPsAu/PEDOT-PLA. **Figure 16** shows 3 peaks: between 1 nm and 10 nm, between 100 nm and 1000 nm (microparticles) and between 1000 nm and 10000 nm (microparticles). The gold nanoparticles correspond to the broad peak in ca. 2 nm (between 1 nm and 10 nm). The other 2 peaks may be due to aggregates of gold nanoparticles or PEDOT-PLA. **Figure 18** shows TEM micrographs of NPsAu/o-EDOT-PLA (**A–D**) and of NPsAu/PEDOT-PLA (**E–H**), being NPsAu/PEDOT-PLA formed by adding potassium peroxydisulfate to the reaction suspension of NPsAu/o-EDOT-PLA. The micrographs show that before the oxidation with potassium peroxydisulfate the nanoparticles (corresponding to the peak of ca. 2 nm in **Figure 16**) are numerous, polydisperse and inhomogeneous. After the oxidation with potassium peroxydisulfate the nanoparticles are slightly smaller and less numerous, demonstrating that Au^0 in the nanoparticles is oxidized to Au(I) or Au(III) species, as it was predicted by **Equation 9** and **Equation 12**, which show that the reactions at the standard conditions are highly thermodynamically spontaneous. The NPs in NPsAu/o-EDOT-PLA are not core-shell NPs, and the matrix of o-EDOT-PLA does not prevent oxidation of gold. **Figure 17** shows that the nanoparticles in NPsAu/PEDOT-PLA are negatively charged.

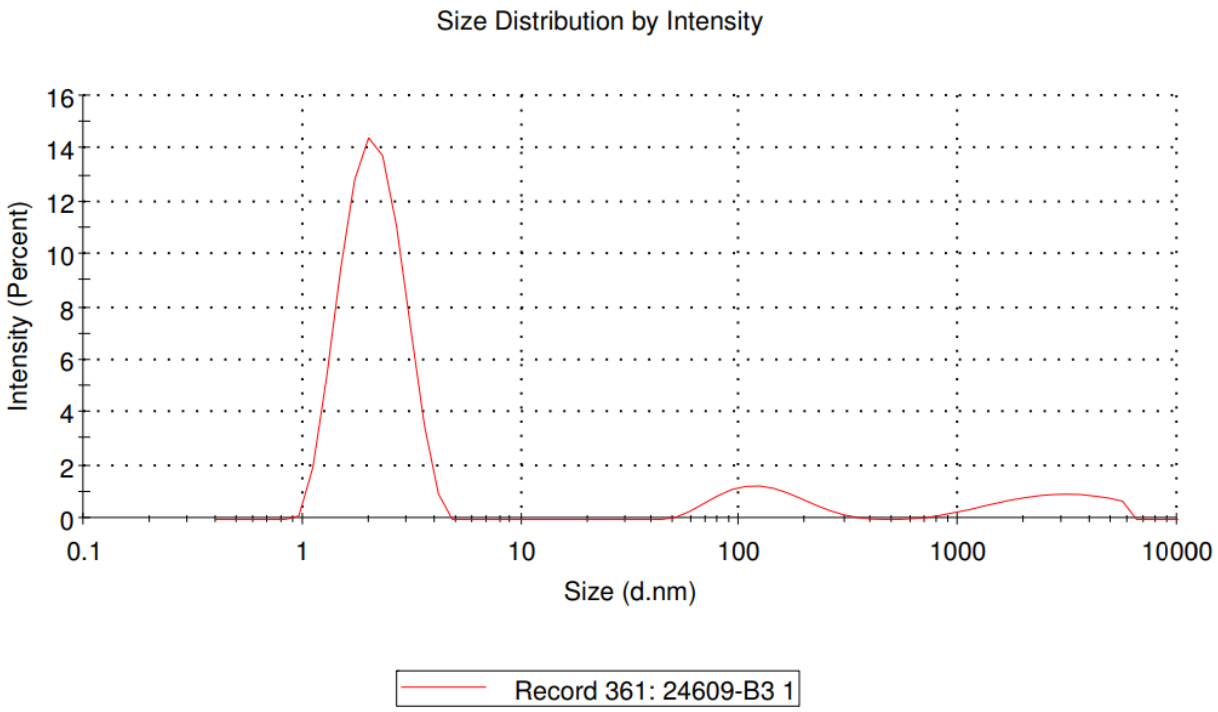

Figure 16. Dynamic light scattering histogram of size of Au nanoparticles on NPsAu/PEDOT-PLA hybrid. x axis is in logarithm scale. NPsAu/PEDOT-PLA formed from the reaction suspension of NPsAu/o-EDOT-PLA and potassium peroxydisulfate in acetonitrile, under stirring for days.

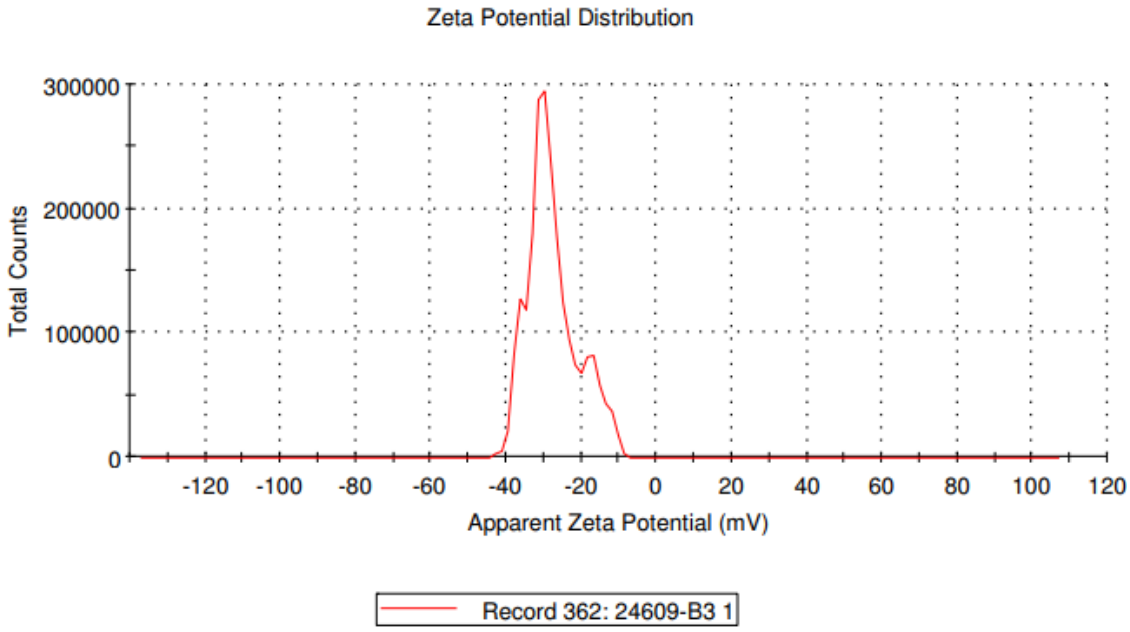

Figure 17. Zeta potential measurements of Au nanoparticles on NPsAu/PEDOT-PLA. NPsAu/PEDOT-PLA formed from the reaction suspension of NPsAu/o-EDOT-PLA and potassium peroxydisulfate in acetonitrile, under stirring for days.

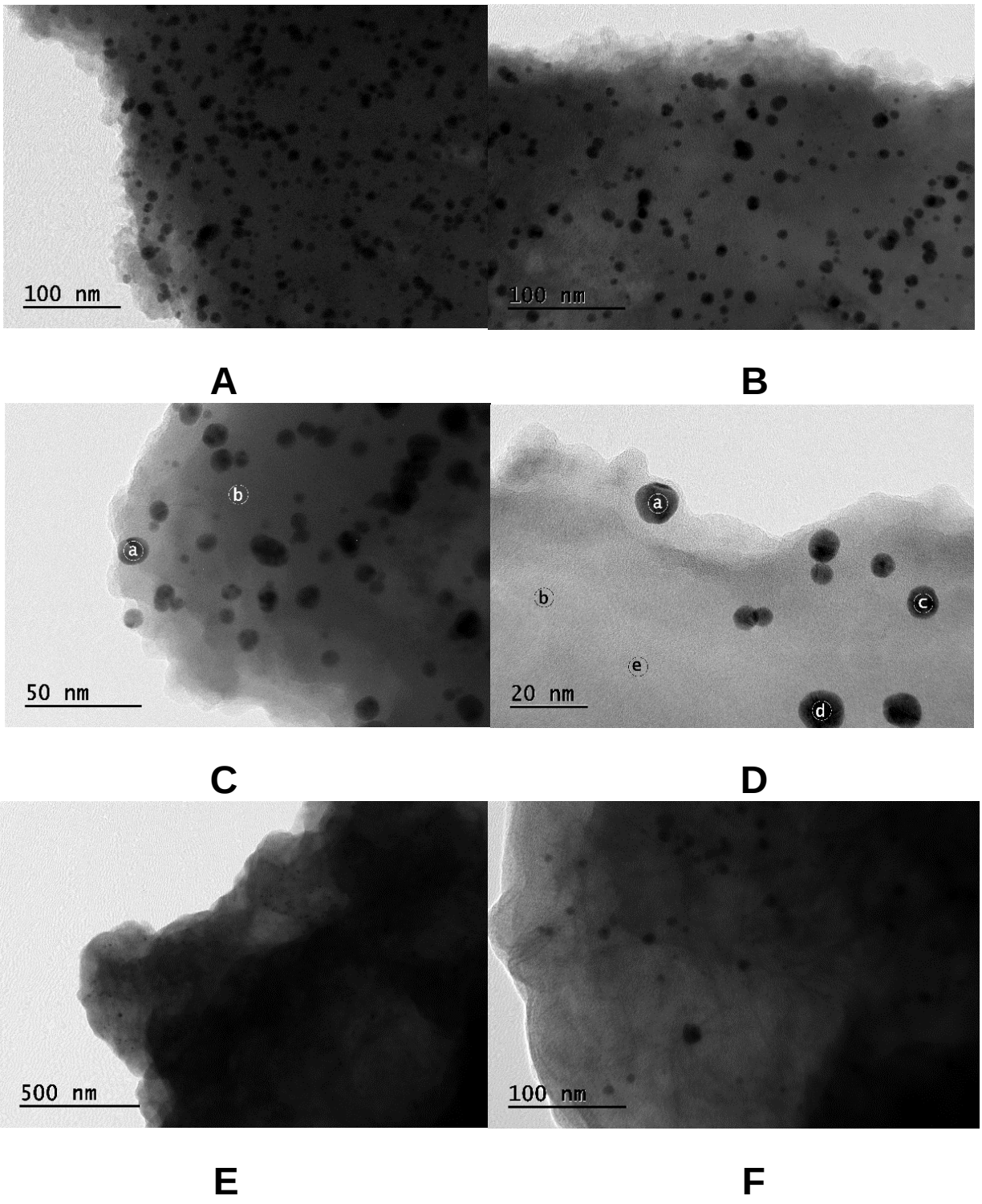

Figure 18. (Continues on next page, legend on next page).

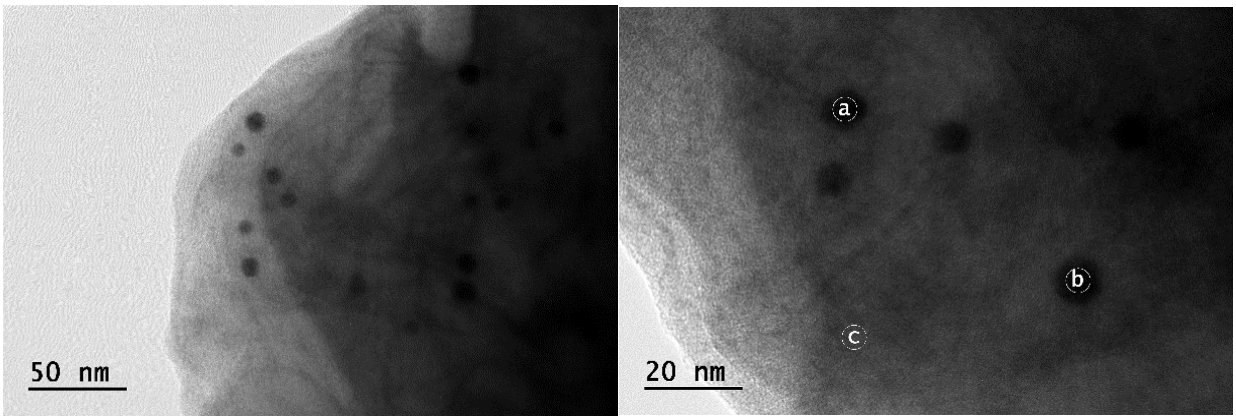

G **H**

Figure 18. (Continuation). Transmission electron micrographs of different nominal magnifications of NPsAu/o-EDOT-PLA (**A–D**) and of NPsAu/PEDOT-PLA (**E–H**). EDS is performed in the depicted regions of C, D and H. C: region a: Au; region b: Au, S. D: regions a, c, d: Au; regions b and e: Au, S. H: regions a and b: Au; region c: Au, S. The reaction suspensions are casted (ca. 2 μL) on transmission electron microscopy grids and let dry. NPsAu/o-EDOT-PLA formed from $HAuCl_4$, EDOT-PLA and NaPSS in acetonitrile. NPsAu/PEDOT-PLA formed from the reaction suspension of NPsAu/o-EDOT-PLA and potassium peroxydisulfate in acetonitrile, under stirring for days.

The sizes of nanoparticles in the synthesized samples were measured by dynamic light scattering (**Figure 9**, **Figure 12** and **Figure 17**) and were also calculated manually by analyzing the TEM micrographs of **Figure 10**, **Figure 13** and **Figure 18** with the software ImageJ. The results are compared in **Table 1**. They are very different, probably due to the methodologies used.

Table 1. Comparison of the mean sizes of nanoparticles observed in the histograms (maximum of peaks of size distributions) by dynamics light scattering and by transmission electron microscopy (counted manually with ImageJ software) for several samples. Data obtained from **Figure 8**, **Figure 10**, **Figure 11**, **Figure 13**, **Figure 16**, **Figure 18** and from the article by Augusto et al. [86]. NPsAu@PEDOT formed from $HAuCl_4$, EDOT and NaPSS in water, under stirring for hours. NPsPt/PEDOT formed from H_2PtCl_6, EDOT and NaPSS in water, under stirring for days. NPsAu/o-EDOT-PLA formed from $HAuCl_4$, EDOT-PLA and NaPSS in acetonitrile. NPsAu/PEDOT-PLA formed from the reaction suspension of NPsAu/o-EDOT-PLA and potassium peroxydisulfate in acetonitrile, under stirring for days.

Samples	**Mean sizes of NPs by DLS / nm**	**Mean sizes of NPs by TEM / nm**
NPsAu@PEDOT	3	3.7 [86]
NPsPt/PEDOT	(2.2±0.2) ; (35±7)	-
NPsAu/o-EDOT-PLA	-	(8.1±0.2)
NPsAu/PEDOT–PDLLA	(2.2±0.7)	(9.0±0.2)

4.2.2. Raman spectroscopy results

The hybrids of noble metal nanoparticles and PEDOTs were immobilized on glass slides by simple casting and analyzed by Raman microscopy. **Figure 19** presents the Raman spectrum of EDOT-$PLA_{(acetonitrile)}$, with its characteristic bands. **Figure 20** presents the spectra of the hybrids NPsAu@PEDOT, NPsPt/PEDOT and NPsAu/PEDOT-PLA. In **Figure 19** it is observed that, even when the background is removed, the noise in very high and the signal-to-noise ratio is low. This occurs due to the fluorescence of EDOT-PLA at stimulating light of 636 nm. This does not occur in the spectra of **Figure 20**, of PEDOT-derived hybrids.

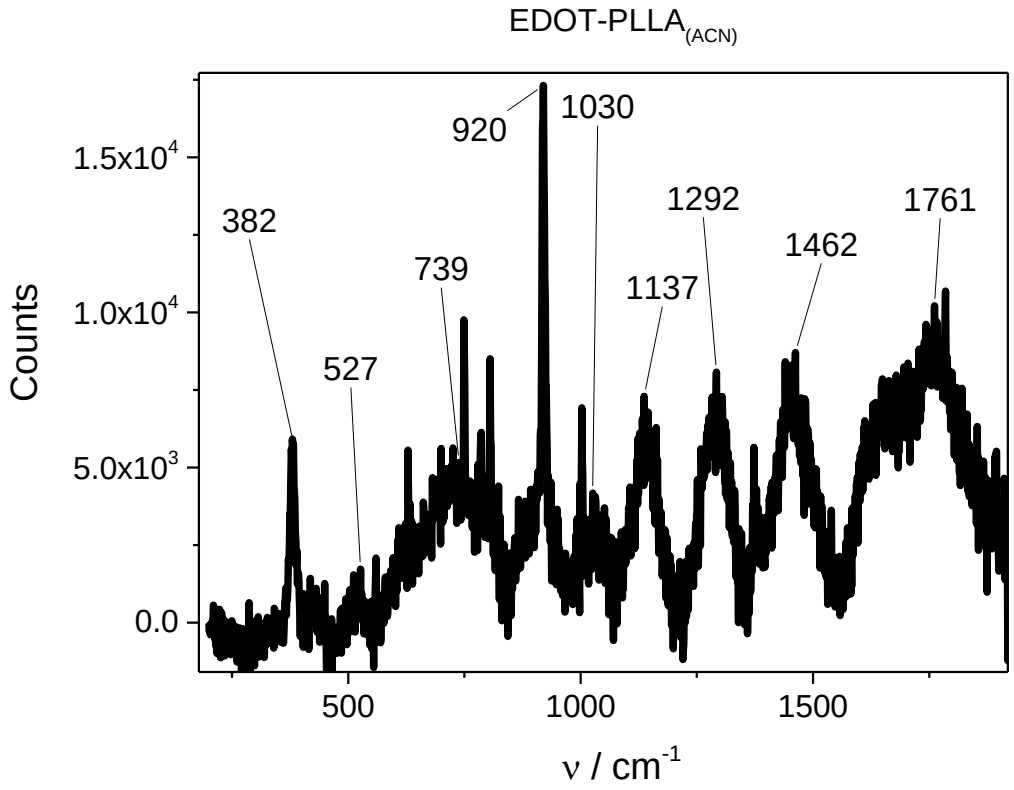

Figure 19. Raman spectrum of EDOT-PLA. The sample is added to a small flask and analyzed in the Raman microscope with a red He/Ne, 636 nm wavelength, laser, with 10% power and integration time of 100 s. The background is subtracted, but the sample presents strong fluorescence at the experimental conditions. EDOT-PLA formed from lactone, Sn(II) 2-ethylhexanoate and lactic acid in toluene, under reflux, at 110 ºC (383 K), and dissolved in acetonitrile previous to the analysis.

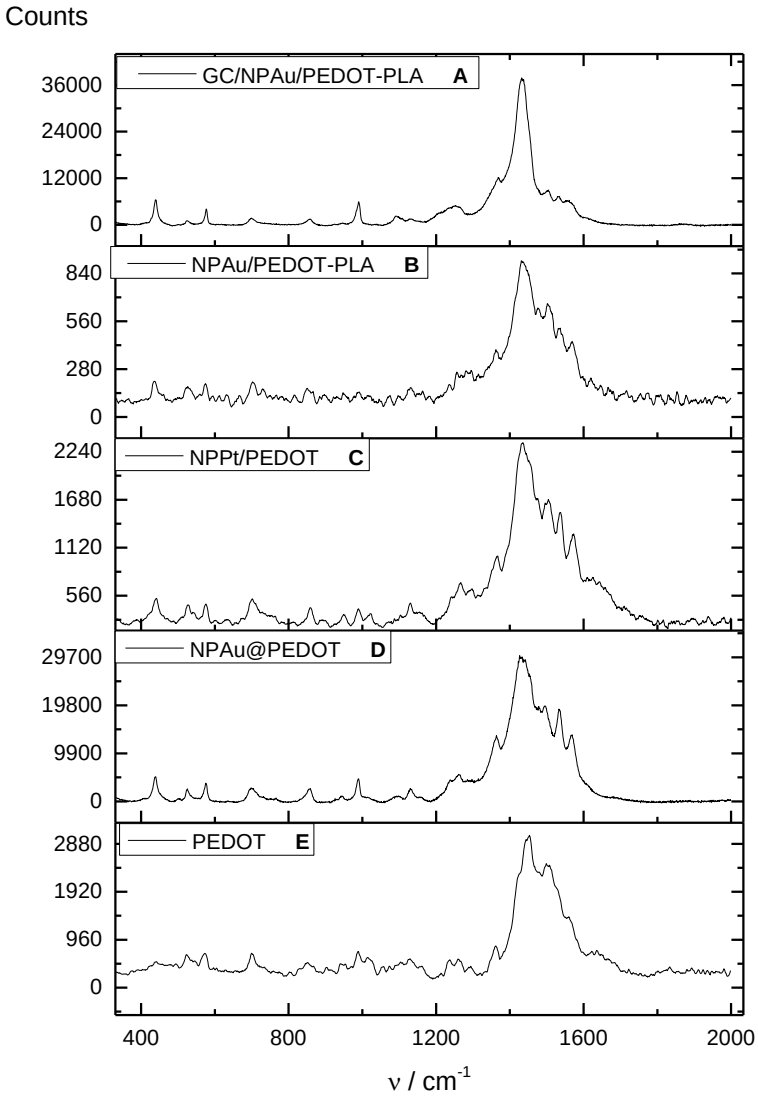

Figure 20. Raman spectra of A: NPsAu/PEDOT-PLA (deposited by casting, 10 steps, on GCE); B: NPsAu/PEDOT-PLA over a glass slide; C: NPsPt/PEDOT over a glass slide; D: NPsAu@PEDOT over a glass slide and E: $PEDOT_{(aq)}$. The laser of the Raman microscope is a He/Ne, 636 nm wavelength laser. A: 10% laser power, 100 s integration time. B: 10% laser power, 10 s integration time. C: 10% laser power, 10 s integration time. D: 10% laser power, 100 s integration time. E: 10% laser power, 10 s integration time, sample diluted 100 x with water previous to the experiment. The backgrounds are subtracted. NPsAu@PEDOT formed from $HAuCl_4$, EDOT and NaPSS in water, under stirring for hours. NPsPt/PEDOT formed from H_2PtCl_6, EDOT and NaPSS in water, under stirring for days. NPsAu/o-EDOT-PLA formed from $HAuCl_4$, EDOT-PLA and NaPSS in acetonitrile. NPsAu/PEDOT-PLA formed from the reaction suspension of NPsAu/o-EDOT-PLA and potassium peroxydisulfate in acetonitrile, under stirring for days.

PEDOT presents the main band in (1426–1453) cm^{-1}, characteristic of oxidized bipolaron PEDOT, and so does all the spectra of the hybrids in **Figure 20**. The main band is due to the symmetrical stretching of C2=C3 and C4=C5 bonds of PEDOTs [94] (sulfur is always C1). In the spectrum of PEDOT/PSS the secondary band is too small to be identified. Duvail et al. [93] hypothesized that this band occurs when PEDOT is synthesized in small and confined structures [89]–[93]. The spectra demonstrate that PEDOTs are present in the samples and PEDOT-PLA is structurally similar to PEDOT, with almost the same bands. The maxima of the spectra, which are the maxima of the main band, present counts from ca. 900 to ca. 37000. The greatest variations among them are attributed to the integration time, which varies from 10 s to 100 s. The counts are not extremely high, and surface enhanced Raman scattering effect seems to not occur. **Table 2** compares the bands of spectra of **Figure 20**. The main band is shifted to lower wavelengths relative to the isolated polymer.

Table 2. Raman bands of **Figure 20** spectra. Bands 1 to 11 are from PEDOTs. 1: symmetric stretching C2=C3 for doped PEDOTs. 2 and 3: unidentified. 4: oxyethylene ring bending. 5 and 6: asymmetric stretching C2=C3. 7: C2=C3 stretching. 8: interring stretching. 9 and 10: C-O-C bending. 11: antyssymetric deformation of double vicinal oxyethyelene rings by movement of the 4 oxygen atoms [94], [95]. NPsAu@PEDOT formed from $HAuCl_4$, EDOT and NaPSS in water, under stirring for hours. NPsPt/PEDOT formed from H_2PtCl_6, EDOT and NaPSS in water, under stirring for days. NPsAu/o-EDOT-PLA formed from $HAuCl_4$, EDOT-PLA and NaPSS in acetonitrile. NPsAu/PEDOT-PLA formed from the reaction suspension of NPsAu/o-EDOT-PLA and potassium peroxydisulfate in acetonitrile, under stirring for days.

Samples / Raman bands / cm^{-1}	**1**	**2**	**3**	**4**	**5**	**6**	**7**	**8**	**9**	**10**	**11**
NPsAu / PEDOT-$PLA_{(s)}$	1431	1501	703	-	-	1536	1363	1268	1131	1096	435
NPsPt / $PEDOT_{(s)}$	1436	1504	702	-	1573	1537	1367	1267	1130	-	442
NPsAu @ $PEDOT_{(s)}$	1426	1494	699	989	1569	1533	1364	1262	1130	-	439
$PEDOT_{(aq)}$	1453	1499	700	989	-	-	1362	1259	1128	-	-
GCE / NPsAu / PEDOT-PLA	1432	1504	700	990	-	1535	1368	1253	1129	-	440

4.3. Deposition of hybrids on GCEs

After synthesizing NPsAu/PEDOT-PLA in acetonitrile the reaction suspension was centrifuged and the supernatant was discarded, obtaining the isolated hybrid in *Eppendorfs*. The NPs were resuspended by adding 1 mL dymethylsulfoxide to the *Eppendorf* and ultrasonicating for the time necessary. The NPsAu/PEDOT-PLA new suspension was then used in casting. The suspension in dymethylsulfoxide produces a much more stable film of NPsAu/PEDOT-PLA in the surface of GCE when compared to the suspension in acetonitrile. The number of casting steps was varied from 1 to 10.

CVs (cyclic voltammograms) of the modified GCEs with different amounts of NPsAu/PEDOT-PLA were performed to study the electroactivity of the hybrids, and the results are presented in **Figure 21**. For each experiment 200 cycles were performed between +600 mV and −400 mV (versus $Ag/AgCl/KCl_{(3\ mol\ L-1)}$) at 10 mV s^{-1} to test the stability of the material. All the profiles of the voltammograms of GCE/NPsAu/PEDOT-PLA are very similar to the profile of bare GCE. **Figure 21A–B** modified GCE-CVs present some unknown redox peaks between ca. +0.2 V and ca. 0 V versus $Ag/AgCl/KCl_{(3\ mol\ L-1)}$, which do not exist in **Figure 21C**. The arrows that cross the CVs indicate the evolution of the current density with the increasing number of cycle. Cycles 1–25 and 176–200 are displayed; cycles 26–175 are omitted. The only characteristic electroactivity observed is at the lower limit of potential range in which there may be a reduction peak at more negative potentials.

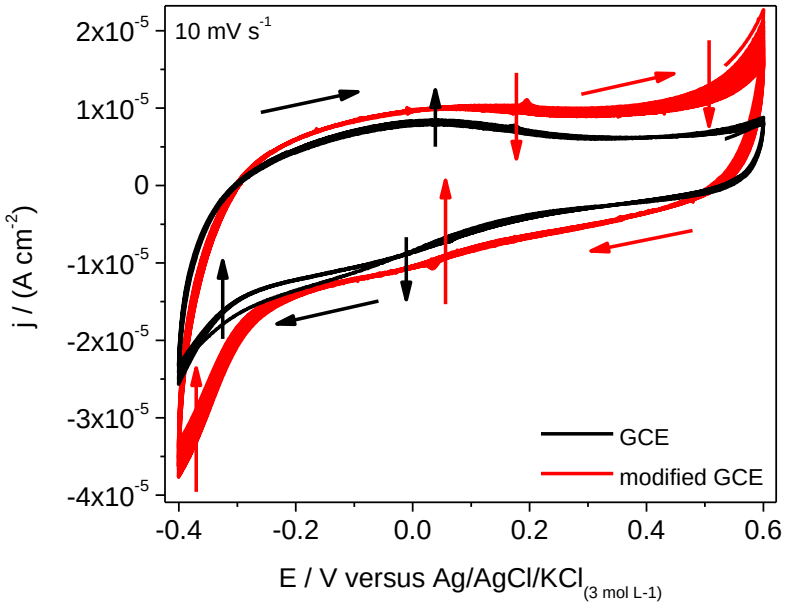

A

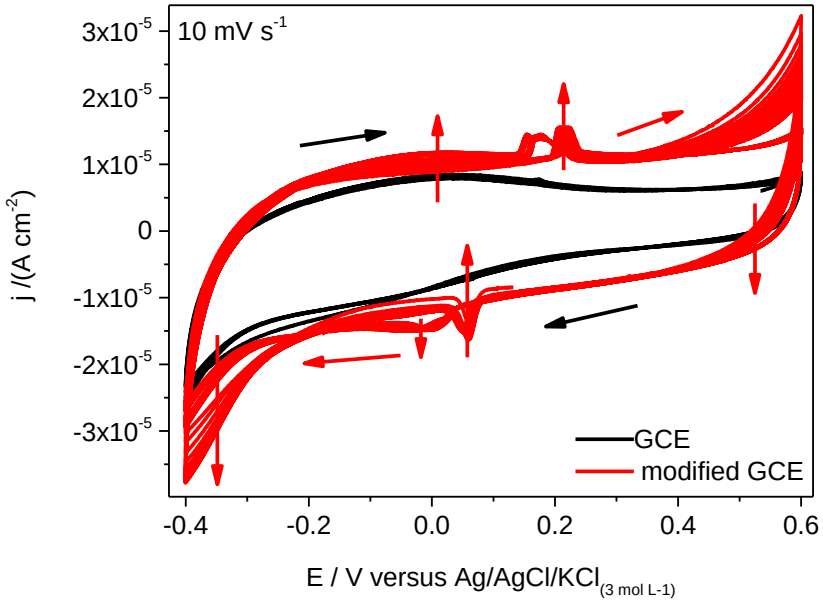

B

Figure 21. (Continues on next page, legend on next page).

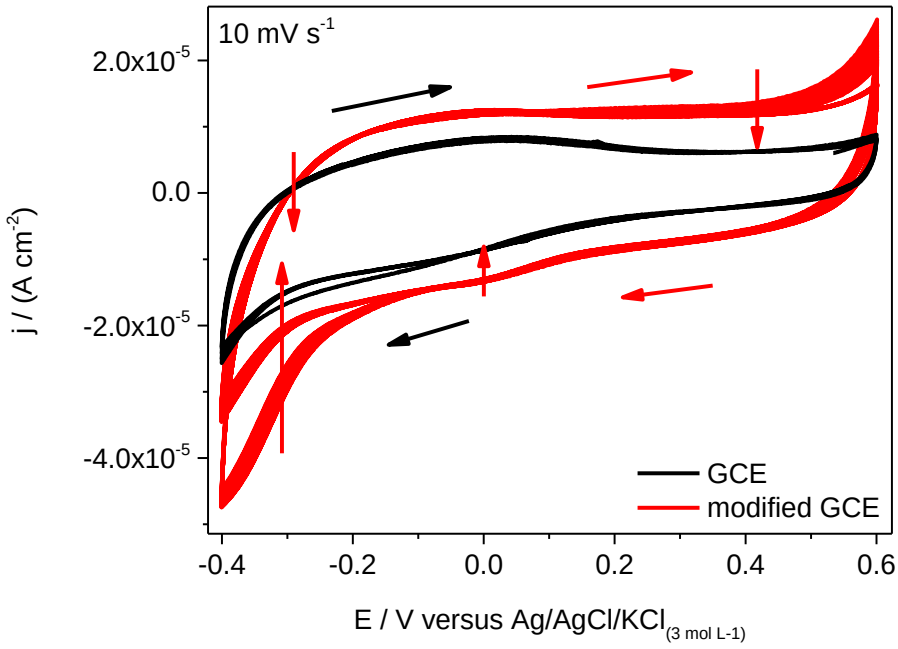

C

Figure 21. (Continuation). Cyclic voltammograms of a GCE (control) (black curves) and of NPsAu/PEDOT-PLA deposited by casting by different numbers of steps on a GCE (red curves). **A**: 1 step. **B**: 5 steps. **C**: 10 steps. The initial potentials were the open circuit potentials: ca. +150 mV. Scan rate: 10 mV s^{-1}. Initial potential scans: increasing potential. The current is normalized by the geometrical area of the electrode (7.07 mm^2). 200 cycles were performed. Cycles 1–25 and 176–200 are showed. Cycles 26–175 are omitted. Arrows that cross the curves indicate the direction of increasing time among the cycles. Working electrode: modified GCEs. Counter electrode: Pt plate. Reference electrode: $Ag/AgCl/KCl_{(3\ mol\ L-1)}$. Electrolyte: dyhydrogenphosphate/hydrogenphosphate buffer 20 mmol L^{-1} pH = 7.4 + NaCl 100 mmol L^{-1}. The electrolyte was deoxygenated by bubbling dry N_2 for at least 15 min prior to the experiment and keeping a N_2 atmosphere over the electrolyte throughout the experiment. NPsAu/PEDOT-PLA deposited on GCEs adding small drops of NPsAu/PEDOT-PLA on GCEs and drying them at 40 ºC (313 K) in vacuum. Prior to the deposition the NPsAu/PEDOT-PLA were centrifuged in their reaction suspension and resuspended in dymethylsulfoxide by ultrasound. NPsAu/PEDOT-PLA formed from the reaction suspension of NPsAu/o-EDOT-PLA and potassium peroxydisulfate in acetonitrile, under stirring for days.

4.4. Syntheses of hydrogels of acrylic acid and acrylamide

Syntheses of hydrogels of poly(acrylic acid) were performed varying the concentrations of reagents like N,N'-methylenebisacrylamide, a bifunctional reagent that reacts with acrylic acid forming bridges between the polymeric chains (as described in **Chapter 3, Experimental**). h-PAAs (PAAs are samples of poly(acrylic acid)) were made in solution by uncatalyzed synthesis with cylindrical templates. The syntheses in cylindrical templates are relatively simple; the gels are mechanically stable and have a good water absorption capability. They increase in volume by more than 2 folds during the complete swelling.

PAA was also synthesized as films over ITOs, which are transparent electrodes suitable for electrochromic experiments. f-h-PAA samples synthesized on ITOs by uncatalyzed syntheses or catalyzed synthesis did not behave as expected. Only increasing the amount of N,N'-methylenebisacrylamide used was not sufficient to produce stable, insoluble polymers. The hydrogels present weak adherence to ITOs and dissolved or detached from the surface of ITOs when immersed in water.

In the case of b-h-PAAs the catalyzed synthesis procedure was modified and 250 μmol L^{-1} N,N'-methylenebisacrylamide were added in the preparation of the precursor solution in the catalyzed synthesis; and 24 μmol L^{-1} N,N'-methylenebisacrylamide in the catalyzed synthesis. The consequent b-h-PAAs presented more stable behavior compared to that produced by adding 12 μmol L^{-1} to the precursor solution. In the long term, though, all b-h-PAAs underwent oxidation reactions and changed its characteristics.

4.4.1. Insertion of nanoparticles in acrylic hydrogels

The insertion of hybrids in hydrogels of PAA and in hydrogels of PAAM was studied. In the case of b-h-PAAs, the insertion was performed by electroinsertion for 12 h at +1.15 V versus ITO, being the electrolyte the reaction suspension of NPsAu@PEDOT. The hydrogel acquires a heterogeneous light-to-dark blue color due to the NPsAu@PEDOT. The successful electroinsertion demonstrates again that the hybrid has negative net charge. The reaction suspension can be roughly estimated (based on the complete formation and oxidation of PEDOT) to have an ionic strength of $7.7x10^{-4}$ mol L^{-1} due to the counter-ions present. The ionic strength impairs the electrodepositions of NPsAu@PEDOT on electrodes, reducing the effect of the electric field and the migration, which may be why some electrodepositions take so long to deposit a desirable amount of material. The reaction suspensions could be dialyzed to purify the hybrids before the electrodepositions, dealing this problem. It was observed that applying +1.15 V for 12 h versus ITO did not have any effect of degrading the electrolyte, but the ITO counter electrode darkens and loses electric conductivity in the process due to the reduction, since the time is too long and the potential difference is high.

In the experiments with f-h-PAAs they were found to not adhere to the ITOs surface, neither those made through the uncatalyzed synthesis nor those made through the catalyzed synthesis. Then PAAM polymer was tested, developing the strategy of bonding with the silane linker and subsequent photopolymerization, described in **Chapter 3, Experimental**. In the formation of ITO/silane/f-h-PAAM the vinyl group of

tris(2-methoxyethoxy)(vinyl)silane is removed, the Si atom bonds to one O atom of ITO surface, and one or more methoxy groups are substituted by N,N'-methylenebisacrylamide or by acrylamide. This way the cross-linked network is formed covalently bonded to the Si atom and to the surface of ITO ($O_{(ITO)}$-(Si-O-CH_2-CH_2)-polymer network). There is a monolayer of the reagent on the surface of ITO, bond to the polymer.

Through the photopolymerization strategy, the stability and adhesion of hydrogel films were increased, allowing them to be used as matrixes for modification by nanoparticles and solving this experimental problem. After the electroinsertion of NPsAu@PEDOT or NPsPt/PEDOT the gel acquires a blue aspect, such as b-h-PAA with NPsAu@PEDOT. For f-h-polyacrylamides the electroinsertions were performed at +2.3 V versus ITOs for 12 h, and the same problems with ITO counter electrode were observed. Films of hydrogels of poly(acrylic acid) formed through uncatalyzed synthesis or catalyzed synthesis were impossible to use or store in aqueous medium. Films of hydrogels of polyacrylamide photopolymerized also degraded in aqueous medium, but far slower. If the hydrogel is immersed in multiple solutions and agitated the process is accelerated. The lack of stability may be also due to the fact that the silane monolayer can underwent hydrolysis.

ITO/silane/f-h-PAAM and ITO/silane/f-h-PAAM&NPsAu@PEDOT were electrochemically studied behavior studied through cyclic voltammetry (**Figure 22**). The CV (cyclic voltammogram) of ITO/silane/f-h-PAAM (**Figure 22A**) shows only 1 reduction shoulder at the negative region of potential and increasing (in module) negative current at the lower limit of potential (unknown). The CV of ITO/silane/f-h-

PAAM&NPsAu@PEDOT (**Figure 22B**) shows a different profile, much more capacitive, depicting the oxidation and reduction peaks of PEDOT, proving that PEDOT is electroactive in the core-shell nanoparticles inserted in the hydrogel. The electroactivity of this hybrid is maintained when they are inserted in the hydrogel.

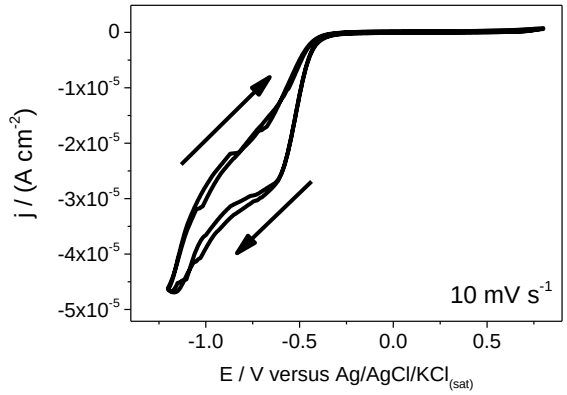

A

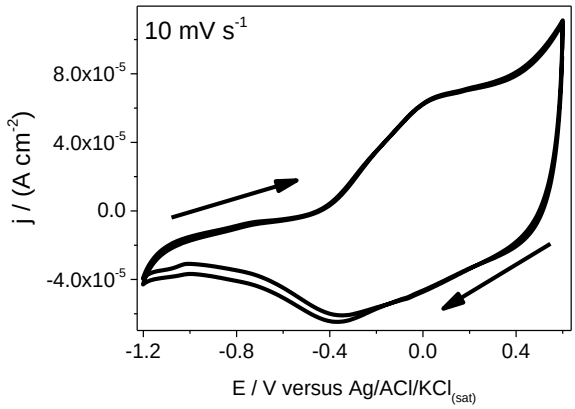

B

Figure 22. **A**: cyclic voltammogram of an ITO/silane/f-h-PAAM (control). **B**: cyclic voltammogram of an ITO/silane/f-h-PAAM&NPsAu@PEDOT. The initial potentials were the open circuit potentials: ca. +150 mV. Scan rate: 10 mV s^{-1}. Initial potential scans: increasing potential. The current is normalized by the geometrical area of the electrode (7.07 mm^2). 3 cycles were performed. Working electrode: modified ITO. Counter electrode: Pt plate. Reference electrode: $Ag/AgCl/KCl_{(sat)}$. Electrolyte: dyhydrogenphosphate/hydrogenphosphate buffer 20 mmol L^{-1} pH = 7.4 + NaCl 100 mmol L^{-1}. The electrolyte was deoxygenated by bubbling dry N_2 for at least 15 min prior to the experiment and keeping a N_2 atmosphere over the electrolyte throughout the experiment. ITO/silane/f-h-PAAM&NPsAu@PEDOT is the [film hydrogel of polyacrylamide on ITO] with core-shell NPsAu@PEDOT inserted by electroinsertion. The electroinsertion is performed applying a positive potential against an ITO, being the electrolyte reaction suspension of NPsAu@PEDOT. The films of hydrogels of polyacrylamide are formed over ITOs silanized in the surface. ITOs are silanized with tris-(2-methoxyethoxy)(vinyl)silane in toluene, removing and heating the ITOs at 100 ºC (373 K). Hydrogels of polyacrylamide are then formed from acrylamide, polyacrylamide, N,N'-methylenebisacrylamide and 2,2-diethoxyacetophenone in water over ITOs/silane, under ultraviolet radiation. NPsAu@PEDOT formed from $HAuCl_4$, EDOT and NaPSS in water, under stirring for hours.

4.5. Electrochromic behavior of NPsAu@PEDOT

After the electrodeposition of core-shell NPsAu@PEDOT on ITOs, described in **Subsection 3.4.4.1**, spectroelectrochemical experiments were done with the modified electrodes. **Figure 24** presents the cyclic voltabsorgrams for ITOs/NPsAu@PEDOT made by electrodeposition for different times (1 h, 2 h and 6 h). The 1 h electrodeposition-CV presents very distinct redox peaks at ca. −100 mV (oxidation peak) and ca. −400 mV (reduction peak), the peaks and CV shape of immobilized PEDOT/PSS. The transmittance at 600 nm was acquired simultaneously to the potential scan. ΔT_{600nm} (T_{600nm} is transmittance at 600 nm, Δ is variation of, ΔT_{600nm} is the electrochromic contrast at 600 nm) is ca. 60% relative to the maximum, demonstrating the electrochromic behavior and the color changes of PEDOT in the film. For 2 h of electrodeposition the CV is very similar. ΔT_{600nm} is greater, ca. 70%. For 5 h of deposition the CV is different, the oxidation peak disappears even though more material is deposited. This may indicate the film has become so thick that in a voltammetry at 10 mV s^{-1} (180 s from minimum to maximum potential) the counter-ions cannot completely diffuse throughout the film, or part of the polymer is losing its electric communication with ITO. Other electrochromic parameters could not be calculated. Therefore, the electrodeposition of NPsAu@PEDOT beyond 2 h impairs the electrochromic properties of the film, being the sample of **Figure 23B** the ideal to electrochromic transmissive layers. The core-shell structure of NPsAu@PEDOT makes the electric communication between PEDOT and the electrode very efficient and so ΔT_{600nm} is high. The performance is superior to that of GCE/PEDOT [86].

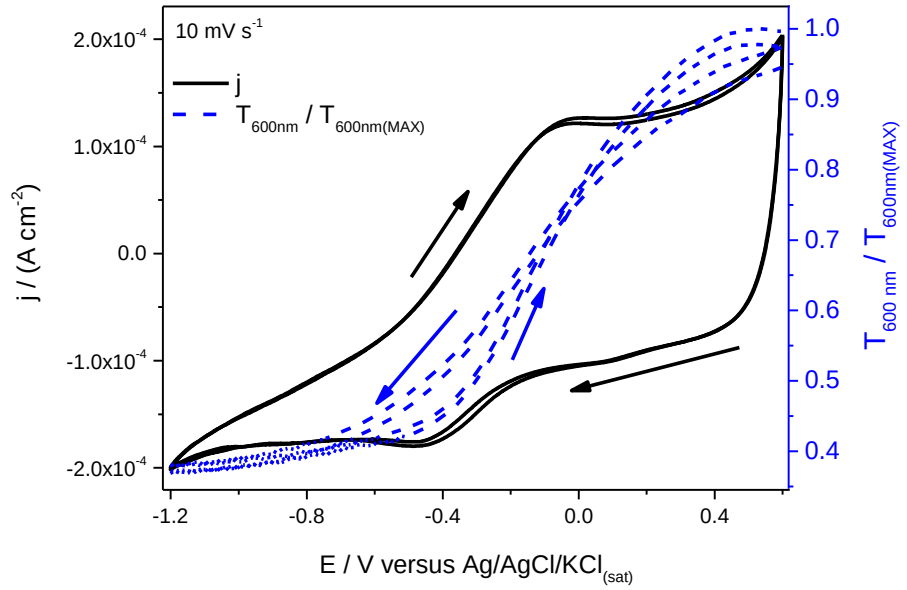

A

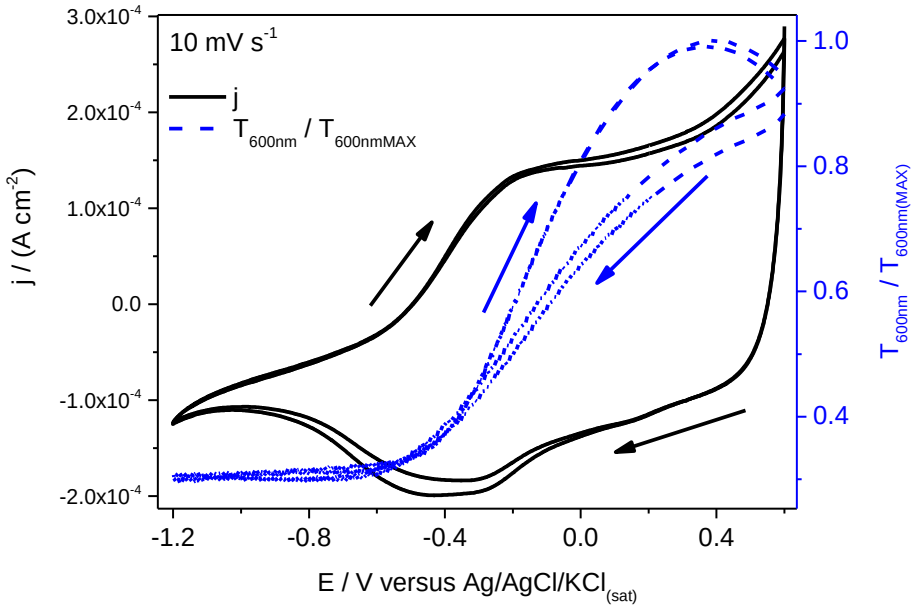

B

Figure 23. (Continues on next page, legend on next page).

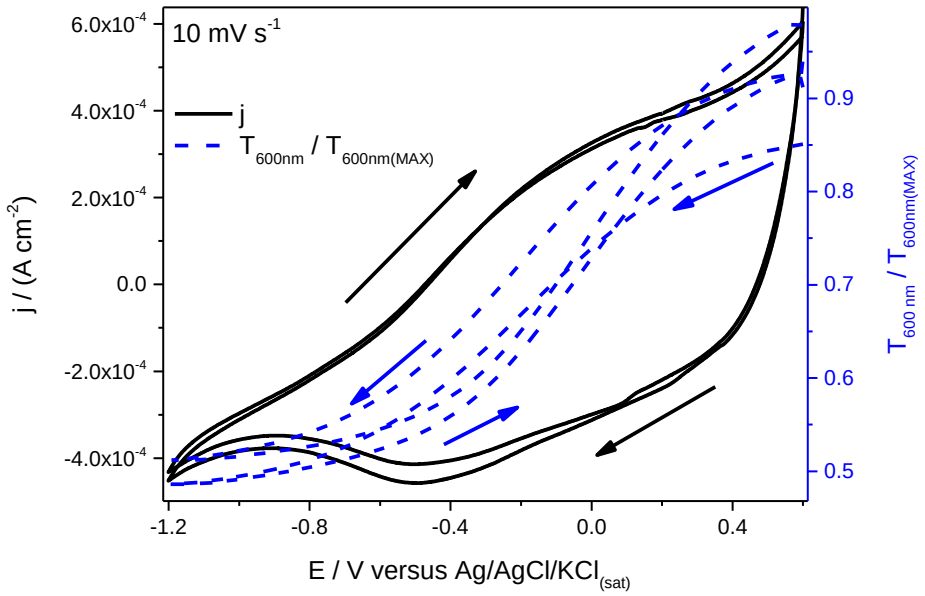

C

Figure 23. (Continuation). Cyclic voltabsorgrams (i (black curve, solid lines) and T (blue curve, dashed lines) x E) of an ITO/NPsAu@PEDOT (i and T x E). Scan rate: 10 mV s^{-1}. Initial potential: +600 mV. Initial scans: decreasing potential. Wavelength of light: 600 nm. The current was normalized by the geometrical area of electrode (0.5 cm^2). 3 cycles were performed, cycles 2 and 3 showed. Working electrode: modified ITO. Counter electrode: Pt plate. Reference electrode: $Ag/AgCl/KCl_{(sat)}$. Electrolyte: dyhydrogenphosphate/hydrogenphosphate buffer 20 mmol L^{-1} pH = 7.4 + NaCl 100 mmol L^{-1}. The electrolyte was deoxygenated by bubbling dry N_2 for at least 15 min prior to the experiment and keeping a N_2 atmosphere over the electrolyte throughout the experiment. NPsAu@PEDOT were deposited on ITO by electrodeposition, applying a positive potential to it versus another ITO, being the electrolyte the reaction suspension of NPsAu@PEDOT. Electrodeposition was performed for 1 h (**A**), 2 h (**B**) and 5 h (**C**). NPsAu@PEDOT formed from $HAuCl_4$, EDOT and NaPSS in water, under stirring for hours.

Figure 24 presents the superimposed ($dAbs_{600nm}$ / dE) x E and j x E. (dAbs600nm / dE) is the derivative of the absorbance relative to E, which was calculated with the data of **Figure 23**. dAbs600nm / dE shows the speed at which the UV-Vis-NIR spectra is changing. For 1 h of electrodeposition, $dAbs_{600nm}$ / dE has 2 peaks at ca. −0.2 V (maximum) and ca. −0.3 V (minimum), near to the peaks of current. For 2 of electrodeposition h the same behavior is observed. The peaks in dAbs600nm / dE are directly related to the redox peaks of the CVs, showing that the injection of charge is promoting the reduction of PEDOT and the change in its optical properties.

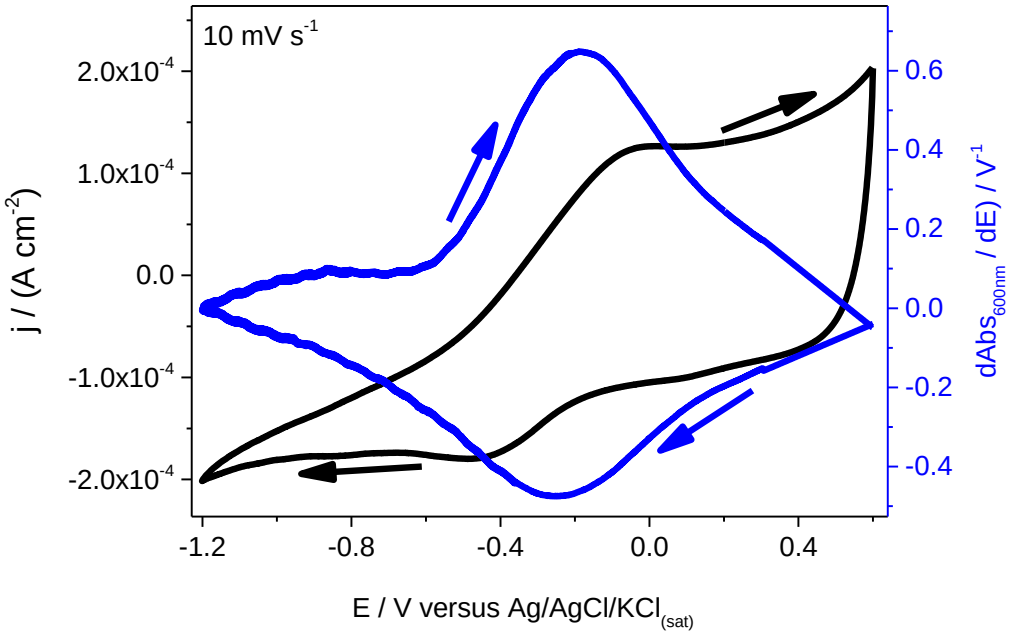

A

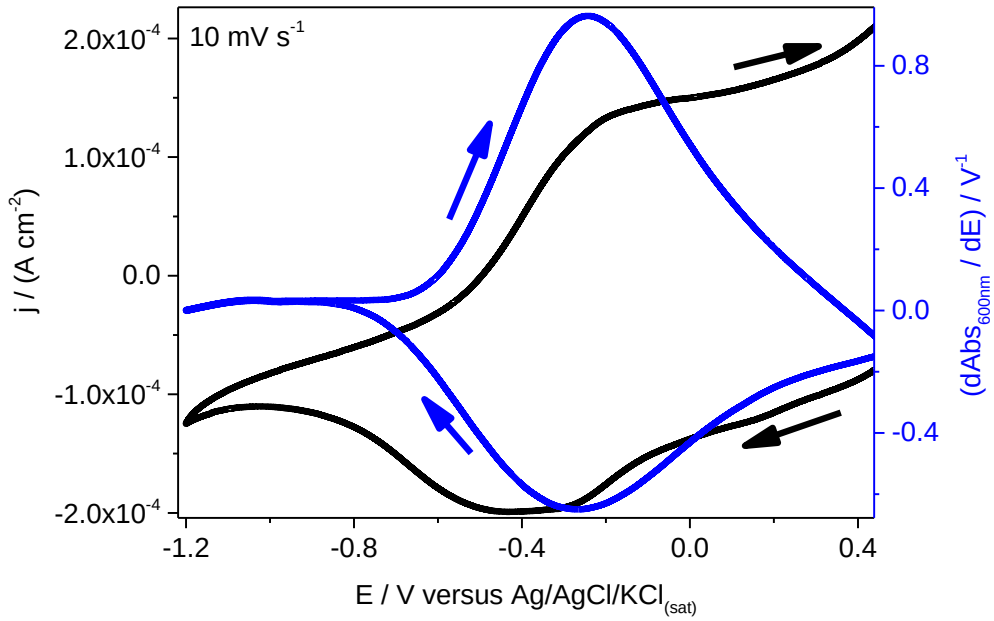

B

Figure 24. (Continues on next page, legend on next page).

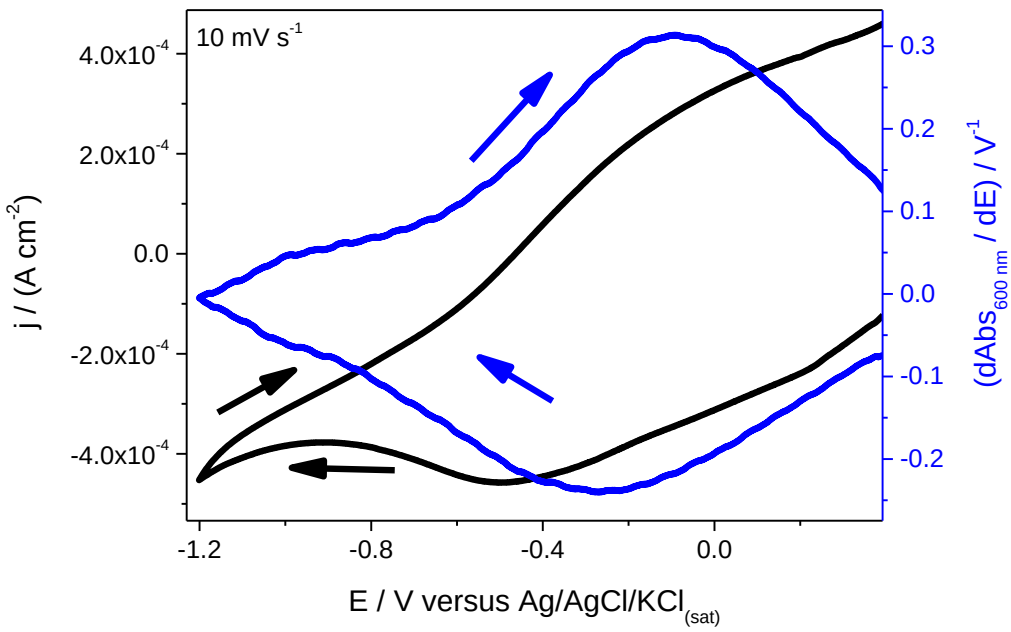

C

Figure 24. (Continuation). Cyclic voltabsorgrams of an ITO/NPsAu@PEDOT of **Figure 23** i (black curve) x E and $dAbs_{600nm}$ / dE (blue curve) x E. The graph is generated calculating $dAbs_{600nm}$/dE for the graph of **Figure 23**. Scan rate: 10 mV s^{-1}. Initial potential: +600 mV. Initial scans: decreasing potential. Wavelength of light: 600 nm. The current was normalized by the geometrical area of electrode (0.5 cm^2). 3 cycles were performed, cycle 3 showed. Working electrode: modified ITO. Counter electrode: Pt plate. Reference electrode: $Ag/AgCl/KCl_{(sat)}$. Electrolyte: dyhydrogenphosphate/hydrogenphosphate buffer 20 mmol L^{-1} pH = 7.4 + NaCl 100 mmol L^{-1}. The electrolyte was deoxygenated by bubbling dry N_2 for at least 15 min prior to the experiment and keeping a N_2 atmosphere over the electrolyte throughout the experiment. NPsAu@PEDOT were deposited on ITO by electrodeposition, applying a positive potential to it versus another ITO, being the electrolyte the reaction suspension of NPsAu@PEDOT. Electrodeposition was performed for 1 h (**A**), 2 h (**B**) and 5 h (**C**). NPsAu@PEDOT formed from $HAuCl_4$, EDOT and NaPSS in water, under stirring for hours.

4.6. Electrochemical detection of H_2O_2 with modified electrodes

After the electrochemical characterization of the modified GCE/NPsAu/PEDOT-PLA (deposited by casting), the electrodes were studied for the electrochemical detection of $H_2O_{2(aq)}$. In alkaline medium, it can be electrochemically reduced to $OH^-_{(aq)}$ through the following reaction (**Equation 13**).

$$H_2O_{2(aq)} + 2e^- \rightarrow 2OH^-_{(aq)}$$

Equation 13. Half-reaction of reduction of H_2O_2 to OH^- in alkaline medium.

Applying a negative potential to the working electrode so that $[H_2O_2]$ in the surface of the electrode is almost 0 allow it to correlate the limit current density of reduction ($j_{RED,L}$) with the bulk $[H_2O_2]$, since $j_{RED,L}$ and $[H_2O_2]$ are in linear relation. Hydrogen peroxide was detected in solution by chronoamperometry at −300 mV (versus $Ag/AgCl/KCl_{(3\ mol\ L-1)}$). **Figure 25** presents the chronoamperograms and calibration curves of GCE and GCE/NPsAu/PEDOT-PLA. At first j was left to stabilize, and the initial current density (j_0) is near 0. In **Figure 25A** the first 10 additions of H_2O_2 (until 6750 s) were nominal (+1 mmol L^{-1}), while the last additions were nominal (+10 mmol L^{-1}). To the (+1 mmol L^{-1}) additions the density current j responses very linear and fast, it increases (in module) and stabilizes. To the (+10 mmol L^{-1}) additions the current density increments are linear but the response time is higher. It is not possible to obtain a control CV without gold nanoparticles for GCE/NPsAu/PEDOT-PLA (which would be a GCE/PEDOT-PLA electrode) because PEDOT-PLA is only formed when o-EDOT-PLA

are oxidized in the presence of gold nanoparticles, which catalyze the reaction. NPsAu increase the conductivity of the material.

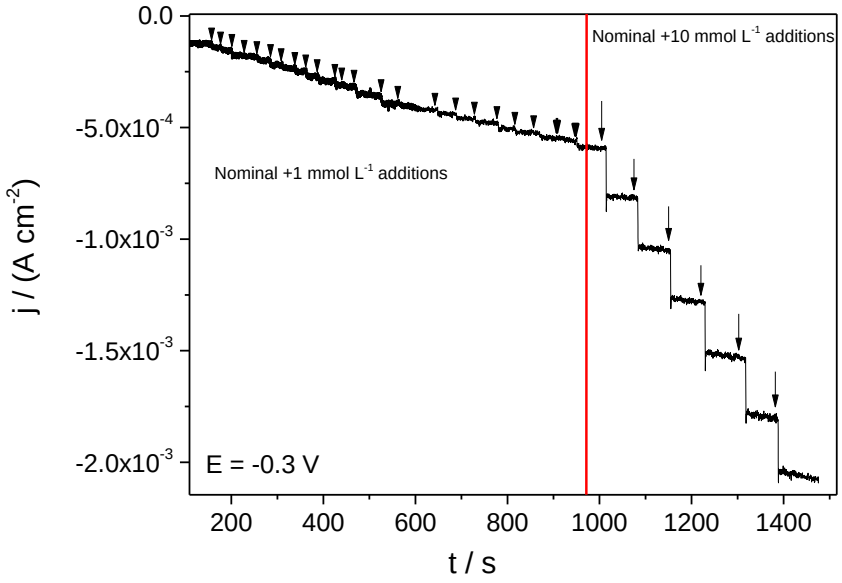

A

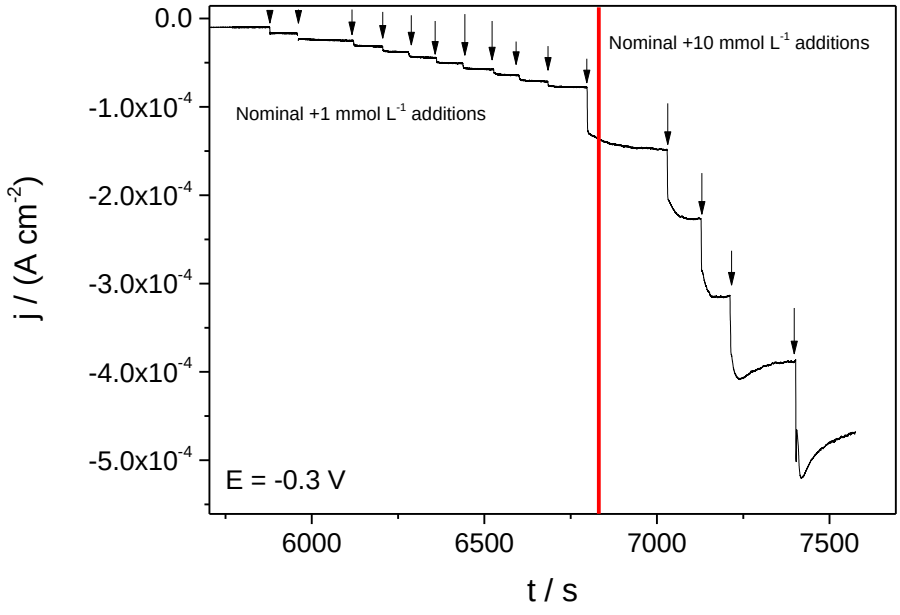

B

Figure 25. (Continuation). **A**: chronoamperogram of a GCE (control) with additions of H_2O_2 to the electrolyte at −300 mV. **B**: chronoamperogram of a GCE/NPsAu/PEDOT-PLA (deposited by casting, 10 steps) with additions of H_2O_2 to the electrolyte at −300 mV. Working electrodes:

GCEs. Counter electrode: Pt plate. Reference electrode: Ag/AgCl/$KCl_{(3\ mol\ L-1)}$. Electrolyte: dyhydrogenphosphate/hydrogenphosphate buffer 20 mmol L^{-1} pH = 7.4 + NaCl 100 mmol L^{-1}. The electrolyte was deoxygenated by bubbling dry N_2 for at least 15 min prior to the experiment and keeping a N_2 atmosphere over the electrolyte throughout the experiment. NPsAu/PEDOT-PLA deposited on GCE adding a small drop of NPsAu/PEDOT-PLA on GCE and drying it at 40 ºC (313 K) in vacuum. NPsAu/PEDOT-PLA formed from the reaction suspension of NPsAu/o-EDOT-PLA and potassium peroxydisulfate in acetonitrile, under stirring for days.

The analytical parameters for the electrochemical sensors of H_2O_2 of **Figure 25** were calculated and are in **Table 3**, compared with analytical parameters of sensors from the literature containing PEDOT. There is a diversity of elements, materials, strategies and technologies to prepare them. The data $(j-j_0)$ x $[H_2O_2]$ was linearly fitted and the value R^2 = 0.993 for GCE and R^2 = 0.996 for GCE/NPsAu/PEDOT-PLA. Therefore, the experimental curves $(j-j_0)$ x $[H_2O_2]$ are linear and the sensors work. The calibration equation of GCE is **Equation 14**, and the calibration equation of GCE/NPsAu/PEDOT-PLA is **Equation 15**. It is observed the sensitivity of GCE/NPsAu/PEDOT-PLA is much higher than that of GCE, and the linear range of GCE/NPsAu/PEDOT-PLA is large and reaches almost two decades of concentration. This linear range suggest GCE/NPsAu/PEDOT-PLA as a sensor of $H_2O_{2(aq)}$ for in situ analysis in aqueous media in which there are reactions happening that form H_2O_2. In **Table 3** the analytical values of the sensors described here are calculated by the geometrical area of GCE electrode, although the film deposited is thick and 3-dimensional. It can be concluded that the hybrid NPsAu/PEDOT-PLA is conducting, highly catalytic to the electroreduction of H_2O_2 and allows the insertion of H_2O_2, which reaches the sites at the gold nanoparticles inside the matrix of polymer. In fact, GCE/NPsAu/PEDOT-PLA has the second highest sensitivity among the sensors of **Table 3** (the first is that of SPC/PEDOT/NPsPt [96], which contains Pt nanoparticles deposited over PEDOT). This indicates high electroactive area and high density of active sites. The sensors from the works of Lin et al. [97] (carbon nanotubes), Chen et al. [98] (nanowiskers of PEDOT) and Nabid et al. [99] (nanofibers of PEDOT) also have great effect of surface area, which increases sensitivity. The limits of detection are calculated

as (3 x standard deviation of blank of analyte / sensitivity). The limits of quantification are calculated as (10 x standard deviation of blank of analyte / sensitivity). In complex, real samples many electroactive chemical species may be present, like organic molecules. At the applied potential of **Figure 25** (−300 mV versus Ag/AgCl/$KCl_{(3\ mol\ L-1)}$) there are no oxidation reactions of uric acid, ascorbic acid, dopamine etc. This is an advantage and favors the selectivity towards H_2O_2 of the sensor. This is important for glucose sensors in blood, which contains these organic molecules. There is also the possibility of non-specific adsorption of proteins on NPsAu. GCE/NPsAu/PEDOT-PLA could be recovered by a permeable layer of polymer to enhance its selectivity. One strategy to determine glucose in blood is chronoamperometric sensing with a working electrode with an immobilized enzyme that oxidizes glucose to H_2O_2, which is then oxidized or reduced at the surface of the electrode. GCE/NPsAu/PEDOT-PLA is suitable for the (mmol L^{-1}) H_2O_2 concentrations range. The density current noise was high during the experiment and the response time varied up to 200 s (for the highest concentrations). The ability of NPsAu/PEDOT-PLA as a stable, biodegradable polymer-based, electrochemical sensor is demonstrated.

Table 3. Potential of detection (E), linear range (LR), sensitivity (Sen), limit of detection (LD) and limit of quantification (LQ) of chronoamperometric sensors of H_2O_2 containing PEDOT hybrids. a: PEDOT and NPsPt hybrid over printed carbon electrode (SPC). b: multiwall carbon nanotubes (MWCNTs) and PEDOT hybrid on GCE. c: hybrid of PEDOT and nanoparticles of Cu and Cu hexacyanoferrate (NPsCu-$Cu_2[Fe(CN)_6]$). d: hybrid of PEDOT nanowiskers (NWs), NPsAu and hemoglobin (Hb). e: PEDOT and Prussian Blue (PB) nanoparticles hybrid. f: PEDOT nanofibers (NFs) and NPsPd (palladium nanoparticles) hybrid. E in this Table refers to $Ag/AgCl/KCl_{(3\ mol\ L-1)}$. The limits of detection are calculated as (3 x standard deviation of blank of analyte / sensitivity). The limits of quantification are calculated as (10 x standard deviation of blank of analyte / sensitivity). Chronoamperometric detection performed in this work: working electrodes: GCEs. Counter electrode: Pt plates. Reference electrode: $Ag/AgCl/KCl_{(3\ mol\ L-1)}$. Electrolyte: dyhydrogenphosphate/hydrogenphosphate buffer 20 mmol L^{-1} pH = 7.4 + NaCl 100 mmol L^{-1}. The electrolyte was deoxygenated by bubbling dry N_2 for at least 15 min prior to the experiment and keeping a N_2 atmosphere over the electrolyte throughout the experiment. NPsAu/PEDOT-PLA deposited on GCE adding a small drop of NPsAu/PEDOT-PLA on GCE and drying it at 40 ºC (313 K) in vacuum. NPsAu/PEDOT-PLA formed from the reaction suspension of NPsAu/o-EDOT-PLA and potassium peroxydisulfate in acetonitrile, under stirring for days.

Sensor	**E / mV**	**LR / (mol L^{-1})**	**Sen / (A cm^{-2} mol^{-1} L)**	**LD / (mol L^{-1})**	**LQ / (mol L^{-1})**	**Reference**
SPC/PEDOT/ NPsPt[a]	−538	$1.62x10^{-6}$ – $6x10^{-3}$	$1.929x10^{-2}$	$1.6x10^{-6}$	$5.3x10^{-6}$	[96]
MWCNTs/ PEDOT[b]	−488	10^{-4} – $9.8x10^{-3}$	-	$5x10^{-5}$ – 10^{-2}	$1.6x10^{-4}$ – $3.3x10^{-2}$	[97]
Pd/PEDOT	−153	$2.84x10^{-6}$ – 10^{-3}	$2.153x10^{-4}$	$2.84x10^{-6}$	$9.5x10^{-6}$	[100]
PEDOT/NPsCu-$Cu_2[Fe(CN_6)]$[c]	−188	10^{-6} – $5.4x10^{-4}$	$1.670x10^{-3}$	10^{-7}	$3.3x10^{-7}$	[101]
GCE/PEDOT/ PSS/Pd	-	10^{-4} – $5x10^{-3}$	-	-	-	[102]
NWsPEDOT/NPs Au/Hb[d]	−253	$6x10^{-4}$ – $1.100x10^{-3}$	$3.13x10^{-4}$	$6x10^{-4}$	$2x10^{-3}$	[98]
GCE/PEDOT/ NPsAg	−28	-	-	$6.1x10^{-7}$	$2.0x10^{-6}$	[103]
PEDOT/NPsPB[e]	+11	$5x10^{-7}$ – $8.39x10^{-6}$	-	$1.6x10^{-7}$	$5.3x10^{-7}$	[104]
NFsPEDOT/NPs Pd[f]	−288	$2x10^{-7}$ – $2.5x10^{-5}$	-	$5x10^{-8}$	$1.6x10^{-7}$	[99]
GCE/NPsAu/ PEDOT-PLA	−300	$5.1x10^{-4}$ – $4.5x10^{-2}$	$8.4x10^{-3}$	$1.7x10^{-4}$	$5.7x10^{-4}$	This Thesis
GCE	−300	$1x10^{-3}$ – $22x10^{-3}$	$1.0x10^{-3}$	$1.9x10^{-3}$	$6.3x10^{-3}$	This Thesis

Sources: Chang et al. [96], Lin et al. [97], Jiang et al. [100], Tsai et al. [101], Smolin et al. [102], Chen et al. [98], Rad et al. [103], Wang et al. [104], Nabid et al. [99].

$$(j_{RED,L} - j_0)\ (\text{in A cm}^{-2}) = 2.4\text{x}10^{-7} - 1.0\text{x}10^{-3}\ \text{x}\ [H_2O_{2(aq)}]\ (\text{in mol L}^{-1})$$

Equation 14. Calibration equation of the sensor GCE/NPsAu/PEDOT-PLA for H_2O_2. Chronoamperometry conditions: working electrodes: GCE/NPsAu/PEDOT-PLA. Counter electrode: Pt plate. Reference electrode: $Ag/AgCl/KCl_{(3\ mol\ L-1)}$. Electrolyte: dyhydrogenphosphate/hydrogenphosphate buffer 20 mmol L^{-1} pH = 7.4 + NaCl 100 mmol L^{-1}. The electrolyte was deoxygenated by bubbling dry N_2 for at least 15 min prior to the experiment and keeping a N_2 atmosphere over the electrolyte throughout the experiment. NPsAu/PEDOT-PLA deposited on GCEs adding a small drop of NPsAu/PEDOT-PLA on GCE and drying it at 40 ºC (313 K) in vacuum (10 steps of casting performed). NPsAu/PEDOT-PLA formed from the reaction suspension of NPsAu/o-EDOT-PLA and potassium peroxydisulfate in acetonitrile, under stirring for days. NPsAu/PEDOT-PLA formed from the reaction suspension of NPsAu/o-EDOT-PLA and potassium peroxydisulfate in acetonitrile, under stirring for days.

$$(j_{RED,L} - j_0)\ (\text{in A cm}^{-2}) = 8.6\text{x}10^{-6} - 8.4\text{x}10^{-3}\ \text{x}\ [H_2O_{2(aq)}]\ (\text{in mol L}^{-1})$$

Equation 15. Calibration equation of the sensor GCE/NPsAu/PEDOT-PLA for H_2O_2. Chronoamperometry conditions: working electrodes: GCE/NPsAu/PEDOT-PLA. Counter electrode: Pt plate. Reference electrode: $Ag/AgCl/KCl_{(3\ mol\ L-1)}$. Electrolyte: dyhydrogenphosphate/hydrogenphosphate buffer 20 mmol L^{-1} pH = 7.4 + NaCl 100 mmol L^{-1}. The electrolyte was deoxygenated by bubbling dry N_2 for at least 15 min prior to the experiment and keeping a N_2 atmosphere over the electrolyte throughout the experiment. NPsAu/PEDOT-PLA deposited on GCEs adding a small drop of NPsAu/PEDOT-PLA on GCE and drying it at 40 ºC (313 K) in vacuum (10 steps of casting performed). NPsAu/PEDOT-PLA formed from the reaction suspension of NPsAu/o-EDOT-PLA and potassium peroxydisulfate in acetonitrile, under stirring for days. NPsAu/PEDOT-PLA formed from the reaction suspension of NPsAu/o-EDOT-PLA and potassium peroxydisulfate in acetonitrile, under stirring for days.

5. CONCLUSIONS

This Thesis described for the first time the synthesis of inorganic/organic hybrids based on EDOT-poly(lactic acid): NPsAu/o-EDOT-PLA (oligomers) and NPsAu/PEDOT-PLA (polymer); and also the complete polymerization of EDOT-PLA catalyzed by Au nanoparticles dispersed in the matrix. PEDOT-PLA is a new conducting polymer based on poly(lactic acid).

The syntheses of core-shell NPsAu@PEDOT and of NPsPt/PEDOT were also studied, followed through UV-Vis-NIR, and the plasmonic bands were observed. NPsPt/PEDOT consists of highly homogenous platinum nanoparticles surrounded by the matrix of PEDOT. All hybrids present nanoparticles with maximum distributions at less than 10 nm.

Nanoparticles/PEDOTs hybrids (negatively charges) were electrodeposited in ITOs, and form stable films which show the electrochromism of PEDOT with high electrochromic contrast due to the structure of the material and the singular electric contact of PEDOT.

Oxidative radical syntheses of hydrogels of poly(acrylic acid) or polyacrylamide were performed. Bulk hydrogels of poly(acrylamide) allow the insertion of gold or platinum nanoparticles driven by the applied potential difference to the system. Catalyzed chemical synthesis and uncatalyzed thermochemical synthesis of poly(acrylic acid) did not form films adherent to ITOs, so a different strategy was created to photopolymerize films of hydrogels of polyacrylamide over ITOs surfaces. With these modified electrodes the insertion of the produced hybrids driven by the applied potential

difference to the systems occurs, modifying the hydrogels. On the other hand, synthesis of gold or platinum nanoparticles directly in the hydrogels does not occur.

GCEs modified with NPsAu/PEDOT-PLA were tested as electrochemical sensors for hydrogen peroxide, by chronoamperometry, and exhibit excellent analytical properties towards it, being able to monitor H_2O_2 in a large range of concentrations. The Thesis demonstrates the versatility of hybrids of PEDOTs and gold or platinum nanoparticles to the development of new electrode materials that can be used in small electrochemical devices.

6. PERSPECTIVES FOR THE FUTURE

Further experiments can be planned with the materials described in this Thesis. Following the strategy of one-pot synthesis of gold and platinum nanoparticles the products can be dialyzed and the hybrids can be analyzed by elemental analysis and the amounts of gold or platinum. The hybrid materials deposited on ITOs can also be analyzed this way, and through the metal load the cost of the materials can be calculated.

The bulk hydrogels of poly(acrylic acid) and polyacrylamide modified with the hybrids of gold or platinum nanoparticles can also be applied to electrochemical detection and insertion/release of chemical species of interest, since they have huge 3-dimensional structure.

Since the biodegradability of EDOT-PLA and of o-EDOT-PLA is well demonstrated, next studies could evaluate the biodegradability of the polymer of EDOT-PLA hybrid NPsAu/PEDOT-PLA, which is the material sensor for H_2O_2.

7. BIBLIOGRAPHY

[1] D. A. Tomalia, “In quest of a systematic framework for unifying and defining nanoscience,” *J. Nanoparticle Res.*, vol. 11, no. 6, pp. 1251–1310, 2009.

[2] D. A. Tomalia and S. N. Khanna, “in Quest of a Systematic Framework for Unifying and Defining Nanoscience,” *Mod. Phys. Lett. B*, vol. 28, no. 03, p. 1430002, 2014.

[3] C. Joachim, “To be nano or not to be nano?,” *Nat. Mater.*, vol. 4, no. 2, pp. 107–109, 2005.

[4] M. A. Watzky and R. G. Finke, “Gold Nanoparticle Formation Kinetics and Mechanism: A Critical Analysis of the ‘Redox Crystallization’ Mechanism,” *ACS Omega*, vol. 3, no. 2, pp. 1555–1563, 2018.

[5] G. Schmid and B. Corain, “Nanoparticulated Gold: Syntheses, Structures, Electronics, and Reactivities,” *Eur. J. Inorg. Chem.*, vol. 2003, no. 17, pp. 3081–3098, 2003.

[6] G. J. Leong *et al.*, “Shape-directed platinum nanoparticle synthesis: Nanoscale design of novel catalysts,” *Appl. Organomet. Chem.*, vol. 28, no. 1, pp. 1–17, 2014.

[7] S. Cheong, J. D. Watt, and R. D. Tilley, “Shape control of platinum and palladium nanoparticles for catalysis,” *Nanoscale*, vol. 2, no. 10, p. 2045, 2010.

[8] I. Saldan, Y. Semenyuk, I. Marchuk, and O. Reshetnyak, “Chemical synthesis and application of palladium nanoparticles,” *J. Mater. Sci.*, vol. 50, no. 6, pp. 2337–2354, 2015.

[9] D. L. Huber, “Synthesis, properties, and applications of iron nanoparticles,” *Small*, vol. 1, no. 5, pp. 482–501, 2005.

[10] L. Chekli *et al.*, “Analytical characterisation of nanoscale zero-valent iron: A methodological review,” *Anal. Chim. Acta*, vol. 903, pp. 13–35, 2016.

[11] J. I. Abd-Elkareem, H. M. Bassuony, S. M. Mohammed, H. M. Fahmy, and N. R. Abd-Elkader, “Eco-friendly methods of copper nanoparticles synthesis,” *J. Bionanoscience*, vol. 10, no. 1, pp. 15–37, 2016.

[12] H. R. Ghorbani, “Chemical synthesis of copper nanoparticles,” *Orient. J. Chem.*, vol. 30, no. 2, pp. 803–806, 2014.

[13] H. Malekzad, P. Sahandi Zangabad, H. Mirshekari, M. Karimi, and M. R. Hamblin, “Noble metal nanoparticles in biosensors: Recent studies and applications,” *Nanotechnol. Rev.*, vol. 6, no. 3, pp. 301–329, 2017.

[14] M. I. Din and R. Rehan, “Synthesis, Characterization, and Applications of Copper Nanoparticles,” *Anal. Lett.*, vol. 50, no. 1, pp. 50–62, 2017.

[15] E. Abbasi *et al.*, “Silver nanoparticles: Synthesis methods, bio-applications and properties,” *Crit. Rev. Microbiol.*, vol. 42, no. 2, pp. 173–180, 2016.

[16] C. Y. Lai, C. F. Cheong, J. S. Mandeep, H. B. Abdullah, N. Amin, and K. W. Lai, “Synthesis and Characterization of Silver Nanoparticles and Silver Inks: Review on the Past and Recent Technology Roadmaps,” *J. Mater. Eng. Perform.*, vol. 23, no. 10, pp. 3541–3550, 2014.

[17] M. Guerrero *et al.*, “About the Use of Rhodium Nanoparticles in Hydrogenation and Hydroformylation Reactions,” *Curr. Org. Chem.*, vol. 17, no. 4, pp. 364–399, 2013.

[18] Y. Yuan, N. Yan, and P. J. Dyson, “Advances in the rational design of rhodium nanoparticle catalysts: Control via manipulation of the nanoparticle core and stabilizer,” *ACS Catal.*, vol. 2, no. 6, pp. 1057–1069, 2012.
[19] J. D. Scholten and J. Dupont, “Catalytic Properties of Soluble Iridium Nanoparticles,” *Iridium Complexes Org. Synth.*, no. I, pp. 369–389, 2009.
[20] L. M. Martínez-Prieto and B. Chaudret, “Organometallic Ruthenium Nanoparticles: Synthesis, Surface Chemistry, and Insights into Ligand Coordination,” *Acc. Chem. Res.*, vol. 51, pp. 970–977, 2018.
[21] P. Lara, K. Philippot, and B. Chaudret, “Organometallic Ruthenium Nanoparticles: A Comparative Study of the Influence of the Stabilizer on their Characteristics and Reactivity,” *ChemCatChem*, vol. 5, no. 1, pp. 28–45, 2013.
[22] G. Elango and S. M. Roopan, “Green synthesis, spectroscopic investigation and photocatalytic activity of lead nanoparticles,” *Spectrochim. Acta - Part A Mol. Biomol. Spectrosc.*, vol. 139, pp. 367–373, 2015.
[23] M. L. Zhang, C. Feng, W. X. Zhang, X. W. Luan, J. Jiang, and L. F. Li, “Synthesis of Bismuth Nanoparticles by a Simple One-Step Solvothermal Reduction Route,” *Appl. Mech. Mater.*, vol. 423–426, no. 3, pp. 155–158, 2013.
[24] M. A. De Paoli and W. A. Gazotti, “Electrochemistry, Polymers and Opto-Electronic Devices: A Combination with a Future,” vol. 13, no. 4, pp. 410–424, 2002.
[25] Q. Pei, G. Zuccarello, M. Ahlskogt, and O. Ingan, “Electrochromic and highly stable poly(3,4- ethylenedioxythiophene) switches between opaque blue-black and transparent sky blue,” *Polym. Pap.*, vol. 35, no. 7, pp. 1347–1351, 1994.
[26] J. Perdew *et al.*, “Atoms, molecules, solids, and surfaces: Applications of the generalized gradient approximation for exchange and correlation,” *Phys. Rev. B*, vol. 46, no. 11, pp. 6671–6687, 1992.
[27] S. Upadhyay, G. R. Rao, M. K. Sharma, B. K. Bhattacharya, V. K. Rao, and R. Vijayaraghavan, “Immobilization of acetylcholineesterase-choline oxidase on a gold-platinum bimetallic nanoparticles modified glassy carbon electrode for the sensitive detection of organophosphate pesticides, carbamates and nerve agents.,” *Biosens. Bioelectron.*, vol. 25, no. 4, pp. 832–8, Dec. 2009.
[28] O. Zhang, H. Yu, L. Lu, Y. Wen, X. Duan, and J. Xu, “Poly(thiophene-3-acetic acid)-palladium nanoparticle composite modified electrodes for supersensitive determination of hydrazine,” *Chinese J. Polym. Sci.*, vol. 31, no. 3, pp. 419–426, Dec. 2012.
[29] Y. Yao, Y. Wen, L. Zhang, J. Xu, Z. Wang, and X. Duan, “A Stable Sandwich-Type Hydrogen Peroxide Sensor Based on Immobilizing Horseradish Peroxidase to a Silver Nanoparticle Monolayer Supported by PEDOT : PSS-Nafion Composite Electrode,” vol. 8, pp. 9348–9359, 2013.
[30] H.-B. Noh, P. Kumar, T. K. Biswas, D.-S. Kim, and Y.-B. Shim, “Improved Performance of an Amperometric Biosensor with Polydiaminonaphthalene on Electrochemically Deposited Au Nanoparticles,” *Electroanalysis*, vol. 22, no. 6, pp. 632–638, Mar. 2010.
[31] S. Tuncagil, C. Ozdemir, D. O. Demirkol, S. Timur, and L. Toppare, “Gold nanoparticle modified conducting polymer of 4-(2,5-di(thiophen-2-yl)-1H-pyrrole-1-l) benzenamine for potential use as a biosensing material,” *Food Chem.*, vol. 127,

no. 3, pp. 1317–1322, Aug. 2011.
[32] M. Atmeh and B. E. Alcock-Earley, “A conducting polymer/Ag nanoparticle composite as a nitrate sensor,” *J. Appl. Electrochem.*, vol. 41, no. 11, pp. 1341–1347, Sep. 2011.
[33] Q. Liu, M. H. Nayfeh, and S.-T. Yau, “A silicon nanoparticle-based polymeric nano-composite material for glucose sensing,” *J. Electroanal. Chem.*, vol. 657, no. 1–2, pp. 172–175, Jul. 2011.
[34] I. Marinov, Y. Ivanov, K. Gabrovska, and T. Godjevargova, “Amperometric acetylthiocholine sensor based on acetylcholinesterase immobilized on nanostructured polymer membrane containing gold nanoparticles,” *J. Mol. Catal. B Enzym.*, vol. 62, no. 1, pp. 66–74, Jan. 2010.
[35] V. Mazeiko, A. Kausaite-Minkstimiene, A. Ramanaviciene, Z. Balevicius, and A. Ramanavicius, “Gold nanoparticle and conducting polymer-polyaniline-based nanocomposites for glucose biosensor design,” *Sensors Actuators B Chem.*, vol. 189, pp. 187–193, Dec. 2013.
[36] N. F. Atta and M. F. El-Kady, “Novel poly(3-methylthiophene)/Pd, Pt nanoparticle sensor: Synthesis, characterization and its application to the simultaneous analysis of dopamine and ascorbic acid in biological fluids,” *Sensors Actuators B Chem.*, vol. 145, no. 1, pp. 299–310, Mar. 2010.
[37] N. German, A. Ramanavicius, J. Voronovic, and A. Ramanaviciene, “Glucose biosensor based on glucose oxidase and gold nanoparticles of different sizes covered by polypyrrole layer,” *Colloids Surfaces A Physicochem. Eng. Asp.*, vol. 413, pp. 224–230, Nov. 2012.
[38] Y. Wen, J. Xu, D. Li, M. Liu, F. Kong, and H. He, “A novel electrochemical biosensing platform based on poly(3,4-ethylenedioxythiophene):poly(styrenesulfonate) composites,” *Synth. Met.*, vol. 162, no. 13–14, pp. 1308–1314, Aug. 2012.
[39] S. Balamurugan, A. Obubuafo, S. A. Soper, and D. A. Spivak, “Surface immobilization methods for aptamer diagnostic applications,” pp. 1009–1021, 2008.
[40] A. Balamurugan and S.-M. Chen, “Silver Nanograins Incorporated PEDOT Modified Electrode for Electrocatalytic Sensing of Hydrogen Peroxide,” *Electroanalysis*, vol. 21, no. 12, pp. 1419–1423, Jun. 2009.
[41] A. Balamurugan, K.-C. Ho, and S.-M. Chen, “One-pot synthesis of highly stable silver nanoparticles-conducting polymer nanocomposite and its catalytic application,” *Synth. Met.*, vol. 159, no. 23–24, pp. 2544–2549, Dec. 2009.
[42] N. G. Semaltianos, W. Perrie, S. Romani, R. J. Potter, G. Dearden, and K. G. Watkins, “Polymer-nanoparticle composites composed of PEDOT:PSS and nanoparticles of Ag synthesised by laser ablation,” *Colloid Polym. Sci.*, vol. 290, no. 3, pp. 213–220, Nov. 2011.
[43] S. Radhakrishnan, C. Sumathi, A. Umar, S. Jae Kim, J. Wilson, and V. Dharuman, “Polypyrrole-poly(3,4-ethylenedioxythiophene)-Ag (PPy-PEDOT-Ag) nanocomposite films for label-free electrochemical DNA sensing.,” *Biosens. Bioelectron.*, vol. 47, pp. 133–40, Sep. 2013.
[44] S.-J. Wang, Y.-J. Choi, and H.-H. Park, “Synthesis and characterization of Pt nanoparticles assembled in poly(3,4-ethylenedioxythiophene):polystyrene

sulfonate," *Ceram. Int.*, vol. 38, pp. S453–S456, Jan. 2012.
[45] S. Adibi, N. Adibi, R. Malekfar, and S. Davatolhagh, "Structural, morphology and optical properties of ITO/PEDOT:PSS and ITO/Ag nanoparticles/PEDOT:PSS thin films," *Eur. Phys. J. Appl. Phys.*, vol. 61, no. 3, p. 30301, Mar. 2013.
[46] S.-J. Wang, Y.-J. Choi, and H.-H. Park, "Investigation of Ag-poly(3,4-ethylenedioxythiophene):polystyrene sulfonate nanocomposite films prepared by a one-step aqueous method," *J. Appl. Phys.*, vol. 109, no. 12, p. 124902, 2011.
[47] S. Woo, J. H. Jeong, H. K. Lyu, Y. S. Han, and Y. Kim, "In situ-prepared composite materials of PEDOT: PSS buffer layer-metal nanoparticles and their application to organic solar cells.," *Nanoscale Res. Lett.*, vol. 7, no. 1, p. 641, Jan. 2012.
[48] P. Xu *et al.*, "Conjugated polymer mediated synthesis of nanoparticle clusters and core/shell nanoparticles," *Polymer (Guildf).*, vol. 54, no. 2, pp. 485–489, Jan. 2013.
[49] C. M. Welch and R. G. Compton, "The use of nanoparticles in electroanalysis: a review.," *Anal. Bioanal. Chem.*, vol. 384, no. 3, pp. 601–19, Feb. 2006.
[50] V. V. Kondratiev, N. a. Pogulaichenko, S. Hui, E. G. Tolstopjatova, and V. V. Malev, "Electroless deposition of gold into poly-3,4-ethylenedioxythiophene films and their characterization performed in chloride-containing solutions," *J. Solid State Electrochem.*, vol. 16, no. 3, pp. 1291–1299, Aug. 2011.
[51] V. V. Kondratiev, N. a. Pogulaichenko, E. G. Tolstopjatova, and V. V. Malev, "Hydrogen peroxide electroreduction on composite PEDOT films with included gold nanoparticles," *J. Solid State Electrochem.*, vol. 15, no. 11–12, pp. 2383–2393, Jul. 2011.
[52] T. He, Y. Ma, Y. Cao, Y. Yin, W. Yang, and J. Yao, "Enhanced visible-light coloration and its mechanism of MoO3 thin fms by Au nanoparticles," *Appl. Surf. Sci.*, vol. 180, pp. 336–340, 2001.
[53] S. Prakash, C. R. K. Rao, and M. Vijayan, "Polyaniline–polyelectrolyte–gold(0) ternary nanocomposites: Synthesis and electrochemical properties," *Electrochim. Acta*, vol. 54, no. 24, pp. 5919–5927, Oct. 2009.
[54] K. W. Park, "Electrochromic properties of Au-WO3 nanocomposite thin-film electrode," *Electrochim. Acta*, vol. 50, no. February, pp. 4690–4693, 2005.
[55] S. H. Cho and S.-M. Park, "Electrochemistry of conductive polymers 39. Contacts between conducting polymers and noble metal nanoparticles studied by current-sensing atomic force microscopy.," *J. Phys. Chem. B*, vol. 110, no. 51, pp. 25656–64, Dec. 2006.
[56] N. F. Atta, A. Galal, and E. H. El-Ads, "Gold nanoparticles-coated poly(3,4-ethylene-dioxythiophene) for the selective determination of sub-nano concentrations of dopamine in presence of sodium dodecyl sulfate," *Electrochim. Acta*, vol. 69, pp. 102–111, May 2012.
[57] Y.-C. Liu and T. C. Chuang, "Synthesis and Characterization of Gold/Polypyrrole Core−Shell Nanocomposites and Elemental Gold Nanoparticles Based on the Gold-Containing Nanocomplexes Prepared by Electrochemical Methods in Aqueous Solutions," *J. Phys. Chem. B*, vol. 107, no. 45, pp. 12383–12386, Nov. 2003.
[58] M. Giannetto, G. Mori, F. Terzi, C. Zanardi, and R. Seeber, "Composite PEDOT/Au Nanoparticles Modified Electrodes for Determination of Mercury at

Trace Levels by Anodic Stripping Voltammetry," *Electroanalysis*, vol. 23, no. 2, pp. 456–462, Feb. 2011.

[59] K. M. Manesh, P. Santhosh, a Gopalan, and K. P. Lee, "Electrocatalytic oxidation of NADH at gold nanoparticles loaded poly(3,4-ethylenedioxythiophene)-poly(styrene sulfonic acid) film modified electrode and integration of alcohol dehydrogenase for alcohol sensing.," *Talanta*, vol. 75, no. 5, pp. 1307–14, Jun. 2008.

[60] S. V. Selvaganesh, J. Mathiyarasu, K. L. N. Phani, and V. Yegnaraman, "Chemical Synthesis of PEDOT–Au Nanocomposite," *Nanoscale Res. Lett.*, vol. 2, no. 11, pp. 546–549, Oct. 2007.

[61] M. Mumtaz *et al.*, "Hybrid PEDOT-Metal Nanoparticles - New Substitutes for PEDOT:PSS in Electrochromic Layers - Towards Improved Performance," *Eur. J. Inorg. Chem.*, vol. 2012, no. 32, pp. 5360–5370, Nov. 2012.

[62] J. S. Lee, Y.-J. Choi, S.-J. Wang, H.-H. Park, and J. C. Pyun, "Characterization of Au-metal nanoparticle-hybridized poly (3,4-ethylenedioxythiophene) films for electrochromic devices," *Phys. Status Solidi*, vol. 208, no. 1, pp. 81–85, Jan. 2011.

[63] B. S. T. Selvan, J. P. Spatz, H. Klok, and M. Möller, "Gold-Polypyrrole Core-Shell Particles in Diblock Copolymer Micelles," no. 2, pp. 1996–1998, 1998.

[64] M. Karbarz, M. Gniadek, and Z. Stojek, "Electroanalytical properties of ITO electrodes modified with environment-sensitive poly(N-isopropylacrylamide) gel and prussian blue," *Electroanalysis*, vol. 21, no. 12, pp. 1363–1368, 2009.

[65] E. Ventosa, a. Colina, a. Heras, V. Ruiz, J. Garoz, and J. López-Palacios, "One-pot synthesis of gold/poly(3,4-ethylendioxythiophene) nanocomposite," *J. Nanoparticle Res.*, vol. 14, no. 1, p. 661, Jan. 2012.

[66] A. Kumar, D. M. Welsh, M. C. Morvant, F. Piroux, K. a. Abboud, and J. R. Reynolds, "Conducting Poly(3,4-alkylenedioxythiophene) Derivatives as Fast Electrochromics with High-Contrast Ratios," *Chem. Mater.*, vol. 10, no. 13, pp. 896–902, 1998.

[67] A. Kumar and J. R. Reynolds, "Soluble Alkyl-Substituted Poly(ethylenedioxythiophenes) as Electrochromic Materials," *Macromolecules*, vol. 29, no. 23, pp. 7629–7630, 1996.

[68] S. S. Kumar, J. Mathiyarasu, and K. L. Phani, "Exploration of synergism between a polymer matrix and gold nanoparticles for selective determination of dopamine," *J. Electroanal. Chem.*, vol. 578, no. 1, pp. 95–103, Apr. 2005.

[69] S. S. Kumar, C. S. Kumar, J. Mathiyarasu, and K. L. Phani, "Stabilized gold nanoparticles by reduction using 3,4-ethylenedioxythiophene-polystyrenesulfonate in aqueous solutions: nanocomposite formation, stability, and application in catalysis.," *Langmuir*, vol. 23, no. 6, pp. 3401–8, Mar. 2007.

[70] P. K. Rastogi, V. Ganesan, and S. Krishnamoorthi, "Palladium nanoparticles incorporated polymer-silica nanocomposite based electrochemical sensing platform for nitrobenzene detection," *Electrochim. Acta*, vol. 147, pp. 442–450, 2014.

[71] O. Zhang, Y. Wen, J. Xu, L. Lu, X. Duan, and H. Yu, "One-step synthesis of poly(3,4-ethylenedioxythiophene)–Au composites and their application for the detection of nitrite," *Synth. Met.*, vol. 164, pp. 47–51, Jan. 2013.

[72] M. Salsamendi *et al.*, "Synthesis and electro-optical characterization of new

conducting PEDOT/Au-nanorods nanocomposites," *Polym. Adv. Technol.*, vol. 22, no. 12, pp. 1665–1672, Dec. 2011.

[73] C. M. Boutry, M. Müller, and C. Hierold, "Junctions between metals and blends of conducting and biodegradable polymers (PLLA-PPy and PCL-PPy)," *Mater. Sci. Eng. C*, vol. 32, no. 6, pp. 1610–1620, 2012.

[74] T. Kuang, L. Chang, F. Chen, Y. Sheng, D. Fu, and X. Peng, "Facile preparation of lightweight high-strength biodegradable polymer / multi-walled carbon nanotubes nanocomposite foams for electromagnetic interference shielding," *Carbon N. Y.*, vol. 105, pp. 305–313, 2016.

[75] C. Xu, G. Yepez, Z. Wei, F. Liu, A. Bugarin, and Y. Hong, "Synthesis and characterization of conductive , biodegradable , elastomeric polyurethanes for biomedical applications," *J. Biomed. Mater. Res. - Part A*, vol. 104A, no. 9, pp. 2305–2314, 2016.

[76] A. Moradpour, A. Ghaffarinejad, A. Maleki, V. Eskandarpourc, and A. Motahariana, "Low loaded palladium nanoparticles on ethylenediamine-functionalized cellulose as an efficient catalyst for electrochemical hydrogen production," *RSC Adv.*, vol. 5, pp. 70668–70674, 2015.

[77] K. Mondal and A. Sharma, "Recent advances in electrospun metal-oxide nano fiber based interfaces for electrochemical biosensing," *RSC Adv.*, vol. 6, pp. 94595–94616, 2016.

[78] T. Tanaka and D. J. Fillmore, "Kinetics of swelling of gels," *J. Chem. Phys.*, vol. 70, no. 3, pp. 1214–1218, 1979.

[79] E. Ye and X. J. Loh, "Polymeric hydrogels and nanoparticles: A merging and emerging field," *Aust. J. Chem.*, vol. 66, no. 9, pp. 997–1007, 2013.

[80] J. C. S. Norton *et al.*, "Poly (3,4-ethylenedioxythiophene) (PEDOT)-Coated Silica Spheres: Electrochemical Modulation of the Optical Properties of a Hydrogel-Stabilized Core-Shell Particle Suspension," *Chem. Mater.*, vol. 18, no. 19, pp. 4570–4575, 2006.

[81] J. Norton, M. G. Han, P. Jiang, S. Creager, and S. H. Foulger, "Electrochemical tuning the optical properties of crystalline colloidal arrays composed of poly(3,4-ethylenedioxythiophene) coated silica particles," *J. Mater. Chem.*, vol. 17, no. 12, p. 1149, 2007.

[82] D. Odaci *et al.*, "In situ synthesis of biomolecule encapsulated gold-cross-linked poly(ethylene glycol) nanocomposite as biosensing platform: a model study.," *Bioelectrochemistry*, vol. 79, no. 2, pp. 211–7, Oct. 2010.

[83] T. Dai, X. Qing, Y. Lu, and Y. Xia, "Conducting hydrogels with enhanced mechanical strength," *Polymer (Guildf).*, vol. 50, no. 22, pp. 5236–5241, Oct. 2009.

[84] H. Xiao, Y. Xia, and C. Cai, "Conducting polymer hydrogel reactor for synthesizing Au nanoparticles and its use in the reduction of p-nitrophenol," *J. Nanoparticle Res.*, vol. 15, 2013.

[85] S. Sekine, Y. Ido, T. Miyake, K. Nagamine, and M. Nishizawa, "Conducting polymer electrodes printed on hydrogel.," *J. Am. Chem. Soc.*, vol. 132, no. 38, pp. 13174–5, Sep. 2010.

[86] T. Augusto, É. Teixeira Neto, Â. A. Teixeira Neto, R. Vichessi, M. Vidotti, and S. I. C. De Torresi, "Electrophoretic deposition of Au@PEDOT nanoparticles towards

the construction of high-performance electrochromic electrodes," *Sol. Energy Mater. Sol. Cells*, vol. 118, pp. 72–80, 2013.

[87] T. Augusto, "Síntese Química de Poli (3,4- etilenodioxitiofeno) (PEDOT): Novas Arquiteturas para Diferentes Aplicações," University of São Paulo, 2012.

[88] A. C. da Silva, T. Augusto, L. H. Andrade, and S. I. Córdoba de Torresi, "One pot biocatalytic synthesis of a biodegradable electroactive macromonomer based on 3,4-ethylenedioxytiophene and poly(l -lactic acid)," *Mater. Sci. Eng. C*, vol. 83, no. April 2017, pp. 35–43, 2018.

[89] S. Garreau, G. Louarn, and J. P. Buisson, "In situ spectroelectrochemical Raman studies of poly(3,4-ethylenedioxythiophene)(PEDT)," *Macromolecules*, vol. 32, pp. 6807–6812, 1999.

[90] A. Garreau and J. L. Duvail, "Recent advances in optically active polymer-based nanowires and nanotubes," *Adv. Opt. Mater.*, vol. 2, no. 12, pp. 1122–1140, 2014.

[91] S. Garreau, J. L. Duvail, and G. Louarn, "Spectroelectrochemical studies of poly(3,4-ethylenedioxythiophene) in aqueous medium," *Synth. Met.*, vol. 125, pp. 325–329, 2002.

[92] F. Tran-Van, S. Garreau, G. Louarn, G. Froyer, and C. Chevrot, "A fully undoped oligo(3,4-ethylenedioxythiophene): Spectroscopic properties," *Synth. Met.*, vol. 119, no. 1–3, pp. 381–382, 2001.

[93] J. L. Duvail, P. Retho, S. Garreau, G. Louarn, C. Godon, and S. Demoustier-Champagne, "Transport and vibrational properties of poly(3,4-ethylenedioxythiophene) nanofibers," *Synth. Met.*, vol. 131, pp. 123–128, 2002.

[94] X. Feng, A. J. East, W. B. Hammond, Y. Zhang, and M. Jaffe, "Overview of advances in sugar-based polymers," *Polym. Adv. Technol.*, vol. 22, no. 1, pp. 139–150, 2011.

[95] P. Slepicka, N. S. Kasalkova, J. Siegel, Z. Kolska, L. Bacakova, and V. Svorcik, "Nano-structured and functionalized surfaces for cytocompatibility improvement and bactericidal action," *Biotechnol. Adv.*, vol. 33, no. 6, pp. 1120–1129, 2015.

[96] L.-C. Chang, H.-N. Wu, C.-Y. Lin, Y.-H. Lai, C.-W. Hu, and K.-C. Ho, "One-pot synthesis of poly (3,4-ethylenedioxythiophene)-Pt nanoparticle composite and its application to electrochemical H_2O_2 sensor.," *Nanoscale Res. Lett.*, vol. 7, no. 1, p. 319, Jan. 2012.

[97] K. Lin, T. Tsai, and S. Chen, "Performing enzyme-free H_2O_2 biosensor and simultaneous determination for AA, DA, and UA by MWCNT–PEDOT film," *Biosens. Bioelectron.*, vol. 26, no. 2, pp. 608–614, 2010.

[98] S. Y. Chen *et al.*, "Fabrication of PEDOT nanowhiskers for electrical connection of the hemoglobin active center for H_2O_2 electrochemical biosensing," *J. Mater. Chem. B*, vol. 1, pp. 3451–3457, 2013.

[99] M. Reza Nabid, S. J. Tabatabaei Rezaei, and S. Zahra Hosseini, "A novel template-free route to synthesis of poly(3,4-ethylenedioxythiophene) with fiber and sphere-like morphologies," *Mater. Lett.*, vol. 84, pp. 128–131, Oct. 2012.

[100] F. Jiang, R. Yue, Y. Du, J. Xu, and P. Yang, "A one-pot 'green' synthesis of Pd-decorated PEDOT nanospheres for nonenzymatic hydrogen peroxide sensing," *Biosens. Bioelectron.*, vol. 44, pp. 127–131, 2013.

[101] T. Tsai, T. Chen, and S. Chen, "Copper Nanoparticles with Copper Hexacyanoferrate and Poly(3,4-ethylenedioxythiophene) Hybrid Film Modified

Electrode for Hydrogen Peroxide Detection," *Int. J. Electrochem. Sci.*, vol. 6, pp. 4628–4637, 2011.

[102] A. M. Smolin, N. P. Novoselov, T. A. Babkova, S. N. Eliseeva, and V. V Kondrat, "Use of Composite Films Based on Poly(3,4-Ethylenedioxythiophene) with Inclusions of Palladium Nanoparticles in Voltammetric Sensors," *Int. J. Electrochem. Sci.*, vol. 70, no. 8, pp. 846–853, 2015.

[103] A. S. Rad, M. Ardjmand, M. Jahanshahi, and A.-A. Safekordi, "AgNPs included GC/Poly(3,4-Ethylenedioxythiophene) Modified Electrode Toward Electrochemical Detection of H_2O_2," *J. Nano Res.*, vol. 16, no. 2011, pp. 77–82, 2012.

[104] J. Wang, Y. Wang, M. Cui, S. Xu, and X. Luo, "Enzymeless voltammetric hydrogen peroxide sensor based on the use of PEDOT doped with Prussian Blue nanoparticles," *Microchim. Acta*, pp. 483–489, 2017.

APPENDIX A — Systematic names of some compounds in this Thesis

Systematic names for some chemical compounds in this Thesis. Prefixes are not considered for the order.

Acetonitrile (ACN).....ethanenitrile

Acrylamide (AAM).....propenamide

Acrylic acid (AA).....propenoic acid

Adipate.....1,6-dihexanoate

Agarose.....poly(D-2,3,4,5-tetrahydroxy-6-hydroxymethyl-tetrahydropyran-*co*-L-3,4,8-trihydroxy-2,6-dioxa-[3,2,1]bicyclooctane)

Ascorbic acid.....3-*R*-6-*S*-3-(1,2-dihydroxyethyl)-4,5-dihydroxy-4-butene-1-lactone

2,2'-bipyridil.....2-(2-pyridil)-1-pyridine

Butylene.....butene

Camphoroquinone.....1,7,7-trimethyl-2,3-dioxo-[2,2,1]bicycloheptane

10-camphorsulfonic acid.....7,7-dimethyl-2-oxo-[2,2,1]bicycloheptane-1-sulfonic acid

Caprolactone.....hexanelactone

Dimethylviologen.....4,4'-di-1-methylpyridinium

Dopamine.....4-(2-aminoethyl)-1,2-diphenol

Ethylenediamine.....1,2-diaminoethane

3,4-ethylenedioxythiophene (EDOT).....[3,4,0]2,5-dioxa-8-thia-2,8-cyclononadiene

Ethyleneglycol.....1,2-dihydroxyethane

1-ethyl-3-vinylimidazolium bromide.....1-ethyl-3-ethenylimidazolium bromide

Lactic acid (LA)….....2-hydroxypropanoic acid

Glucose.....2,3,4,5-tetrahydroxy-6-hydroxymethyl-tetrahydropyran

N,N’-methylenebisacrylamide.....3,7-dioxo-4,6-diaza-1,8-nonadiene

Prussian Blue.....iron(III) hexacyanoferrate

Phenylene vinylene…….....ethenylbenzene

Pyrrole.....1-aza-2,4-cyclopentadiene

Sarin.....2-(fluoro-methylphosphoryl)isopropoxy

4-styrenesulfonate (SS).....4-ethenylbenzenesulfonate

Terephtalate.....1,4-dibenzoate

N,N,N',N'-tetramethylethane-1,2-diamine.....2,5-diaza-2,5-dimethylhexane

Thiophene.....1-thia-2,4-cyclopentediene

Toluene.....methylbenzene

Tris(2-methoxyethoxy)(vinyl)silane.....tri-(2-methoxyethoxy)-ethenylsilane

Uric acid.....2,4,7,9-tetraaza-3,5,8-trioxo-[4,3,0]-(1-6)-bicyclononene

Urethane.....ethyl 1-aminomethanoate

CURRICULUM VITAE

Personal data

- Full name: Marco Antonio de Oliveira Santos Minadeo.
- Names in publications: Minadeo, Marco A. O. S.; Marco A. O. S. Minadeo; Minadeo, M. A. O. S.; M. A. O. S. Minadeo; Marco A. O. S. M..
- Born in São Paulo, São Paulo, Brazil, in 1991.
- ORCID ID: 0000000163105801.

Scholar and academic education

2006–2007. **Secondary Education**. Federal Institute of São Paulo, São Paulo, São Paulo, Brazil.

2008–2008. **Secondary Education**. Colégio Integrado Objetivo, São Paulo, São Paulo, Brazil.

2009–2012. **BSc in Chemistry**. USP, São Paulo, São Paulo, Brazil. Main research performed during the course: Laboratory: Laboratory of Electroactive Materials. Supervisor: Professor Doctor Susana Inés Córdoba de Torresi. Scholarship from: Research Support Agency of the State of São Paulo. Title of the project: "**Study of the Direct Electron Transfer of Redox Proteins Aiming the Construction of Enzymatic Biosensors**".

2013–2018. **PhD in Chemistry**. USP, São Paulo, São Paulo, Brazil. Scholarships received from: Nacional Council of Research and Research Support Agency of the State of São Paulo (this Thesis).

Supplementary education

- Short course in **Stereochemistry**. USP, 2009.
- Short course in **Origin of Life**. USP, 2010.
- Scientific diffusion formal open course in **Introduction to Astronomy and Astrophysics**. USP, 2011.
- Short course in **Green Chemistry**. USP, 2011.
- **Italian Language and Culture**. ELIS Association, Rome, Italy, 2012.
- **Scanning Electrochemical Microscopy**. Brazilian Chemical Society, 2012.
- Short course in **Paintings and Polymers BASF**. BASF, 2012.
- Subject course in **Synthesis and Applications of Dyes and Pigments**. USP, 2012.
- **Summer Course of the Institute of Physics of USP**. USP, 2013.
- Short course in **Electrochemical Impedance Spectroscopy**. Metrohm, 2013.
- Subject course in **Electron Microscopy**. Theoretical and experimental course. USP, 2013.

- Subject course in **Atomic Force Microscopy**. USP, 2014.
- **Simulation in Electrochemistry**. USP, 2016.
- Short course in **Electrochemical Impedance Spectroscopy**. Ametek, 2017.
- Short course in **Microscale Scanning Electrochemical Techniques**. Ametek, 2017.
- Subject course in **Light-activated Electrochemistry: Fundaments and Applications**. USP, 2017.
- Subject course in **Teaching in the Higher Education: a First Approach**. USP, 2018.
- **Spectroscopic Methods Applied to the Study of Materials: X Ray Photoelectron Spectroscopy**. USP, 2018.
- **Scientific Dissemination on the Internet**. USP, 2018.

Works with received scholarships

- BSc student research, scholarship from FAPESP, 2011–2012.
- PhD student research, scholarship from CNPq, 2013–2013 (this Thesis).
- PhD student research, scholarship from FAPESP, 2013–2018 (this Thesis).

Scientific production

Articles published in journals

- V. R. Gonçales, R. N. P. Colombo, Marco A. O. S. Minadeo, E. Y. Matsubara, J. M. Rosolen, S. I. Córdoba de Torresi; “Three-dimensional graphene/carbon nanotubes hybrid composites for exploring interaction between glucose oxidase and carbon based electrodes”; *Journal of Electroanalytical Chemistry*; v. 775, p. 235–242 (2016).
- F. Wolfart, B. M. Hryniewicz, M. S. Góes, C. M. Corrêa, R. Torresi, Marco A. O. S. Minadeo, S. I. Córdoba de Torresi, R. D. Oliveira, L. F. Marchesi, M. Vidotti; “Conducting polymers revisited: applications in energy, electrochromism and molecular recognition”; *Journal of Solid State Electrochemistry*; v. 21, p. 2489–2515 (2017).

Submitted articles

- Marco A. O. S. Minadeo, A. C. da Silva, S. I. Córdoba de Torresi; “Gold nanoparticles and [PEDOT-poly(lactic acid)] composite. Synthesis, characterization and application to H_2O_2 sensing” (2019).

Works presented at congresses

Several works among them are abstracts published in congresses annals.

- 10^{th} Spring Meeting of the International Society of Electrochemistry, Perth (2012).

"Wiring glucose oxidase enzymes with CNTs and conducting polymer for direct electron transfer".

- 35th Annual Meeting of the Brazilian Chemical Society, Águas de Lindóia (2012). "Direct electron transfer between glucose oxidase and nanostructured carbon composite electrodes" (double presentation).
- 63th Annual Meeting of the International Society of Electrochemistry, Prague (2012). "Carbon micro/nanostructures for third generation biosensors".
- 20th International Symposium of Research of Tertiary Education Students of USP, São Paulo (2012). "Direct electron transfer between glucose oxidase and nanostructured carbon composite electrodes".
- XIX Brazilian Symposium in Electrochemistry and Electroanalytics, Campos do Jordão (2013). "Study of the electroactivity of glucose oxidase onto a felt/CSCNT carbon composite for the development of biosensors".
- Workshop Electrochemistry, from Sensing to Energy Conversion and Storage, São Paulo (2015). "Synthesis and characterization of hybrid nanoparticles for electrochemical devices".
- I Meeting in Electrochemistry and Electroanalytics of IQ-USP, São Paulo (2017). "Synthesis of gold nanoparticles/PEDOT-PLLA hybrid materials and applications in electrochemical detection".
- XXI Brazilian Symposium in Electrochemistry and Electroanalytics, Natal (2017). "Synthesis of gold/PEDOT-PLLA hybrids and applications in electrochemical detection".
- 46th IUPAC World Chemistry Congress / 40th Annual Meeting of the Brazilian Chemical Society, São Paulo (2017). "Synthesis of gold nanoparticles/PEDOT-PLLA hybrids and applications in electrochemical detection".

Teaching experience

- Teacher of experimental electrochemistry at the 6th (2011), 7th (2012), 8th (2013), 9th (2014), 10th (2015) and 11th (2016) Paulo Teng An Sumodjo School of Electrochemistry, being the 9th Paulo Teng An Sumodjo School of Electrochemistry also called *FAPESP São Paulo School of Advanced Sciences on Electrochemistry, Energy Conversion and Storage* (2014).
- Volunteer teacher of experimental chemistry at extracurricular courses (2018–2018).
- Freelancer teacher of Chemistry of private classes at private classes schools (2018–now).

Appraiser activities

Participated as appraiser at the 22th (2014), 23th (2015), 24th (2016) and 25th (2017) International Symposium of Research of Tertiary Education Students of USP.

ABOUT THIS THESIS

This is the version of the Thesis corrected after the Thesis defense. The physical copy of the text can be found at the Library of Chemical Sciences Set of the University of São Paulo, in the *campus* of São Paulo, São Paulo, Brazil. The physical copy of the original version of the Thesis (for the Thesis defense) can be found at the Secretary of Graduate Courses at the Institute of Chemistry of the University of São Paulo, in the *campus* of São Paulo, São Paulo, Brazil. The digital corrected version and the digital original version of the Thesis can be found and downloaded at The Digital Library of Theses and Dissertations of the University of São Paulo (in English):

http://www.teses.usp.br/index.php?lang=en

The original version of the Thesis was delivered to the Secretary of Graduate Courses on November 5th, 2018, and defended on December 14th, 2018. The corrected version of the Thesis was delivered to the Secretary of Graduate Courses in February 2019.

If the images in the physical versions were difficult to read, please check the digital versions. To write to the author send an e-mail to marco.minadeo@alumni.usp.br.